Humboldt Universität zu Berlin

DISSERTATION

Influence of HCMV proteins pUL71 and pUL77 on viral maturation

zur Erlangung des akademischen Grades
d o c t o r r e r u m n a t u r a l i u m (Dr. rer. nat.)
im Fach Biologie

eingereicht an der
Mathematisch-Naturwissenschaftlichen Fakultät I
der Humboldt-Universität zu Berlin

von

Mag. rer. nat. Christina Sylvia Meissner

Präsident der Humboldt-Universität zu Berlin
Prof. Dr. Jan-Hendrik Olbertz

Dekan der Mathematisch-Naturwissenschaftlichen Fakultät I
Prof. Dr. Andreas Herrmann

Gutachter: 1. Prof. Dr. Elke Bogner
2. Prof. Dr. Martin Messerle
3. PD Dr. Thorsten Wolff

eingereicht: 27.06.2011
Datum der Promotion: 14.11.2011

Zusammenfassung

Die Bildung infektiöser Viruspartikel des humanen *Zytomegalievirus* (*HCMV*) ist ein mehrstufiger Prozess. Sie beginnt mit der Verpackung der DNA in die Kapside im Kern, gefolgt von weiterer Reifung während des Transports durch das Zytoplasma und der abschließenden Freisetzung aus der Zelle. Im Zuge dieser Arbeit wurden zwei Proteine, die Einfluss auf die ebengenannten Prozesse haben, analysiert.

Der erste Teil der Arbeit befasst sich mit der funktionellen Charakterisierung des *HCMV* Proteins pUL77. Es ist bekannt, dass das homologe Protein pUL25 in α-*Herpesvirinae* essentiell für die DNA-Verpackung ist. Zunächst konnte das Protein als Kapsid-assoziiertes strukturelles Protein identifiziert werden. Es wurden Interaktionen von pUL77 mit DNA-Verpackungs- und Kapsidproteinen gezeigt. Weiterhin wurde die DNA-Bindungsfähigkeit von pUL77 in verschiedenen „*in vitro*"-Experimenten untersucht. Zusammengefasst weisen unsere Ergebnisse auf eine Funktion von HCMV pUL77 bei der DNA-Verpackung hin.

Im zweiten Teil der Arbeit wurde das *HCMV* Protein pUL71 charakterisiert, das in allen Herpesviren konserviert vorkommt, dessen Funktion jedoch nicht charakterisiert ist. Zunächst wurde das Protein als strukturelles Tegumentprotein mit "early-late" Expressionskinetik klassifiziert. Weiterhin wurden die subzelluläre Lokalisation sowie virale und zelluläre Interaktionspartner untersucht. Die Ergebnisse weisen auf eine Funktion von HCMV pUL71 bei der Reifung und beim Transport der Virionen im Zytoplasma hin. „*In silico*"-Vorhersagen zeigten ein „Leuzin Zipper"-Motiv in pUL71, das als mögliche Oligomerisationsdomäne dienen könnte. Mutationen wurden in dieses Motiv eingebracht und die resultierenden Proteine auf ihre Oligomerisationsfähigkeit mit „in vitro"-Methoden und in rekombinanten Viren untersucht. Zusammenfassend konnten wir zeigen, dass das „Leuzin Zipper"-Motiv wichtig für die Funktion von pUL71 ist und diese mit einer unbeeinträchtigten Oligomerisation des Proteins zusammen hängt.

Schlagwörter:

Humanes Zytomegalievirus, DNA Verpackung, Transport und Reifung von Viruspartikel, Oligomerisierung

Abstract

The morphogenesis of Human *cytomegalovirus* (*HCMV*) virions starts with the capsid assembly and DNA insertion in the nucleus followed by maturation during transport through the cytoplasm prior to release of virus progeny. In this study we are functionally characterising two proteins that are involved in those steps.

The function of essential *HCMV* protein pUL77 is characterised in the first part of the study. *HCMV* pUL77 was shown to be a structural protein associated with capsids. Furthermore, our experiments demonstrated that *HCMV* pUL77 interacts with DNA packaging motor components and capsid proteins. The ability of *HCMV* pUL77 to bind double-stranded DNA was studied in "*in vitro"* assays designed for this study. The homologue *α-Herpesvirinae* protein pUL25 is described to be involved in processes connected with DNA packaging. Data obtained in this study demonstrates that *HCMV* pUL77 might serve a similar function.

In the second part of the study *HCMV* pUL71, conserved throughout the Herpesvirus family but to date unclassified, was functionally characterised. *HCMV* pUL71 was defined a structural tegument protein with early-late expression kinetics. We studied the sub-cellular localisation and interactions of pUL71 with a subset of cellular and viral proteins. Thereby we could show that *HCMV* pUL71 function might be connected with processes of viral egress. By *in silico* analyses we identified a leucine zipper motif in pUL71 that might serve as a putative oligomerisation domain. In order to investigate the function of the leucine zipper motif, we performed *in vitro* assays and investigated the alterations of the motif in the viral context. Taken together we can conclude that (i) an intact leucine zipper motif is crucial for the function of pUL71 and (ii) this function is dependent upon undisturbed oligomerisation of the protein.

Keywords:

Human *cytomegalovirus*, DNA packaging, egress, oligomerisation

Table of content

1 Introduction

1.1 *HCMV* and the *Herpesviridae*

The human cytomegalovirus (*HCMV*) is taxonomically classified in the family of *Herpesviridae* according to the international committee on virus taxonomy (=ICTV) (194). Characteristics *Herpesviridae* comprise are (i) structural similarities like composition of the virus particle (1.1.1.) as well as (ii) encoding their own viral DNA-polymerase and (iii) establishment of a life-long persistence in their host. (2)

Taking biologic properties such as host range and growth kinetics into account the *Herpesviridae* can be subclassified into three subfamilies: α-, β- and γ-*Herpesvirinae*.

α- *Herpesvirinae* are characterised by common features like broad host range, a comparatively short replication cycle (<1 day) and fast cell-to-cell spread. Persistence takes place in sensory neurons. Members of this subfamily causing pathogenicity in humans are *herpes simplex virus type 1* and *2* (*HSV-1, HSV-2*) as well as *varizella zoster virus* (*VZV*) (2, 194).

β- *Herpesvirinae* are characterised by a narrow host range, comparatively long replication cycles (>1 day) and slow cell-to-cell spread. Persistence takes place in lymphotropic organs, secretory glands and renal tissue. Human pathogenic members of this subfamily are *HCMV*, *human herpes virus type 6* (*HHV-6*) and *human herpes virus type 7* (*HHV-7*) (2, 194).

γ- *Herpesvirinae* are characterised by a strict host range and even restricted towards B- and T-cells. Furthermore they are convincingly linked to oncogenesis. Human pathogenic members of this subfamily are *Epstein-Barr virus* (*EBV*) and *human herpes virus type 8* (*HHV-8*) (2, 194).

HCMV infection of host cells is characterised by a strong cytopathic effect causing enlargement of the cells, eponymously called cytomegaly. Considering the characteristics for *β-Herpesvirinae* mentioned above *HCMV* can infect a remarkably broad range of cells within its human host, including parenchymal cells and connective tissue cells of virtually any organ and various hematopoietic cell types. Epithelial cells, endothelial cells, fibroblasts and smooth muscle cells are the predominant targets for virus replication (214).

Following primary infection, *HCMV* establishes lifelong latency and periodically reactivates without causing symptoms in healthy individuals (7, 61, 117). In the absence of an adequate host-derived immune response, like in prenatal and postnatal infants (40, 75, 191), patients

receiving organ transplants (197) or such suffering from AIDS (55), *HCMV* can subsequently cause invasive disease (65).

Although the exact mode of *HCMV* infection is still unknown, it is assumed to be through direct contact with body fluids from an infected person (1). Putative routes of transmission are via sexual contacts through saliva, sperm and cervix fluid (86), from mother to child congenitally (97) or later through breast feeding (147) and via blood transfusions and organ transplants (197).

HCMV is world-widely endemic but persistence in the population differs between economically well developed countries of northern Europe (40% seropositive adults) to developing countries were almost 100% of adults are seropositive (7, 28).

1.1.1 The viral particles

One common feature of the *Herpesviridae* is the composition of its virions.

For *HCMV* the virion is between 150-200 nm in diameter in total. From the inside to the outside composed of the genome surrounded by a protein matrix in its centre (core), encapsidated by a protein shell (capsid), covered by an amorphous protein layer (tegument) and a host-derived lipid bilayer with inserted viral glycoproteins (envelope) (91, Figure 1).

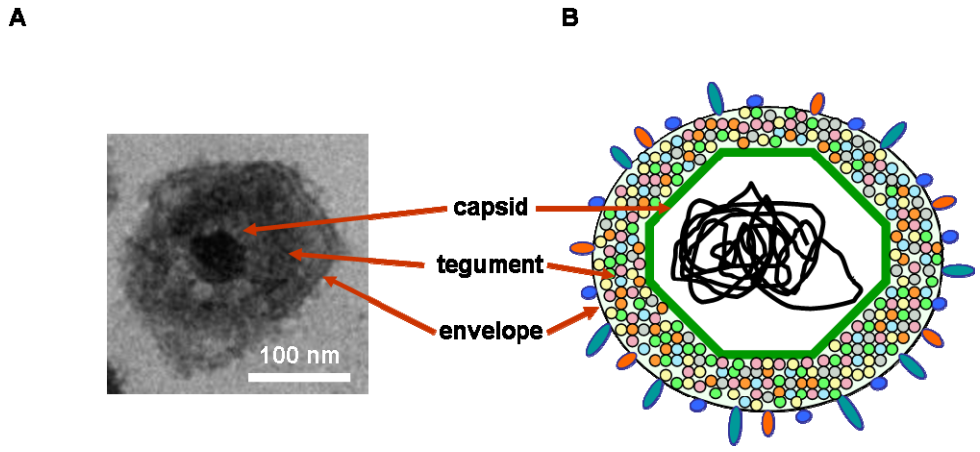

Figure 1: Composition of the virion (A) EM analysis of a mature extracellular virion from *HCMV* (*TB40E*). Sample was embedded and ultra thin sectioned prior analysis by transmission electron microscopy (TEM). Magnifications are indicated by the bar. (B) Schematically drawing of the virion. Capsid, tegument and envelope layers are indicated by red arrows in both representations.

The central core is composed of the linear dsDNA genome and a fibrillic protein matrix. (249). Together core and capsid are termed nucleocapsid.

The capsid has an icosahedral symmetry (T=16) composed of 162 capsomers. These capsomers itself are build up from a subset of structural proteins including the major capsid protein (MCP), minor capsid protein (mCP), minor capsid binding protein (mC-BP), smallest capsid protein (SCP) as well as parts of the DNA packaging machinery with portal protein (pUL104) and large terminase subunit (pUL56). (91)

Capsid assembly has been studied in *α-Herpesvirinae* in *in vitro* cell free assembly assays of *HSV-1* capsids (164). Many *HSV-1* capsid proteins share structural and functional homology to *HCMV* capsid proteins and cryo-electron microscopic analysis of both viruses suggests similar, but not identical, capsid structure (44, 54, 95, 234, 255, 256).

The tegument is composed of a number of phosphor proteins. This arrangement does not seem to follow any obvious symmetry and is therefore called amorphous (38). So far 20 proteins are assigned to the tegument that facilitates important functions during viral replication (112). For example they facilitate morphogenesis during egress (e.g. pp150 (26, 156)), viral transport (pUL47, pUL48 (136, 216), immune evasion (e.g. pp65 **,** pIRS1/pTRS1 (41, 58) as well as regulation of early gene expression by transactivation (e.g. pp71**,** pUL69, (133, 247)).

In comparison to other *Herpesvirinae* the most structurally diverse region of the *HCMV* virion seems to be the tegument which is composed of a lot of unique proteins. Although proteins with homologous functions localised to the tegument, only a limited number of these proteins show significant structural homologies (6).

The envelope is a host derived lipid-bilayer with inserted viral glycoproteins (185) that are arranged in three complexes. Glycoprotein complex I (gCI) is a homodimer predominately composed of glycoprotein gB (37, 38). glycoprotein complex II (gCII) is arranged of glycoproteins gM and gN (137, 138) and glycoprotein complex III (gCIII) from gH, gL and gO (104, 132). These complexes are important for attachment to the host cell and fusion between the viral envelope and the plasma membrane for entry into the cell, as well as for the induction of neutralising antibodies in the host's immune response (39).

Among infectious virions a number of other non-infectious viral particles are build during *HCMV* infections. Though these particles are not infectious for not containing the genome they are important for the host's immune response (178). Examples are dense bodies (DB) that are composed of enveloped tegument proteins (204) or so called non-infectious enveloped particles (NIEPs), empty capsids that underwent further maturation steps like tegumentation and envelopment (108).

1.1.2 The viral genome

The *HCMV* genome has the largest coding capacity of all *Herpesviridae* with 230kb in length and a molecular weight of 1,5 x 10^8 Dalton (24, 52). It is comprised of linear double stranded (ds) DNA and contains two non repetitive regions that are termed *unique long* (UL)- and unique *short* (US)-segment, flanked by *terminal* (TR_L, TR_S) and *internal repeats* (IR_L, IR_S) (11). The open reading frames (ORFs) are named and numbered according to their position on the genome within one of those regions.

An important motif for DNA packaging is found in the internal repeat regions, the so called a-region that encodes the cis-acting packaging elements pac 1 and pac 2 (115, 146, 159, 163). These elements are an important trigger for nuclease- and binding activity of the terminase during packaging of DNA into preformed capsids, a crucial step in viral maturation (31, 161).

The lab strain *AD169* that is predominantly used in this study is completely sequenced and contains 208 ORFs (52). Through passaging mutations in comparison to wild type virus have accumulated in *AD169* likes frame shifts in genes RL5A, RL13 and UL131A (14, 72, 252) and a substitution of gene UL36. Those regions are hypothesised to facilitate pathogenicity and cell tropisms in other *HCMV* strains (48, 143).

1.2 From structural components to infectious particles

The *HCMV* lifecycle is determined by four crucial events: (i) the entry into the host cell, (ii) the exploiting of the cellular machinery to produce dsDNA and protein, (iii) the assembly of the capsids and DNA insertion and (iv) the release of virus progeny from the cell. In the following those events will be discussed in more detail. Figure 2 is a schematically drawing of the events mapping viral replication steps to cellular compartments.

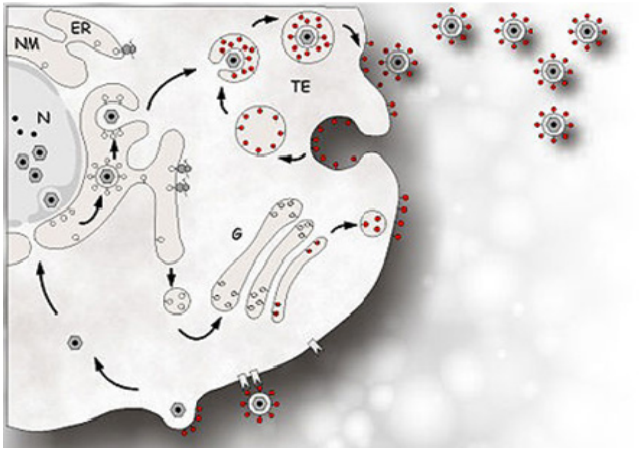

Figure 2: The *HCMV* life cycle. Processes of *HCMV* lifecycle are summarised starting with attachment and entry, followed by transport to the nucleus. Further synthesis of viral components is carried out as well as assembly of capsids in the nucleus prior to packaging of DNA into these preformed capsids. Egress starts with perinuclear budding and transport to the cytoplasmic cisternae where virions undergo the final envelopment. The last step is release of virus progeny by exocytosis. Adapted from E. Bogner (30).

1.2.1 Attachment and virus entry

The process of *HCMV* entering the host cell is classified into three events: (i) attachment, (ii) receptor binding or activation and (iii) fusion (98).

Attachment of the virus to the surface of the host cell is the first step in viral replication. On the viral side the three glycoprotein complexes I-III (gC I-III) are involved. Not all interaction partners in this event are fully characterised to date. Still we know that firstly attachment to cell surface is mediated by binding of gB and gM to heparan sulphate proteoglycans (63, 113). Complexes of gH/gL/UL128-131 are necessary for entry in epithelial cells (198).
Further a couple of receptors were suggested as *HCMV* entry receptors. For instance Annexin II was described to bind gB and enhances *HCMV* binding and fusion to phospholipid-membranes (182, 188). To the contrary, cells that do not express Annexin II are permissive for *HCMV* too (182). Another candidate was human aminopeptidase N (CD13) that was discussed to mediate interactions between gH and cell surface (218). Epidermal growth factor receptor (EGFR) as another putative *HCMV* receptor and integrin αvβ3 as a co-receptor were described by Wang et al. (242, 243). Still, it is important to note cells that do not express EGFR are susceptible for *HCMV* infection in *HELF* cells. Taken together, neither one of the entry receptors proposed so far are likely to be the *HCMV* entry receptor nor seem this event to be dependent on one receptor alone in all cell types. Therefore further investigations need to be carried out to elucidate the underlying mechanism of attachment.

Still, these processes are followed by membrane fusion between envelope and host cell plasma membrane (62). Again glycoproteins seem to be involved but the exact events remain poorly understood (34, 114, 190). In the case of *HSV-1* the specific mode of entry is cell-type dependent. Either the route via direct fusion at the plasma membrane and subsequent release of the capsid into the cytosol or endocytosis is used (142, 168). An equivalent scenario is likely for *HCMV*.

Once the virus has entered the cell its nucleocapsid is transported to the nuclear pore by hijacking cellular motor proteins. Kinesin or dynein and dynactin transport capsids on microtubules from the plasma membrane to the nuclear pore (76, 80, 187, 217). At the nuclear

pore the DNA is released and circulised to ensure proper nuclear import of functional genomes (172, 193).

1.2.2 Gene expression and replication

Once the dsDNA genome has reached the nucleus gene expression will start in a cascade manner modulated by multiple transcription activators. Within this cascade proteins are characterised according to their expression kinetics in (i) immediate-early, (ii) early and (iii) late proteins (244). Within the first three hours of infection immediate early genes (IE1/2 (221)) are expressed triggered by cellular RNA-Polymerase II together with viral proteins pp71 and pUL69 (22, 247). Expression is independent from *de novo*-synthesised viral proteins. Immediate early proteins regulate expression of so called early genes (219). Expressed between three and 36 hours post infection (h p.i.) early genes regulate initiation of viral replication and expression of the majority of viral proteins so called late proteins that often have structural functions (expression 36-72h p.i.) (90). Expression of late proteins starts with DNA-synthesis that is carried out following the *rolling circle-mechanism (*17*,* 103, 145) first described for genome replication in bacteriophage λ (5). DNA-synthesis is restricted to centralised areas in the nucleus termed replication centres (73, 74). According to the rolling cycle mechanism so called concatamers, linear linkage of several unique-length genomes, are synthesised from the circular template that will be later on processed for DNA packaging.

1.2.3 Capsid assembly and DNA packaging

During the process of capsid assembly three different forms of capsid are described: empty A-capsids, protein containing B-capsids and DNA filled C-capsids (91, 192).

Assembly of the capsid takes place in the proximity of viral replication centres in the nucleus of host cells. All components needed for assembly are transported inside the nucleus.

For *HSV-1* extensive *in vitro* cell free assembly assays of capsids have been performed (164) to identify important players in this process. For *HCMV* it was shown that first of all the two alternatively translated gene products of UL80 a*ssembly protein precursor* (pAP) and *proteinase precursor* (pPR) together with the MCP form higher order complexes in the cytoplasm (pAP_{12}-MCP_6) (91). Those are transported into the nucleus together with SCP (56, 127). There they build up the pro-capsids together with mCP and mc-BP (92, 164). Thereby pAP and pPR form a so called scaffold to stabilise the structural viral proteins at their correct positions during assembly (91). At the same time the portal protein pUL104 (77, 167, 213) is

inserted as well. Once assembly is completed capsids are called B-capsid, containing two layers of protein one composed of structural components on the outside and the scaffold within.

Before DNA can be packaged the capsid needs to be matured by removing the scaffold by proteolytic activity of pPR derived protease PR (192, 245).

The process of DNA packaging shows homologies to that described for dsDNA bacteriophages belonging to the order of *Caudovirales* (21). As mentioned above DNA is synthesised as concatamers that need to be processed in unique length genomes during packaging. Seven viral gene products have been indentified due to the homologies between bacteriophages and *Herpesviridae*. For *HCMV* those are pUL104, pUL93, pUL89, pUL77, pUL56, pUL52 und pUL51 (52). The most important among them are the two subunits of the terminase pUL56 and pUL89 that specifically bind to the a-sequence of viral DNA, have an endonuclease activity and produce energy needed for packaging by ATP-hydrolysis (31, 32, 105, 206, 207). The terminase translocates the DNA via the portal inside the capsids (77, 78). If DNA packaging is successful, the capsids containing the genome are now termed C-capsids while abortive packaging leads to so called DNA-free A-capsids (179).

DNA processing and packaging, as well as the turn over from B to C-capsid is hypothesised to be synchronised and conserved in all *Herpesviridae* (125).

1.2.4 Maturation and egress

After the capsids have undergone packaging they are interacting with first tegument and cellular proteins of the nuclear lamina to drive egress. For example it has been described that viral kinase pUL97 in HCMV or pUL31 and pUL34 in *α-Herpesvirinae* polarise and thereby destabilise the nuclear lamina to allow capsids to leave the nucleus (51, 88, 122, 184, 195, 201). This transport is described as a perinuclear budding event (186). Glycoproteins gB and gH (33, 155, 184) facilitate a first temporal envelopment at the inner nuclear membrane followed by a de-envelopment at the outer nuclear membrane (8). Further they bud into the cytoplasm and get transported to the cytoplasmic cisternae. Morphogenesis of the virions will occur on the capsids itself through tegumentation while been transported through the cytosol as well (202) as on the future envelopment site (151, 152). The exact underlying mechanisms of morphogenesis are controversially discussed in the field. Recently, it was hypothesised that the virus reconstructs the cell for its morphogenesis upon infection by inducing formation of a compartment that combines endoplasmatic reticulum (ER), Golgi and trans-Golgi network (TGN) in close proximity. It has been reported that many vesicles derived from the TGN,

secretory, and endosomal pathway (66, 71, 87, 202, 233) concentrate in a junxtanuclear position to form a structure termed “assembly compartment” or “assembly complex” (AC) (101, 202). Besides these cellular structures, tegument, envelope, and non-structural proteins have been found to accumulate in this AC during infection (70, 99, 101, 138, 202, 209, 227). Anyhow, ultrastructural analysis of HCMV infected cells revealed that final envelopment takes place at the cisternae of the tubular endosomes or TGN (233). There the viral particles acquire their final envelope by budding into membrane compartment containing both TGN and endosomes (47).

The cellular processes of membrane budding which are normally part of endosome sorting are controlled by the cellular endosomal sorting complex required for transport (ESCRT). Recent data showed that ESCRT specific proteins are recruited to the AC thereby suggesting that ESCRT machinery is involved in final maturation steps (225)

After completion of morphogenesis mature virions will leave the cell by exocytosis (151, 152, 153, 154).

1.3 Aim of the study

In this study proteins are functionally characterised that are proposed to be involved in two important steps of virion morphogenesis. At the beginning of this study and partially still to date nothing is described about the function of *HCMV* essential protein pUL77 and pUL71, though being nonessential, its loss causes severe growth impairments (82, 239). Homologues in *α-Herpesvirinae* are partially characterised and therefore we tried to draw conclusions from these homologies.

Firstly HCMV pUL77 is analysed in comparison to its *α-Herpesvirinae* homologue pUL25 (52). This protein is described to have a proposed function as an assisting factor during DNA packaging, to generate a headfull signal to stop the packaging process or to function as a cap to seal the portal and hold DNA within packaged capsids (15, 118, 144, 171, 235). More recently, an additional function early in the viral lifecycle is discussed. *HSV-1* pUL25 is described to trigger the release of genomic DNA at the nuclear pore during entry (175, 193)

The 1911 bp long gene product of ORF UL77 is defined as a core gene and situated on position 112227 and 114137 in the *HCMV* genome (NC_006273.2, 81) between UL76 and UL78 partially overlapping with the C-Terminus of pUL76. The translated protein is 636 aa in length and the calculated molecular weight (MW) and isoelectric point (pI) is 73028.53 (~ 73kDa) and 5.73, respectively.

In this study we hypothesise that *HCMV* pUL77 shares equivalent properties with its *α-Herpesvirinae* homologues and plays a role in similar processes. Therefore we generate a specific antibody to analyse the subviral localisation of pUL77, interactions with certain viral proteins by ultracentrifugation and various protein-protein interactions *in vitro*. Furthermore, we analyse whether pUL77 has the capacity to bind dsDNA, a prerequisite for the proposed functions in DNA packaging or release, by generating a new assay that allows us to use defined DNA fragments for our interaction studies.

The *α-Herpesvirinae* homologue for pUL71 is pUL51 (52). However, *HCMV* pUL71 and *HSV-1* pUL51 are not structural homologues, but both are members of the *Herpesvirus* U44 superfamily, containing the conserved, but functionally unclassified, U44 domain (140).

At the beginning of this study, only studies in animal herpesviruses and *HSV*-1 were performed (67, 96, 131). Most of them concentrated on localisation but some also connected the protein to processes of egress either at the stage of perinuclear budding or at a later step like secondary envelopment (119, 131, 169, 170).

The 1086 bp long gene product of ORF UL71 is defined as a core gene and situated on position 104703 and 105788 in the *HCMV* genome (NC_006273.2, 81) between UL70 and UL72 partially overlapping with the N-terminus of the opposed UL70. The translated protein is 361 aa in length and the calculated MW and pI is 39885.86 (~ 40kDa) and 4.99, respectively.

In this study we analyse whether the functions described for *α-Herpesvirinae* are applicable for pUL71. Again we start our analysis by generating a specific antibody that will be further used to identify subviral localisation and the interaction with other viral and cellular proteins in different *in vitro* protein-protein interaction studies and immunofluorescence. In addition, analyses are performed to determine the time point of expression of pUL71 within the *HCMV* transcription cascade and the intracellular distribution of the protein. Oligomerisation of pUL71 is analysed by single particle EM analysis, *in vitro* protein-protein interaction studies and in the viral context using recombinant viruses.

2 Materials and Methods

2.1 Materials

2.1.1 Chemicals, consumables and equipment

2.1.1.1 Chemicals

All chemicals were purchased at highest purity and used according to the manufacturer indicated below. Buffers and media for cell culture are indicated in the appropriate section.

Name	Manufacturer
Acetone ($(CH_3)_2CO$) [Cat. No. 8002]	JT Baker, Phillipsburg, NJ
Acrylamide stock [Cat. No. 10687] (acrylamide- bis solution (29:1) 30%)	Serva Electrophoresis, Heidelberg
-Ade/-His/-Leu/-Trp DO Supplement [10 g Cat. No. 630428]	Clontech, Otsu, Japan
Agar (agar-agar bacteriological) [Cat. No. 2266.3]	Carl-Roth, Karlsruhe
Agarose- electrophoresis grade [Cat. No. 15510-027]	Invitrogen, Paisley, UK
Ampiciline Na-salt [Cat. No. 13399]	Serva Electrophoresis, Heidelberg
APS (ammonium peroxodisulfate) [Cat. No. 09913]	Fluka, Steinheim
3-AT (3-amino-1,2,4-triazole) [Cat. No. A-8056-10G]	Sigma-Aldrich, St. Louis, MO
Bis-Tris Pufferan [Cat. No. 9140.2] (bis-(2-hydroxyethyl)-imino-tris(hydroxymethyl)-methan)	Carl-Roth, Karlsruhe
Boric acid (H_3BO_3) [Cat. No. 1.00165.5000]	Merck, Darmstadt
Bromephenole blue sodium salt [Cat. No. 32768]	Riedel-de Haen, Steinheim
BSA (albumin bovine fraction V) [Cat. No. 11930]	Serva Electrophoresis, Heidelberg
$CaCl_2$ (calcium chloride) [Cat. No.C-7902]	Sigma, Deisenhofen
CH_3COOH (acetic acid) Rotipuran [Cat. No. 37385]	Carl-Roth, Karlsruhe
Chloroform [Cat. No. 1.02431.1000]	Merck, Darmstadt
cOmplete Mini, [Cat. No. 04693159001] EDTA-free Protease Inhibitor Mix	Roche Diagnostics, Mannheim
Coomassie brilliant blue R250 [Cat. No. 21553]	Merck, Darmstadt
DABCO(1,4-diazabicyclo[2.2.2]octan) [Cat. No. D-2522]	Sigma, St.Louis, MO

Name	Manufacturer
DAPI (4',6-diamidino-2-phenylindole) [Cat. No. 6335.1]	Carl-Roth, Karlsruhe
DMF (N, N Dimethylformamide) Rotipuran [Cat. No. T921.1]	Carl-Roth, Karlsruhe
dNTP Mix (10mM total) [Cat. No. BIO-39044]	Bioline, Luckenwalde
DTT (dithiothreitol) [Cat. No. D-9779]	Sigma, St.Louis, MO
EDTA (ethylendiamine tetraacetic acid) [Cat. No. 8040.2]	Carl-Roth, Karlsruhe
1,2-Epoxypropane (propylene oxide) [Cat. No. 56671]	Carl-Roth, Karlsruhe
Ethanolamine [Cat. No. E-6133]	Sigma, St.Louis, MO
$EtOH_{den.}$ (ethanol 96% +MEK 1%) [Cat. No. T171.3]	Carl-Roth, Karlsruhe
EtOH (ethanol 96% EMPROVE exp.) [Cat. No. 1.00971.1000]	Merck, Darmstadt
Fluoroprep [Cat. No. REF-75521]	bioMerieux, Marcy l'Etoile, France
Glucose (α-D(+) glucose monohydrate) [Cat. No. 6887.1]	Carl-Roth, Karlsruhe
Glutaraldehyd 25% solution [Cat. No. 74157.1]	Carl-Roth, Karlsruhe
L-Gluthadione reduced [Cat. No. 6382.2]	Carl-Roth, Karlsruhe
Glycerol Rotipuran [Cat. No. 3783.1]	Carl-Roth, Karlsruhe
Glycid ether 100 [Cat. No. 8619.1]	Carl-Roth, Karlsruhe
Glycine [Cat. No. 3908.3]	Carl-Roth, Karlsruhe
Hardener DBA [Cat. No. 8623]	Carl-Roth, Karlsruhe
Hardener MNA [Cat. No. 8639]	Carl-Roth, Karlsruhe
HEPES Pufferan [Cat. No. 9105.2] (4-(2-hydroxyethyl)-1-piperazineethanesulfonic acid)	Carl-Roth, Karlsruhe
HCl 37% Rotipuran (hydrochloric acid) [Cat. No. 4625.2]	Carl-Roth, Karlsruhe
Herring sperm DNA 10mg/ml [Cat. No. D181B]	Promega, Madison, WI
IPTG (isopropyl-1-thio-ß-D-galactopyranoside) [Cat. No. CN08.2]	Carl-Roth, Karlsruhe
Isopropyl alcohol (2-propanol) Rotipuran [Cat. No.6752.3]	Carl-Roth, Karlsruhe
Kanamycine sulphate [Cat. No. T832.1]	Carl-Roth, Karlsruhe
KCH_3CO_2 (potassium acetate) [Cat. No. T874.1]	Carl-Roth, Karlsruhe
KCl (potassium chloride) [Cat. No. 6781.3]	Carl-Roth, Karlsruhe
KH_2PO_4 (potassium dihydrogen phosphate) [Cat. No. 3904.2]	Carl-Roth, Karlsruhe

Name	Manufacturer
Lead citrate (Lead(II) citrate tribasic trihydrate) [Cat. No. 15326-25G]	Sigma, St.Louis, MO
L-Leucine [Cat. No. L8000-25G]	Sigma, St.Louis, MO
-Leu/-Trp DO supplement (10g Cat No. 630417)	Clontech, Otsu, Japan
LiOAc (lithium acetate dehydrate) [Cat. No. 62395]	Fluka, Steinheim
β-mercaptoethanole (2-mercaptoethanole) [Cat. No. 4227.1]	Carl-Roth, Karlsruhe
MES Pufferan [Cat. No. 4256.2] (2-(N-morpholino)ethanesulfonic acid)	Carl-Roth, Karlsruhe
Methocel MC [Cat. No. M-64605-100G-F]	Sigma, St.Louis, MO
$MgCl_2$ (magnesium chloride hexahydrate) [Cat. No. A450933]	Merck, Darmstadt
$MgSO_4$ (magnesium sulfate) [Cat. No. 0261.2]	Carl-Roth, Karlsruhe
Milk powder- blotting grade [Cat. No. T145.3]	Carl-Roth, Karlsruhe
$MnCl_2$ (manganese(II) chloride) [Cat. No. T881.3]	Carl-Roth, Karlsruhe
MOPS (3-(N-morpholino) propanesulfonic acid) [Cat. No. M-1254]	Sigma, St.Louis, MO
NaCl (sodium chloride) [Cat. No. 1.06404.5000]	Merck, Darmstadt
Na-desoxycholat (sodium desoxycholat) [Cat. No. 685304]	Merck, Darmstadt
Na_2HPO_4 x $2H_2O$ [Cat. No. K11432680] (di-sodium hydrogenphosphate dihydrate)	Merck, Darmstadt
NaH_2PO_4 x H_2O [Cat. No. A983346807] (sodium dihydrogenphosphate monohydrate)	Merck, Darmstadt
NaN_3 (sodium azide) [Cat. No. K305.1]	Carl-Roth, Karlsruhe
NaOH (sodium hydroxide) [Cat. No. P031.2]	Carl-Roth, Karlsruhe
Na_2SO_4 (sodium sulphate) [Cat. No. 8560.3]	Carl-Roth, Karlsruhe
NH_4Cl (ammonium chloride) [Cat. No. P726.1]	Carl-Roth, Karlsruhe
$(NH_4)_2SO_4$ (ammonium sulphate) [Cat. No. 3746.1]	Carl-Roth, Karlsruhe
NP-40 (nonidet P-40) non-ionic detergent [Cat. No. N-6507]	Sigma, St.Louis, MO
Osmium tetroxide 4% solution [Cat. No. 8088.1]	Carl-Roth, Karlsruhe
PAA (phosphonoacetic acid) [Cat. No. 195425]	ICN-Biomedicals INC, Aurora, OH
PEG4000 (polyethylene glycol MW 4000) [Cat. No. 0156.1]	Carl-Roth, Karlsruhe

Name	Manufacturer
Peptone/Tryptone [Cat. No. 211705] (bacto-tryptone pancreatic digest of casein)	BD, Le Ponnt de Claix, France
PFA (paraformaldehyde) [Cat. No. 0335.2]	Carl-Roth, Karlsruhe
Phenole (Rotiphenol for separation of DNA/RNA) [Cat. No. 0038.2]	Carl-Roth, Karlsruhe
Ponceau S [Cat. No. 33429]	Serva, Boehringer Ingelheim Bioproducts, Heidelberg
RbCl (rubidium chloride) [Cat. No. 4471.1]	Carl-Roth, Karlsruhe
RedSafe [Cat. No. 21141] (nucleic acid staining solution)	Intron Biotechnology, INC. Gyeonggi-do, Korea
[^{35}S] methionine/cystein (10 mCi/ml) [Cat. No. IS103/074]	Hartmann Analytic, Braunschweig
SDS (sodium dodecyl sulfate) pellets [Cat. No. CN30.3]	Carl-Roth, Karlsruhe
Sodium tatrate (di-sodium tartrate dihydrate) [Cat. No.T110.1]	Carl-Roth, Karlsruhe
Sucrose [Cat. No. S-0389]	Sigma, St.Louis, MO
Tannin [Cat. No. 4239.1]	Carl-Roth, Karlsruhe
TCA (trichloro acidic acid) [Cat. No. 8074.0100]	Merck, Darmstadt
TEMED (N,N,N',N'-tetramethyl-ethane-1,2-diamine) [Cat. No. T-9281]	Sigma, St.Louis, MO
Tetracycline hydrochloride [Cat. No. A2228.0025]	AppliChem, Darmstadt
Tris Pufferan [Cat. No. 4955.3] (2-Amino-2-hydroxymethyl-propane-1,3-diol)	Carl-Roth, Karlsruhe
Triton X-100 detergent [Cat. No. 648466] (Polyethylene glycol mono [4-(1,1,3,3-tetramethylbutyl)phenyl] ether)	Calbiochem, La Jolla, CA
L-Tryptophan [Cat. No. T-0254-5G]	Sigma, St.Louis, MO
Tween-20 non ionic detergent [Cat. No. 9127.2] (Polyoxyethylene (20) sorbitan monolaurate)	Carl-Roth, Karlsruhe
Uranyl acetate dihydrate [Cat. No. 19481]	Ted Pella INC., Redding, CA
Yeast extract granulated [Cat. No. 2904.2]	Carl-Roth, Karlsruhe
Yeast nitrogen base without amino acids [Cat. No. HP26.1]	Carl-Roth, Karlsruhe
X-Gal [Cat. No. R0404] (5-bromo-4-chloro-3-indolyl- beta-D-galactopyranoside)	Fermentas, Mannheim

2.1.1.2 Consumables

Name	Manufacturer
Amicon Ultra centrifugal filters Ultracel 30K/50K	Millipore, Cork, Ireland
Amicon Ultra centrifugal filters Ultracel 0.5mL 30K/50K	Millipore, Cork, Ireland
Botteltop filter 500ml SFCA 0.45µm	Nalgene, Rochester, NY
Centrifuge tubes 1x 3 1/2 in. (25x89mm) for SW32Ti	Beckmann Coulter, Krefeld
Centrifuge tubes 7/16x 2 3/8 in. (11x60mm) for SW60Ti	Beckmann Coulter, Krefeld
Centrifuge tubes 9/16x 3 3/4 in. (14x95mm) for SW40	Beckmann Coulter, Krefeld
Cell culture dishes Falcon 6 well ($1x10^6$ cells per well); 12 well ($5x10^5$ cells per well); 24 well ($2x10^5$ cells per well); 96 well ($4x10^4$ cells per well)	BD, Heidelberg
Cell culture flasks Falcon 25 ml ($1x10^6$ cells); 75 ml ($1x10^7$ cells); 175 ml ($2x10^7$ cells)	BD, Heidelberg
Conical test tubes 17x120 (15ml)	Carl-Roth, Karlsruhe
Conical test tubes 30x115 (50ml)	Carl-Roth, Karlsruhe
Econo-Pac 10 disposable columns	BioRad Laboratories, Muenchen
Injekt 20ml luer solo syringe	Braun, Melsungen
Injekt-F 1ml luer solo syringe	Braun, Melsungen
Multiply® -Pro cup PCR tube 0.2ml PP	Sarstedt, Nuembrecht
Nitrocellulose membrane 0.2µm	Schleicher & Schuell BioScience GmbH, Dassel
Rotilab reaction tubes 1.5ml	Carl-Roth, Karlsruhe
Rotilab syringe filters PVDF 0.22µm	Carl-Roth, Karlsruhe
Rotilab syringe filters PVDF 0.45µm	Carl-Roth, Karlsruhe
Whatmann blotting paper (WM Whatmann 3MM)	GE Healthcare, Freiburg
Visking dialysis tube type 20/32	Carl-Roth, Karlsruhe

2.1.1.3 Equipment

Name	Manufacturer
Centrifuges	
Benchtop Centrifuge 3K20 Rotor: #12158 for 1x 3 1/2 in. (25x89mm)	Sigma Laborzentrifugen GmbH, Osterode
Eppendorf Centrifuge 5417R	Eppendorf, Wesseling-Berzdorf
Rotors: Fixed-angle rotor FA-45-30-11, Swing-bucket rotor A-8-11	
Function Line Labofuge 400 Rotor: Swinging bucket rotor #75008179	Heraeus, Osterode
Optima L-90K Ultracentrifuge Rotors: SW60Ti; SW40, SW32Ti	Beckmann Coulter, Krefeld
Sorvall RC24 Rotor: GSA	Thermo, Scientific, Dreieich
Chromatography	
Affi Gel® 10 Gel active ester agarose	BioRad Laboratories, Hercules, CA
Affi Gel® 15 Gel active ester agarose	BioRad Laboratories, Hercules, CA
ÄKTA FPLC system	GE Healthcare, Freiburg
(Elements: CU-950, Frac-920, INV-907, M-925, P-920, UPC-900)	
Deoxyribonucleic acid-cellulose (double stranded, from calf thymus DNA)	Sigma-Aldrich, St Louis, MO
Glutathione Sepharose 4B	GE Healthcare, Freiburg
GSTrap™ 1ml column	GE Healthcare, Freiburg
HiPrep 16/60 Sephacryl HR column	GE Healthcare, Freiburg
HiTrap™ Heparin HP column	GE Healthcare, Freiburg
Pierce Avidin Agarose	Thermo Scientific, Dreieich
Protein A Sepharose CL-4B	GE Healthcare, Freiburg
Resource Q™ 1ml column	GE Healthcare, Freiburg

Name	Manufacturer
Documentation	
Biometra BioDoc Analyse Ti5	Biometra Goettingen
CCD-Camera Fusion SL	Vilber Lourmat, Eberhardzell
Molecular Dynamics Phosphorimager SI	Amersham Pharmacia, Uppsala, Sweden
Generals	
Bronson sonifier II W-450	Heinemann, Schwaebisch Gmuend
Beaker resonator 101-147-046	Heinemann, Schwaebisch Gmuend
Consort EV243 Electrophoresis power supply	Carl-Roth, Karlsruhe
Horizontal electrophoresis system	university workshop, Erlangen
MC1 precision balance LC420	Satorius, Goettingen
Model 583 Gel Dryer	BioRad Laboratories, Muenchen
Sterile safety bench Antair BSK 4MP S/N 8261	Heraeus, Osterode
TE 70XP Semi-Dry Transfer Unit w/built-in Power Supply	Hoefer, San Francisco, CA
Thermocycler Primus 25 advanced	Peqlab, Erlangen
Vertical electrophoresis system	Kreutz Labortechnik, Reiskirchen
Vortex Genie 2	Scientific Industries, INC., Bohemia, NY
Microscopes and Equipment	
Axio-Observer.Z1 fluorescence microscope	Carl Zeiss MicroImaging GmbH, Jena
Eclipse A1 laser scanning microscope	Nikon Instruments, Tokyo, Japan
Olympus BX60 wide field	Olympus, Tokyo, Japan
TEM Tecnai^{TM} G2	FEI Company, Eindhoven
Turbo Carbon Coater 208	Cressington Scientific Instruments Ltd., Watford, UK
Ultracut S Ultra microtome	Leica Microsystems, Wetzlar

Name	Manufacturer
Pipetting	
Eppendorf Reference 1000	Eppendorf, Wesseling-Berzdorf
Eppendorf Reference 100	Eppendorf, Wesseling-Berzdorf
Eppendorf Research 10	Eppendorf, Wesseling-Berzdorf
Eppendorf Research 2.5	Eppendorf, Wesseling-Berzdorf
Pipetus®	Hirschmann Laborgeraete, Eberstadt
Spectrometers	
Nanodrop 1000	Peqlab, Erlangen
Ultraspec 4000 UV/Vis spectrometer	Pharmacia Biotech, Uppsala, Sweden
Software	
Axiovision 4.8 software for Zeiss microscopes	Carl Zeiss MicroImaging GmbH, Jena
Biometra BioDoc Analyse 2.1	Biometra, Goettingen
Cell D Imaging software for Olympus microscopes	Olympus, Tokyo, Japan
ImageJ 1.41o	NIH Bethesda, MD
Image Quant for Phosphorimager	Amersham Pharmacia, Uppsala Sweden
NIS-Elements software for Nikon microscopes	Nikon Instruments, Tokyo, Japan
Unicorn 5.1 for ÄKTA FPLC	GE Healtcare, Freiburg

2.1.2 Enzymes, Markers and Kits

Name	Manufacturer
Enzymes modifying DNA, RNA and proteins	
*BamH*I [Cat. No. ER0051]	Fermentas, Mannheim
*Bgl*II [Cat. No. ER0081]	Fermentas, Mannheim
DNase I from bovine pancreas [Cat. No. 11284932001]	Roche Diagnostics, Mannheim
*Dpn*I [Cat. No. ER1701]	Fermentas, Mannheim
*EcoR*I [Cat. No. ER0271]	Fermentas, Mannheim
Lysozyme 20 000 U/mg [Cat. No. 8259.3]	Carl-Roth, Karlsruhe
*Nde*I [Cat. No. ER0581]	Fermentas, Mannheim
*Not*I [Cat. No. ER0591]	Fermentas, Mannheim
peqGOLD *Pwo*-DNA-Polymerase [Cat. No. 01-5020]	Peqlab, Erlangen
PreScission Protease 500U [Cat. No. 27-0843-01]	GE Healtcare, Freiburg
RNase A 100mg [Cat. No. 740505]	Machery-Nagel, Dueren
T4 DNA Ligase 1000 units [Cat. No. EL0011]	Fermentas, Mannheim
Taq DNA-Polymerase (recombinant) 100 units [Cat. No.EP0401]	Fermentas, Mannheim
*Xba*I [Cat. No. ER0681]	Fermentas, Mannheim
DNA marker	
Generuler ^{TM} Low Range DNA Ladder [Cat. No. SM1911]	Fermentas, Mannheim
Generuler ^{TM} 1kb DNA Ladder [Cat. No. SM0311]	Fermentas, Mannheim
Protein marker	
PageRuler ^{TM} Prestained Protein Ladder [Cat. No. SM0671]	Fermentas, Mannheim
PageRuler ^{TM} Unstained Protein Ladder [Cat. No. SM0661]	Fermentas, Mannheim

Name	Manufacturer
Kits	
AEC-Staining Kit [Cat. No. AEC101]	Sigma-Aldrich, St. Louis, MO
ECL kit [Cat. No. 34075] SuperSignal West Dura Extended Duration Substrate	Thermo Scientific, Dreieich
NucleoSpin Extract II Kit [Cat. No. 740609.250]	Machery-Nagel, Dueren
GeneJET™ Plasmid Miniprep kit [Cat. No. K0503]	Fermentas, Mannheim
PureLink™ HiPure Plasmid Midiprep kit [Cat. No. K210014]	Invitrogen, Karlsruhe
TnT® T7 [Cat. No. L1170] Quick Coupled Transcription/Translation System	Promega, Mannheim
TurboFect™ in vitro Transfection Reagent [Cat. No. R0531]	Fermentas, Mannheim

2.1.3 Bacteria, cells and virus

	Features	reference
Bacteria (E. coli)		
BL21	B, F-, dcm, ompT, hsdS(r_B- m_B-), gal, [$malB^+$], $_{K-12}$(λ^S)	223, Stratagene
DH10Bac	endA1, gyrA96, hsdR17 (r_{k-}, m_{k+}), recA1, relA1, supE44 thi-1-,deoR (lacZYA-argF)-U169f80lac M15	Invitrogen
XL1-blue	endA1, gyrA96, hsdR17 (r_k-m_{K+}), lac, recA1, relA1, supE44, thi, (F´, $lacI^q$, lacZΔM15, $proAB^+$, tet)	Stratagene
Yeast (Saccharomyces cerevisiae)		
AH109	*MATa, his3-200, leu2-3/ 112, trp1-901, ura3-52*; *gal4*Δ, *gal80*Δ, *LYS2::GAL1UAS-GAL1TATA-HIS3; GAL2UAS-GAL2TATA-ADE2, URA3:: MEL1UAS-MEL1TATA-lacZ, MEL1*	Clontech
Y187	*MAT*α, *ade2-101, his3-200, leu2-3/ 112, trp1-901, ura3-52*, *gal4*Δ, *met–*, *gal80*Δ, *URA3*::*GAL1UAS -GAL1TATA-lacZ, MEL1*	Clontech
Insect cells		
High5	5B1-4, *Trichoplusia ni* embryonic cell line	Invitrogen
Sf9	*Spodoptera frugiperda* ovarian tissue cell line	Invitrogen
Mammalian cells		
Hela	human cervix carcinoma cell line	ATCC.CCL-2
HFF	Primary human foreskin fibroblast isolate passages 10-15	T. Stamminger , Uni. Erlangen
293T	Human Embryonic Kidney (*HEK*) epithelial cell line transformed by human adenovirus 5 + SV40 T-antigen	ATCC.CRL-11268, 177
Viruses (HCMV)		
AD169	Lab strain, additional 929 bp after nucleotide, 54612 causing frame shift effecting UL42, UL43	68, 196
recombinant BACs		
71_ΔLZ-BAC	pTBs-UL71del34-41_res (d3-24)	150, *
71_L1-BAC	pTBs-UL71L34A-L41A_res (I1-15)	150, *
71_wt-BAC	pTB4- *HCMV TB40E*-4 BAC (endotheliotropic)	215, *

***** Constructed in cooperation with Dr. Jens von Einem, University Hospital Ulm

2.1.4 Buffers and media

Buffers that are specific for certain procedures are directly indicated in the Methods section.

2.1.4.1 General buffers and solutions (9):

PBS (phosphate buffered saline)- 137mM NaCl, 2,7mM KCl, 8mM Na_2HPO_4 x 2 H_2O,

1.76mM KH_2PO_4; pH 7.4

TE (Tris-EDTA) Buffer- 10 mM Tris-HCl, 1mM EDTA; pH 8.0

Tris-HCl Buffer- Tris is adjusted with HCl to right pH (between 6.8 - 9.0)

Sodium phosphate buffer (3): e.g. 1L 20mM pH7.4: 19ml 0,2M Na_2HPO_4 x 2 H_2O +

81ml 0,2M NaH_2PO_4

2.1.4.2 Media and supplements for cultivation of bacteria (*E.coli*)

LB	Soc I
10g/L Peptone/Tryptone 5g/L Yeast extract 5g/L NaCl 15g/L Agar (plates) pH 7.5	20g/L Peptone/Tryptone 5g/L Yeast extract 0.5g/L NaCl pH 7.5 after autoclaving: 10mM $MgCl_2$ 2.5mM KCl 56mM Glucose

Used supplements

Antibiotic	working concentration	comment
Ampiciline	100µg/ml	in ddH_2O, -20°C
Gentamycine	7µg/ml	4°C
IPTG	40µg/ml	in ddH_2O, at -20°C
Kanamycine	50µg/ml	in ddH_2O, -20°C
Tetracycline	10µg/ml	in 70% EtOH, light protected, -20°C
X-Gal	100µg/ml	in DMF, light protected, -20°C

2.1.4.3 Media and supplements for cultivation of yeast

YPD	Minimal media
20g/L Peptone/Tryptone 10g/L Yeast extract 20g/L Agar (plates) 2% Glucose pH 6.5	6,7g /L Yeast nitrogen base without amino acids 20g/L Agar 2% Glucose 2.5mM 3-AT pH 5.8
-Leu selective media	-Trp- selective media
Minimal media +0.64 g/L-Leu/-Trp DO supplement +20µg/L L-Tryptophan	Minimal media +0.64 g/L-Leu/-Trp DO supplement +100mg/L L-Leucine
-Leu/-Trp selective media	-Leu/-Trp/-Ade/-His selective media
Minimal media +0.64 g/L-Leu/-Trp DO supplement	Minimal media +0.60 g/L -Ade/-His/-Leu/-Trp DO supplement

2.1.4.4 Media and supplements for cultivation of insect cells

Name	Manufacturer
FCS (fetal calf serum) (#CH 30 160.30)	Prebio Science, Bonn
Gentamycine sulphate 50mg/ml (#17-518 L)	Lonza, Basel, Switzerland
Grace's Insect Medium suppl. (#11605-045)	Gibco-BRL Life Technologies, Eggenstein

Sf9 or *High5* cells were grown in Grace's Insect Medium supplemented with 10% FCS and 50µg/ml Gentamycine sulphate.

2.1.4.5 Media and supplements for cultivation of mammalian cells

Name	Manufacturer
L-alanyl-L-glutamine (#K0302)	Biochrom AG, Lankwitz
FCS (fetal calf serum) (#CH 30 160.30)	Prebio Science, Bonn
Gentamycine sulphate 50mg/ml (#17-518 L)	Lonza, Basel, Switzerland
MEM (Minimum essential Medium Eagle) (#12-136F)	Lonza, Basel, Switzerland
NEAA (non essential amino acids) 100x (#K0293)	Biochrom AG, Lankwitz
OptiMEM I (1x) (#11058-021)	Lonza, Basel, Switzerland
PBS (Phosphate buffered saline) I(#17-512F)	Lonza, Basel, Switzerland
Sodium pyruvate 100x (#L0473)	Biochrom AG, Lankwitz
Trypsin/EDTA 0.25% pH 7,0 (#2500-056)	Gibco-BRL Life Technologies, Eggenstein

Growth medium for *HFF*, *293T*		Growth medium for *Hela*	
MEM	500ml	MEM	500ml
Supplements:		Supplements:	
Gentamycine sulphate 500µl		Gentamycine sulphate 500µl	
L-alanyl-L-glutamine	5ml	L-alanyl-L-glutamine	5ml
Sodium pyruvate	5ml	Sodium pyruvate	5ml
NEAA	5ml		

HFF, *Hela* or *293T* cells were grown in their appropriate media supplemented with 10% FCS. For infection and transfection FCS concentration was reduced to 2%, for transfection for BiFCs to 0.1%. Unsupplemented OptiMEM I was used to prepare transfection mixes.

Inhibitors of viral replication:

Phosphonoacetic acid (PAA) in PBS pH 7.3 (stock concentration 1mg/ml / working concentration 200µg/ml)

2.1.5 Plasmids

Plasmid	Features	Reference
bMON14272	Baculovirus shuttle vector, present in DH10Bac™ *E. coli*, Bacmid	Invitrogen
pcDNA-YC	C-term. YFP (YC) in pcDNA3.1+, for BiFC	J. von Einem
pcDNA3.1+	Mammalian expression vector T7prom, f1 ori,pBR322 ori, AmpR, pCMV, pSV40, NeoR.,	Invitrogen
pcDNA3.1-GFP	GFP in pcDNA3.1+ for assaying expression capacity of cells in BiFC	J. von Einem
pcDNA3.1-mcherry	mCherry in pcDNA3.1+ for assaying expression capacity of cells in BiFC	J. von Einem
pcDNA3.1/HisC	Mammalian expression vector T7prom, f1 ori, pBR322 ori , AmpR, pCMV, pSV40, NeoR., 6xHis, Xpress_EK	Invitrogen
pcDNA56	UL56wt in pcDNA3.1/HisC	E. Bogner
pcDNA71	UL71wt in pcDNA3.1/HisB	This study
pcDNA71_ΔLZ-YC	UL71 Δ34-55 + C-term. YC in pcDNA3.1+	This study
pcDNA71_L1-YC	UL71 L34/41A + C-term. YC in pcDNA3.1+	This study
pcDNA71_L2-YC	UL71 L34/41/55A + C-term. YC in pcDNA3.1+	This study
pcDNA71_L3-YC	UL71 L34/41/48/55A + C-term. YC in pcDNA3.1+	This study
pcDNA71_wt-YC	UL71wt + C-term. YFP (YC) in pcDNA3.1+	This study
pcDNA71_wt-YN	BiFC YN-construct UL71wt + N-term. YFP (YN) in pcDNA3.1+	J. von Einem
pcDNA71_ΔLZ-myc	UL71 Δ34-55 pHM1580	This study
pcDNA71_L1-myc	UL71 L34/41A in pHM1580	This study

pcDNA71_L2-myc	UL71 L34/41/55A in pHM1580	This study
pcDNA71_L3-myc	UL71 L34/41/48/55A in pHM1580	This study
pcDNA71-myc	UL71wt in pHM1580	E. Bogner
pcDNA77	UL77wt in pcDNA3.1 HisC	E. Bogner
pcDNA77-myc	UL77wt in pHM1580	E. Bogner
pcDNA89	UL89wt in pcDNA3.1 HisB	E. Bogner
pcDNA104	UL104wt in pcDNA3.1 HisB	E. Bogner
pcDNAMCP	UL86wt in pcDNA3.1 HisC	E. Bogner
pCM1029	Cosmid	85
pGADT-7	Gal-4 AD Vector for Yeast pBR322 ori, AmpR, 2µ ori, LEU2	57
pGAD56	UL56wt Gal4-AD construct for Y2H	This study
pGAD71	UL71wt Gal4-AD construct for Y2H	This study
pGAD77	UL77wt Gal4-AD construct for Y2H	This study
pGAD89	UL89wt Gal4-AD construct for Y2H	This study
pGAD104	UL104wt Gal4-AD construct for Y2H	This study
pGADMCP	UL86wt Gal4-AD construct for Y2H	This study
pGBKT-7	DNA-BD Vector for Yeast pBR322 ori, KanR, 2µ ori, TRP1	134
pGBD71	UL71wt DNA-BD construct for Y2H	This study
pGBD77	UL77wt DNA-BD construct for Y2H	This study

pGBD56	UL56wt DNA-BD construct for Y2H	This study
pGBD89	UL89wt DNA-BD construct for Y2H	This study
pGBD104	UL104wt DNA-BD construct for Y2H	This study
pGBDMCP	UL86wt DNA-BD construct for Y2H	This study
pFastBacHT B	Cloning vector for Baculovirus f1ori, pBR322ori, AmpR, PHprom, SV40 pA, Tn7-R, Tn7L GentR, 6x His, TEV_EK	Invitrogen
pFast71	UL71 in pFastBac HT B	This study
pGEX-6P-1	*E. coli* (*BL21*) expression vector ptac, pBR322 ori, lac I q, AmpR, GST, PreScission_EK	GE Healthcare
pGEX-UL71	UL71wt in pGex6p-1	E. Bogner
pGEX-UL77	UL77wt in pGex6p-1	E. Bogner
pHM123	IE1 in pcDNA3	183
pHM1580	Mammalian expression vector pcDNA3.1+, N-terminal Myc-tag	100
pUC-aseq	Herpesvirus a-sequence cloned into pUC18	199

2.1.6 Primers

The primers were designed with help of Gene Runner Version 3.01 (http://www.generunner.net) software and received by Invitrogen, Karlsruhe. DNA of cosmids (85) and plasmids indicated in the table above were used as template. Constructs were tested for accuracy by sequencing using vector and insert specific primers (LGC Genomics, Berlin).

Primer	Sequence
BiFC_YC_for	5′-CACCAGATCTGATATCGGTGGCGGTGGCTCTGGAGGTGGTGG GTCCTACCCATACGATGTTCCAGATTACG-3′
BiFC_YC_rev	5′-AGTGCGGCCGCGTTAACTTACTTGTACAGCTCGTCCATGCC-3′
BiFC_71_for	5′-TACGGGATCCATGCAGCTGGCCCAGCGC-3′
BiFC_71_rev	5′-TCAGGATCCCGCGGAGGACAGCAAGGCC-3′
MCP_GR_for	5′-CTGCATATGGCCATGGAGGCCGAATTCCCGGGGATGTTTGAG GCCTTACGCATCTA C-3′
MCP_GR_rev	5′-GGGTTATGCTAGTTATGCGGCCGCTGCAGGTCGACGCTCACG AGTTAAATAACATGGATTG-3′
MCP_Nde_for	5′-TACATATGTTTGAGGCCTTACGCATCTAC-3′
MCP_Eco_rev	5′-CAGAATTCCTCACGAGTTAAATAACATGGATTG-3′
UL56_Nde_for	5′-TACATATGGAGATGAATTTGTTACAGAAAC-3′
UL56_Eco_rev	5′-CAGAATTCTTAACGCAGACTACCAGGCA-3′
UL71_Eco_for	5′-TAGAATTCATGCAGCTGGCCCAGC-3′
UL71_Bam_rev	5′-CAGGATCCTCACGCGGAGGACAGC-3′
UL77_Nde_for	5′-TACATATGAGTCTGTTGCACACCTTTT-3′
UL77_Eco_rev	5′-CAGAATTCTTACAACACCGCCACGCT-3′
UL89_Nde_for	5′-TACATATGTTGCGCGGAGACTC-3′
UL89_Eco_rev	5′-CAGAATTCCTAGCTGACCCTGAAACGG-3′
UL104_Eco_for	5′-TAGAATTCATGGAGCGAAACCACTGGA-3′
UL104_Bam_rev	5′-CAGGATCCTAGTGAAATCCGTATGGACCT-3′
71_L1_QC_for	5′-GAGGACGTGGAGGCTCGCGAGCTGCAGGCGTTTGCTGACGA GAAC-3′
71_L1_QC_rev	5′-AGTTCTCGTCAGCAAACGCCTGCAGCTCGCGAGCCTCCTCGT CC-3′
71_L2_QC_for	5′-CTTTAAGCAGGCTGAGATCACCCCGGCCGACGCTCGAACCTT TTCTC-3′
71_L2_QC_rev	5′-CGAGAAAAGGTTCGAGCGTCGGCCGGGGTGATCTCAGCCTG CTTAAAG-3′

Primers	Sequence
71_Bam_for	5′-CGGGATCCATGCAGCTGGCCCAGC-3′
71_Xba_rev	5′-CATCTAGATCACGCGGAGGACAGC-3′
$71_{1\text{-}33}$_Bam_rev	5′-ACGGATCCCTCCACGTCCTCGCTAG-3′
$71_{56\text{-}361}$_BglII_for	5′-ACAGATCTACCTTTTCTCGCGACACG-3′
bio-250	5′-CGTGCACACAGCCCAGC-3′
bio-500	5′-CTACCAGCGGTGGTTTGTTTG-3′
bio-1000	5′-AATTAATAGACTGGATGGAGGCGG-3′
bio-pac1	5′ ATTTCACCCCCCCGCTAAAAACACCCCCCCGCCCAC-3′
pac1 rev	5′-GTGGGCGGGGGGGTGTTTTTAGCGGGGGGGTGAAAT-3′
pUC18-pac	5′-ATTTCACCCCCCCGCTAAAAACTCCGCCCCCCTGACGAG-3′

2.1.7 Used antibodies

Primary antibodies:

Primary antibodies for immunofluorescence (IF) were diluted in PBS only, whereas they were diluted in PBS + 0.1% Tween-20 +0.3% BSA +0.02% NaN_3 for immunostaining (WB), stored at 4°C and used multiple times.

Viral targets

Cytotect	Cytotect CP Biotest, a hyper immune serum against *HCMV*, 100E/ml (PZN-1469325; Biotest Pharma GmbH, Dreieich) For WB: [1:5000]
mAbgB	"CMV gB" (1-M-12) mouse mAb against pUL55 = gB (sc-52400; Santa Cruz Biotechnology, INC., Heidelberg) for IF: [1:75] /for WB: [1:400]
mAbIE1	mAb63-27 mouse mAb specific for IE1 (183) for IF: [conc.] / for WB: [conc.]/ for IP: [1:50]
mAbMCP	mAb28-4 mouse monoclonal antibody (mAb) specific for the major capsid protein (MCP) (53) for IF: [conc.] / for WB: [1:10]/ for IP: [1:50]
mAbpp28	"CMV pp28" (5C3) mouse mAb against pUL99 = pp28 (sc-56975; Santa Cruz Biotechnology, INC., Heidelberg) for IF: [1:75] / for WB: [1:250]
mAbpp150	(XP-1) mouse mAb against pp150 = UL32 (110) for IF: [1:10]
mAbUL44	"CMV pp52" (CH16) mouse mAb against pUL44 = pp52 (sc-69744; Santa Cruz Biotechnology, INC., Heidelberg) for IF: [1:50] / for WB: [1:400]
pAbUL56	affinity purified from *HCMV* positive patient Sera (31) for WB: F1 [conc.]/ for IP: F1 [1:50]
pAbUL71	affinity purified from *HCMV* positive patient Sera (this study) for IF: F1 [conc.]/ for WB: F1 [1:20]/ for IP: F1 [1:50]
pAbUL77	affinity purified from *HCMV* positive patient Sera (this study) for IF: F1 1:5/ for WB: F1 [1:10]/ for IP: [1:50]
pAbUL104	affinity purified from *HCMV* positive patient Sera (77) for WB: F3 [conc.] / for IP:F3 [1:50]

Cellular targets

mAbGM130 "purified mouse anti-GM130" against Golgi matrix protein GM130 (#610822; Becton, Dickinson and Company Transduction Laboratories, Franklin Lakes, NJ)
for IF: [1:75]

mAbp230 "purified mouse anti-Human p230 trans Golgi" against peripheral membrane protein associated with cytosolic face of TGN p230 (#611280; Becton, Dickinson and Company Transduction Laboratories, Franklin Lakes, NJ)
for IF: [1:75]

pAbβ-actin affinity purified rabbit sera against cellular filament protein β-actin (#600-401-886; Rockland, Gilbertsville, PA)
for WB: [1:5000]

Epitope-tags:

mAbGFP GFP (4B10) mouse mAb (#2955; Cell Signalling, Beverly MA)
for WB: [1:1000]

pAbHA HA Epitope-tag affinity purified rabbit sera against synthetic peptide (YPYDVPDYA); (#OPA-1-10980; ABR, Golden, CO)
for WB: [1:200]

mAbHis His-tag (27E8) mouse mAb against 6x-His (HHHHHH) (#2366; Cell Signalling, Beverly MA)
for WB: [1:1000]

mAbMyc_m Myc-tag (9B11) mouse mAb against c-Myc (EQKLISEEDL) (#2276; Cell Signalling, Beverly MA)
for WB: [1:1000]/ for IP: [1:500]

mAbMyc_r Myc-tag (71D10) rabbit mAb against c-Myc (EQKLISEEDL) (#2278; Cell Signalling, Beverly MA)
for WB: [1:1000]/ for IP: [1:200]

mAbXpress Anti-Xpress™ –tag mouse mAb against synthetic peptide (DLYDDDDK) (#R910-25; Invitrogen, Karlsruhe)
for WB: [1:1000]

Secondary Antibodies:

Secondary antibodies for immunofluorescence (IF) were diluted together with DAPI (1:10.000) in PBS whereas in PBS + 0.1% Tween-20 immunostaining (WB). Both were discarded after use.

anti-human^{green}	DyLight^{TM}488-conjugated AffiniPure F(ab')$_2$ Fragment Goat Anti-Human IgG, Amax=493nm; Emax=518nm (#109-486-006; Jackson Immuno Research Laboratories, INC.; Baltimore, MD) for IF: [1:250]
anti-human^{HRP}	Peroxidase-conjugated AffiniPure Goat Anti-Human IgG (H+L) (#109-035-003; Jackson Immuno Research Laboratories, INC., Baltimore, MD) for WB: [1:5000]
anti-human^{red}	Cy^{TM}3-conjugated AffiniPure F(ab')$_2$ Fragment Goat Anti-Human IgG Amax=550nm, Emax=570nm (#109-166-006; Jackson Immuno Research Laboratories, INC., Baltimore, MD) for IF: [1:300]
anti-mouse^{HRP}	Peroxidase-conjugated polyclonal Rabbit Anti-Mouse IgG's (#P0161; DakoCytomation, Glostrup, Denmark) for WB: [1:5000]
anti-mouse^{red}	DyLight^{TM}549-conjugated AffiniPure F(ab')$_2$ Fragment Goat Anti-Mouse IgG, Amax=555nm, Emax=568nm (#115-505-006; Jackson Immuno Research Laboratories, INC., Baltimore, MD) for IF: [1:350]
anti-rabbit^{HRP}	Stabilised Goat Anti-Rabbit HRP-Conjugated (#1858415, Perbio, Bonn) for WB: [1:1000]

2.2 Methods

2.2.1 Cultivation of bacteria (*E. coli* methods)

2.2.1.1 MOPS competent cells

With an overnight (o/n) culture of *E. coli* strains (*DH10Bac, BL21, XL1-blue*) 100ml LB medium were inoculated. Bacteria were incubated at 37°C until an OD_{600} of 0.6 was reached followed collection by centrifugation (5‘ at 1.000 x *g*, 4°C). The pellet was resuspended in 40ml ice cold MOPS I (100mM MOPS, 10mM $CaCl_2$, 10mM RbCl, pH 7.0) and incubated on ice for 10‘. Bacteria were centrifuged for 5‘ at 1.000 x *g,* 4°C and resuspended in 40ml ice cold MOPS II (100mM MOPS ,70mM $CaCl_2$, 10mM RbCl, pH 6.5). After incubation for 30’ on ice, bacteria were collected by centrifugation (5‘ at 1.000 x *g*, 4°C). The sediment was suspended in 2ml ice cold MOPS IIa (MOPS II + 15% glycerol) and incubated for 10’on ice. Afterwards aliquots of 100µl were taken. These were used immediately or stored at -80°C.

2.2.1.2 Transformation of MOPS competent cells

To competent cells 1 µl plasmid DNA or 15µl ligation mixture were added. Bacteria were incubated for 30’ on ice. Afterwards cells were treated 2’ at 42°C (heat shock), followed by a short incubation on ice. Bacteria were regenerated in 300µl LB (*XL1-blue*) or 1ml SOC I (*BL21*) medium for 30’ or 60’ at 37°C, respectively. Then 100µl batches were plated on LB plates with the corresponding antibiotics. The plates were incubated o/n at 37°C.

2.2.1.3 Overexpression of recombinant proteins in *E. coli* (*BL21*)

For over expression of GST-fusion proteins UL71-GST or UL77-GST, *BL21* were transformed with constructs pGEX-UL71 and pGEX-UL77, respectively as described above (2.2.1.2). A fresh overnight culture was grown in LB media supplemented with 100µg/ml ampiciline at 37°C. After an OD_{600} of 0.3 was reached the GST-protein expression was induced by addition of IPTG to a final concentration of 1mM and growth was continued for 2h at 37°C. Bacteria were harvested by centrifugation (10’ at 1.000 x *g*, 4°C) and sediments stored at -20°C until further usage.

2.2.2 Cultivation of yeast cells

Methods described in the following and for Y2H section (2.2.8.2.3) are modified from Sanderson et al. (10), Matchmaker™ GAL4 Two-Hybrid System 3 & Libraries User Manual 2007, Clontech (12) and Yeast Protocols Handbook 2008, Clontech (13).

2.2.2.1 Propagation and handling of yeast

To prepare yeast stains for transfection *AH109* and *Y187* were grown in YPD full media firstly on plates for 3 days and then in liquid media o/n at 30°C. It is very important to work with fresh cultures to avoid too thick cell walls that interfere with transfection efficiency.

2.2.2.2 Transfection of yeast

10ml YPD media was inoculated with fresh o/n culture of yeast strain *AH109* or *Y187*, respectively. Reaching an OD_{600} of 0.5 cells were harvested by centrifugation (5', 700 x g, RT). The sediment was resuspended in 5ml 100mM LiOAc and again centrifuged (5', 700 x g, RT). After this washing step, cells were well suspended in 230µl PEG 4000 followed by addition of 46µl dH_2O, 35µl 1M LiOAc and 9µl herring sperm DNA to the mixture. In contrast, for gap repair reaction instead of 46µl dH_2O, 45µl dH_2O and 1µl *BamH*I digested vector were added.

Mixture was split in 10x 32µl aliquots in PCR tubes and either 4µl constructs or PCR products were added. For pGADT-7 constructs mating strain MAT-a *AH109* whereas for pGBK-T Mat-α *Y187* was transfected.

After thoroughly mixing a Thermocycler was used for incubation for 30' at 30°C, followed by 25' at 42°C and finally 1' at 30°C, followed by plating pGADT-7 constructs (prey) on –Leu and pGBKT-7 (bait) on -Trp selective media plates, respectively. After growing for 3-5 days at 30°C, colonies should be visible that were further tested (i) to confirm insert size by colony PCR and (ii) for reactivation by plating them on selective plates lacking both marker amino acids leucine and tryptophan.

2.2.3 Cultivation of insect cells

2.2.3.1 Propagation and handling of insect cells

Two species of insect cells, *Sf9* for preparation of recombinant baculoviruses and *High5* for protein over-expression, were cultivated at 27°C in growth media.

2.2.3.2 Preparation of recombinant baculovirus

The gene of interest was inserted into Bacmid bMON14272 by site-specific transposition in *E.coli* prior to transfection into *Sf9* cells as described by Luckow et al. (135). Amounts of DNA, unsupplemented Grace's Insect Medium and Turbofect (Fermentas) are outlined in the manufacturer's protocol. After resuspending the mixture was incubated for 15' at room temperature (RT) and drop wisely added on top of the cells. Transfection mixture was changed after 5h into growth media. Virus in the supernatant was harvested 48h, sterile filtered (0.22µm) and stored at 4°C.

2.2.3.3 Baculovirus expression system

For harvesting recombinant baculovirus expressed protein, *High5* cells were infected with virus harvested above (2.2.3.2). Cells were washed with unsupplemented Grace's Insect Medium prior to infection. Medium was changed into growth media after 5h. Viruses in the supernatant as well as cells were harvested after 48h. Supernatant was sterile filtered (0.22µm) and stored at 4°C whereas cell extracts were subjected to protein purification (2.2.6.3.2).

2.2.4 Cultivation of mammalian cells

2.2.4.1 Propagation and handling of mammalian cells

All types of used adherent mammalian cells (*Hela, HFF, 293T*) were cultivated at 37°C and 5% CO_2 atmosphere.

Confluent monolayers were passaged after washing with PBS, detached with 0.25% trypsin-EDTA and taken up in total amount of 10ml growth media containing 10% FCS. After the effect of trypsin was reversed by FCS of the media, cells were either counted in a Neubauer counting chamber for seeding of distinct cell numbers for transfection or splitted 1:5 in growth media for further passaging.

2.2.4.2 Propagation and titration of virus

For *AD169* propagation 2 x 10^7 *HFF*s were infected at a low multiplicity of infection (MOI) of 0.1. Medium was changed after 50% cytopathic effect and virus in the media was harvested after 10-12 days.

Recombinant viruses *71_ΔLZ-BAC* and *71_L1-BAC*, *71_wt-BAC* were propagated similarly to *AD169* by infecting 2 x 10^7 *HFF* at a low MOI of 0.1. In contrast to previous method, infected cells were splitted before confluence for propagation. The virus in the media was harvested 21 days post infection (p.i.).

Cells and cell fragments were removed by centrifugation (5', 1.000 x *g*, 4 °C) and filtration (0.45µm), aliquoted and stored at –80°C.

Viral titres were determined by infection of confluent *HFF*s in 12 or 96 well dishes with logarithmic dilutions (10^{-2}-10^{-8}) following visualisation of infected cells by *HCMV* specific antibodies (mAbIE1) 24h p.i. Cells were fixed with cold EtOH: acetone for 30' at -20°C prior to multiple washing steps and antibody reactions. Infected cells were stained with AEC staining kit (Sigma), against anti-mouse^{HRP} and plaques counted under the microscope at different dilutions.

2.2.4.3 Experimental virus infection

Confluent monolayers of *HFF* were infected at MOI 1 to 3. Virus was applied in growth media without FCS and incubated for 2h at 37°C, 5% CO_2. After virus absorption supernatant was exchanged with growth media containing 2% FCS.

If expression of proteins at specific time points of infection is examined inhibitors of viral replication will be applied. In this study the chemical inhibitor PAA (2.1.4), a specific inhibitor of viral DNA-polymerase, was used. Inhibitor was added during infection and propagation in growth media.

2.2.4.4 Transient expression of viral proteins

Plasmid DNA was transfected into *Hela* and *293T* cells using Turbofect system (Fermentas) according to manufacturers' protocol.

Briefly, 4 x 10^4 *Hela* or 4 x 10^5 *293T* cells were seeded per 12 and 6 well, respectively. For biomolecular fluorescence complementation (BiFC) assays, *Hela* cells were grown in growth media supplemented with 0.1% FCS for all other purposes 2% FCS. After confluence of 70-90% was reached transfection was carried out. Amounts of DNA, Optimem I and Turbofect are outlined in "Turbofect™ in vitro Transfection" manual (Fermentas,

http://www.fermentas.com/templates/files/tiny_mce/coa_pdf/coa_r0531.pdf). After resuspending the mixture was incubated for 17' at RT and drop wisely added on top of the cells. Cells were harvested 14h (*Hela* for BiFC), 24h (*Hela*) or 48h (*293T*s) after transfection, respectively.

2.2.4.5 Harvesting cell extracts

Cell monolayers were washed with PBS prior to mechanical detachment. Harvested cells were collected by centrifugation (5', 1.000 x *g*, 4 °C) and sediments taken up in RIPA-Buffer (50mM Tris-HCl pH 7.5, 150mM NaCl, 1% NP-40, 0.5% Na-desoxycholate, 0.1% SDS) prior to ultrasonic treatment. Cell debris was removed by centrifugation (30', 10.000 x *g*, 4 °C) and cell extracts subjected to either co-immunoprecipitation (2.2.8.2.2) or directly to polyacrylamide gel electrophoresis (PAGE) (2.2.6.1) followed by immunostaining (2.2.7.3.).

All Buffers contained Protease Inhibitor mix cOmplete Mini (Roche) as instructed by the manufacturer.

2.2.4.6 Isolation and fragmentation of *HCMV* extracellular virions

Extracellular virions of *AD169* were separated from dense bodies and non-infectious particles 96h after infection by sedimentation through a sodium-tartrate gradient according to Talbot and Almeida (224). Isolated virions were incubated with non-ionic detergent (1% NP-40) for 10' on ice prior to separation through a 15% sucrose cushion in TE buffer (1h, 100.000 x *g*, 4°C). The supernatant contained the envelope fraction. The sediment which constituted of the capsid/tegument fraction was treated with 1% ß-mercaptoethanol for 10' on ice. Following this treatment, the capsid/tegument fraction was loaded onto another 15% sucrose cushion and separated by centrifugation (1h, 100.000 x *g*, 4°C). The supernatant contained the tegument and the sediment the capsid fraction. The tegument as well as the envelope fraction were precipitated with 10% TCA and dissolved in TE buffer. The capsid, tegument and envelope fraction as well as extracellular virions were subjected to SDS-PAGE (2.2.6.1.1) prior to immunostaining (2.2.7.3).

2.2.5 Cloning strategies and molecular biological methods

2.2.5.1 Plasmid constructions

Amplification of DNA fragments was carried out as described in 2.2.5.2.1.

Restriction enzymes as well as T4-DNA Ligase and recommended buffers were obtained from Fermentas and used as indicated in manufacturer's protocols and sections 2.2.5.2.2 or 2.2.5.2.3, respectively.

2.2.5.1.1 Constructs for bimolecular fluorescence complementation (BiFC)

The constructs for BiFC were designed in a two step amplification process; firstly the specific UL71 and the fluorophore parts were amplified independently, ligated and amplified as one piece prior to ligation into the appropriate vector pcDNA3.1+.

Briefly, for pcDNA71_wt-YC construct pcDNA71-myc served as a template for PCR using the primers BiFC_71_for and BiFC_71_rev resulting in PCR-71. For amplification of the C-terminal part of the fused fluorophore YFP (YC) pcDNA-YC served as a template and BiFC_YC_for and BiFC_YC_rev as primers resulting in PCR-YC. Both PCR fragments were digested with restriction endonucleases, PCR-71 with *BamH*I and PCR-YC with *Bgl*II and because of the similar restriction sites ligated together resulting in disruption of the site. The ligated fragment was amplified using primers BiFC_71_for and BiFC_YC_rev resulting in PCR-71-YC. The resulting fragment as well as the cloning plasmid pcDNA3.1+ was digested with restriction endonucleases *BamH*I and *Not*I, ligated together and transformed into *XL1-blue* as described previously.

Constructs pcDNA71_ΔLZ-YC, pcDNA71_L1-YC, pcDNA71_L2-YC and pcDNA71_L3-YC were constructed in the same manner using pcDNA71_ΔLZ-myc, pcDNA71_L1-myc, pcDNA71_L2-myc and pcDNA71_L3-myc as templates for PCR-71.

2.2.5.1.2 Constructs for co-immunoprecipitation

Constructs used for elucidating oligomerisation ability of pUL71 using co-immunoprecipitation are discussed in the following. The wild type construct with the Myc-tag pcDNA71-myc was already in the lab's collection whereas the Xpress-tagged version pcDNA71 needed to be constructed in this study. For PCR pcDNA71-myc served as template and 71_Bam_for and 71_Xba_rev served as primers for amplification. The product as well as cloning vector pcDNA3.1/HisC was subjected to restriction using *BamH*I and *Xba*I, followed by ligation and transformed into *XL1-blue*.

For construction of Leucine zipper-like motif deletion mutant 71_ΔLZ-myc a two step amplification protocol similar as for BiFC constructs was used to remove aa 34-55 of UL71. As a first step aa 1-33 were amplified using pcDNA71-myc as template and 71_Bam_for and 71_{1-33}_Bam_rev as primers resulting in PCR_{1-33} whereas aa 56-361 using 71_{56-361}_BglII_for and 71_Xba_rev resulting in PCR_{56-361}. Both PCR fragments were cut with restriction endonucleases, PCR_{1-33} with *BamH*I and PCR_{56-361} with *Bgl*II and because of the similar restriction sites ligated together resulting in disruption of the site. The resulting fragment was amplified using primers 71_Bam_for and 71_Xba_rev. The product as well as cloning vector pcDNA3.1/His C was subjected to endonuclease digestion using *BamH*I and *Xba*I, followed by ligation and transformed into *XL1-blue*.

The point mutations in the Leucine zipper motif were constructed using a two step Quick change site-directed mutagenesis protocol modified from Stratagene. In the first mutagenesis round aa 34 and 41 were exchanged from Leucines (L) to Alanine (A) resulting in no alteration of the coiled-coil structure but in hydrophobicity of the motif. As for the other constructs pcDNA71-myc served as the template for amplification using primers 71_L1_QC_for and 71_L1_QC_rev, prior to digest of template using *Dpn*I and transformation into *XL1-blue* resulting in pcDNA71_L1-myc (L34/41A). To mutate aa 48 and 55 in the same manner another round of Quick Change mutagenesis was performed using pcDNA71_L1-myc as template and primers 71_L2_QC_for and 71_L2_QC_rev proceeding as described above. The second mutagenesis resulted in two constructs identified by sequencing, pcDNA71_L2-myc (L34/41/55A) and pcDNA71_L3-myc (L34/41/48/55A).

2.2.5.1.3 Constructs for protein purification using baculovirus system

To construct a recombinant baculovirus expressing the gene of interest pUL71 the Bac-To-Bac system (Invitrogen) was used according to manufactures protocol. Firstly UL71 needed to be cloned into Vector pFastBacHT B carrying the sequences later on needed for site recombination by site-specific transposition. In the first step UL71 was amplified from cosmid pCM1029 using primers UL71_Eco_for and UL71_Bam_rev prior to digesting both vector and insert with *BamH*I and *EcoR*I, ligation and transfection into *XL1-blue*. The accurate construct was transfected into *DH10Bac*, an *E.coli* strain carrying the baculovirus genome in the bacmid *bMON14272*, where site-specific recombination took place *in vivo*. The bacmid was extracted from the cells using methods described in the following (2.2.5.2.5.1).

2.2.5.1.4 Constructs for yeast two hybrid assay (Y2H)

To construct a viral gene library, genes important for DNA packaging and egress discussed in this study were cloned into bait and prey vectors pGBKT-7 and pGADT-7 using same PCR products, respectively.

For construction of UL56 yeast vectors, amplification from pcDNA56 using primers UL56_Nde_for and UL56_Eco_rev was performed. The insert as well as both vectors pGBKT-7 and pGADT-7 were subjected to restriction using endonucleases *Nde*I and *EcoR*I, resulting in pGBD56 and pGAD56, respectively.

The other constructs were designed in the same manner e.g. using primers UL71_Eco_for and UL71_Bam_rev and cosmid pCM1029 resulting in pGBD71 and pGAD71, respectively. Constructs pGBD77 and pGAD77 were constructed using primers UL77_Nde_for and UL77_Eco_rev and pcDNA77; further pGBD89 and pGAD89 were constructed using primers UL89_Nde_for and UL89_Bam_rev and pcDNA89; pGBD104 and pGAD104 were constructed using primers UL104_Eco_for and UL104_Bam_rev and pcDNA104 and finally pGADMCP was constructed using template pcDNAMCP and primers MCP_Nde_for and MCP_Eco_rev. The corresponding restriction endonucleases indicated in the primer names were subjected for digestion of insert and vector prior to ligation as described previously. For pGBD71 and pGAD71 that are *EcoR*I and *BamH*I, for pGBD77 and pGAD77 *Nde*I and *EcoR*I, for pGBD89 and pGAD89 *Nde*I and *BamH*I, for pGBD104 and pGAD104 *BamH*I and *EcoR*I and for pGADMCP *Nde*I and *EcoR*I, respectively.

It was not possible to clone pGBDMCP using conventional methods therefore the yeast based gap repair was used amplifying MCP from pcDNAMCP using primers MCP_GR_for and MCP_GR_rev encoding motifs for site specific recombination in yeast. In the following, PCR product was transfected together with *BamH*I linearised pGBKT-7 and site specific recombination took place in yeast strain *Y187*.

2.2.5.2 Molecular biological methods

2.2.5.2.1 Polymerase chain reaction (PCR)

This method was used in the following for amplification of certain DNA fragments later on used for cloning, identification of proper constructs or recombination reactions of the cells.

Batches were completed according to the manufacturers' protocols: 100µl reaction batch for preparative usage contained 10 – 15ng DNA template, 500ng of each primer, 20nmol dNTPs and 2 units of DNA polymerase plus associated buffers. Half the batch was used for PCRs preformed for analytical purpose. Concerning temperature program double strand melting

took place at 95°C. Temperature for following annealing process was dependent on used primers (5°C below melting point of the primer) and elongation process was dependent on the used polymerase in terms of temperature and on length of DNA fragment in terms of time. This cycle was repeated until an optimum in accuracy and amount was obtained. PCRs were performed using a Thermocycler.

Either PWO-DNA-Polymerase with proof reading activity (Peqlab) at 72°C or Taq-DNA-Polymerase (Fermentas) at 68°C elongation temperature were used.

2.2.5.2.2 Restriction of DNA

Restriction enzymes from Fermentas were used indicated in the 2.2.5.1 as referred by manufacturer's protocol. Briefly, 1 unit of endonuclease in its supplied reaction buffer was incubated with 0.5µg DNA for 3h at 37°C for digestion. Double digests were performed as calculated by the Double Digest™ software from Fermentas (http://fermentas.com/en/tools/doubledigest/).

2.2.5.2.3 Ligation of DNA

For ligation, fragment and vector DNA were set in a ratio of 1: 4. T4 DNA Ligase (Fermentas) and associated buffer were added. The reaction batch was incubated 3h at RT or o/n at 16°C.

2.2.5.2.4 Purification of PCR- and DNA-fragments after Restriction

The DNA was purified using spin columns from Machery-Nagel following manufacturer's protocol.

2.2.5.2.5 DNA purification

The procedures discussed in the following were performed with strain of *E. coli*.

Plasmids were purified from growing cultures. The used methods are depended on form and size of plasmid and which grade of purity is needed for later on performed procedures, respectively.

2.2.5.2.5.1 Preparation of bacmid DNA

Colonies positive for insertion of gene of interest into *bMON14272* in *DH10Bac* were tested (i) for destruction of LacZ operon and therefore missing β-galactosidase activity on LB plates containing 50µg/ml kanamycine, 100µg/ml X-Gal, 40µg/ml IPTG, 7µg/ml gentamycin, 5µg/ml tetracycline and (ii) by PCR using specific primers. 1.5ml of culture was collected by centrifugation. Pellet was resuspended in 0.3ml Solution I (25mM Tris-HCl pH 8.0, 50mM glucose, 10mM EDTA), prior to addition of 0.3ml Solution II (1% SDS, 0.2M NaOH) and gentle mixing. After incubation at RT until suspension became almost translucent, 0.3ml 3M

KCH_3CO_2 pH 5.5 were added and incubated for 10' on ice. Precipitate was sedimented by centrifugation (10' 14.000 x *g*, RT) and supernatant was added to 0.8ml isopropyl alcohol. Bacmid DNA was precipitated by incubation o/n at -20°C followed by centrifugation step (10' 14.000xg, RT). DNA pellet was washed twice with 70% EtOH, dried at RT, suspended in 40µl TE buffer and stored at 4°C.

2.2.5.2.5.2 Preparation of plasmids using kits

DNA used for cloning in *E.coli* was purified with Plasmid Miniprep kit (Fermentas), whereas for large amounts of transfection grade pure DNA Midiprep kit (Invitrogen) was used both according to manufacturers' protocols. Briefly, pellets were collected and subjected to alkaline lysis (9). Firstly pellets were resuspended in 25mM Tris-HCl (pH 8.0)/ 50mM glucose/ 10 mM EDTA), for lysis 1% SDS/ 0.2M NaOH were added and vigorously mixed prior to precipitation of cell debris by addition of 5M KCH_3O_2 (pH 4.8) and again vigorous mixing. The cell debris was removed by centrifugation (10', 10 000 x *g*, RT) and supernatant was applied to columns purchased from Fermentas and Invitrogen. Plasmid DNA was bound to the columns, washed and eluted prior to precipitation with 96% isopropyl alcohol (30', 15 000 x *g*, 4°C).

2.2.5.2.5.3 Quick preparation method

Bacteria (300µl) were collected and resuspended in 5 x DNA sample buffer (25% sucrose, 0.05% bromphenole blue, 0.1% SDS, 50mM Tris-HCl, pH 8.2). To precipitate proteins phenol/chloroform (1:1) were added. The sample was mixed by vortexing followed by centrifugation to pellet debris. This method will be used for crude purification to screen for positive clones if no other manipulations are performed with the plasmid afterwards.

2.2.5.2.6 Separation of DNA fragments according to their size

DNA purified after PCR or enzymatic manipulations (2.2.5.2.4) as well as plasmids (2.2.5.2.5) were analysed using the following methods.

2.2.5.2.6.1 Agarose gel electrophoresis

Agarose 1% was melted in 1 x TBE (89mM Tris, 89mM boric acid, 2mM EDTA, pH 8.0) in the microwave until the solution became clear. For DNA staining 50µl/L RedSafe (Intron Biotechnology INC.) were added afterwards. Samples were taken up in 5 x DNA sample buffer and loaded onto gel. Electrophoresis was carried out at 100V in a horizontal system.

2.2.5.2.6.2 Polyacrylamide electrophoresis

Acrylamide stock was diluted with 1 x TBE till desired percentage. Polymerisation was induced by addition of APS and TEMED. Sample preparation was done corresponding to 2.2.5.2.6.1.Further separation was carried out in a vertical system at 70V. The DNA was stained in an ethidium bromide (0.5g/L) solution. This method using 8.5% polyacrylamide was used for separating bands in a range from 30-1000bp.

2.2.5.2.7 Determination of DNA concentration

DNA amount was determined by spectroscopic measurements at 260 nm using Nanodrop (Peqlab) or quantification of gel bands after separation (2.2.5.2.6) using image processing software ImageJ 1.41o (National Institute of Health, USA).

2.2.5.2.8 *In vitro* translation.

The plasmids pcDNAUL77, pcDNAUL56 or pcDNAMCP (1µg each) were incubated with [^{35}S] methionine/cystein (10mCi/ml) and 40µl TNT® T7 Quick Master Mix (TNT-T7 Quick kit, Promega) in a final volume of 50µl for 1.5h at 30°C. Translation products were analysed by SDS-PAGE (2.2.6.1.1) or subjected to Protein-DNA-Interaction studies (2.2.8.1).

2.2.6 Protein methods

2.2.6.1 Polyacrylamide gel electrophoresis (PAGE)

Used for protein separation according to molecular weight followed by visualisation through Coomassie (2.2.6.2) or immunostaining (2.2.7.3).

2.2.6.1.1 SDS-PAGE (126)

Composition	resolving gel 8.5-10%	stacking gel 4%
Acrylamide stock	1417-1667µl	267µl
1.5M Tris-HCl, pH 8.8 0.4% SDS	1250µl	-
0.5M Tris-HCl, pH 6.8 0.4% SDS	-	500µl
ddH_2O	xµl	1233µl
total volume	5000µl	2000µl
10% APS	60µl	20µl
TEMED	10µl	5µl

10-30µl Protein samples were added per slot. SDS running buffer (10 x: 250mM Tris, 1,9M glycine, 35mM SDS) was used for separation in a vertical system. Electrophoresis was with constant 15mA per gel.

2.2.6.1.2 NATIVE-PAGE

Composition	resolving gel 8.5-10%	stacking gel 4%
Acrylamide stock	1417-1667µl	267µl
1.5M Tris-HCl, pH 8.8	1250µl	-
0.5M Tris-HCl, pH 6.8	-	500µl
ddH_2O	xµl	1233µl
total volume	5000µl	2000µl
10% APS	60µl	20µl
TEMED	10µl	5µl

Native running buffer (10 x: 250mM Tris, 1.9M glycine) was used for separation in a vertical system. Electrophoresis conditions were used similar to SDS-PAGE (2.2.6.1.1)

2.2.6.1.3 Electrophoresis conditions

Standard SDS-PAGE under denaturating conditions was performed as described by Laemmli et al. using SDS- loading buffer (2 x buffer: 0.12mM Tris-HCl pH 6.8, 4% SDS, 17.4% glycerol, 2% β-mercaptoethanol, 0.02% bromphenole blue) with boiling for 5' at 95°C prior to loading onto SDS-polyacrylamide gels (126). For SDS-PAGE under non reducing conditions (209) samples are taken up in native- loading buffer (2 x buffer: 0.12mM Tris-HCl pH6.8, 0.1% SDS, 17.4% glycerol, 0.02 % bromphenole blue) and subjected to SDS-polyacrylamide gels without boiling. While for NATIVE-PAGE samples were taken up in native- loading buffer and directly loaded on native polyacrylamide gel.

2.2.6.2 Coomassie staining

To visualise separated proteins on the polyacrylamide gels Coomassie staining was used. Gels were incubated in Coomassie staining solution (45% $EtOH_{den.}$, 9% CH_3COOH, 0,1% Coomassie Brilliant Blue R250) until complete staining. The destaining was carried out in two steps; incubation with 45% $EtOH_{den.}$/ 12% CH_3COOH for 30' followed by complete destaining with 5% $EtOH_{den.}$/ 5% CH_3COOH. After neutralizing in H_2O gels were dried in a frame between wet cellophane sheets.

2.2.6.3 Purification of recombinantly expressed proteins

2.2.6.3.1 Purification of GST-proteins for column affinity chromatography

Protein production was induced in *BL21* as described above (2.2.1.3). Sedimented cells were lysed in binding buffer (20mM sodium phosphate buffer pH 7.4, 0.15M NaCl) containing 250µM $MgCl_2$, 25µM $MnCl_2$, 400µg DNase I and 4mg lysozyme, incubated for 30' and sonicated on ice. Undissolved material was removed by centrifugation at 5.000 x *g* at 4°C and supernatant passed through a 0.22µm filter.

The purification was performed with ÄKTA FPLC system (GE Healthcare) using a GSTrap™ 1ml column (GE Healthcare). The column was washed with three bed volumes binding buffer prior to loading the proteins. Proteins were eluted from the column with 10 bed volumes of elution buffer (50mM Tris-HCl, 10mM glutathione, pH 8.0).

For usage as antigen in antibody purification GST-tag needs to be removed. For cleavage, eluted protein was dialysed in PreScission buffer (50mM Tris-HCl pH 7.0, 150mM NaCl, 1mM EDTA, 1mM DTT) and incubated with 80 units of PreScission protease (GE Healthcare) for 12 h at 4°C. After removal of the GST-tag fraction was supplied to Glutathione Sepharose 4B slurry (GE Healthcare) for 16 h at 4°C to bind free GST and

uncleaved fusion protein. Supernatant containing the proteins rpUL71_E.coli or rpUL77_E.coli were stored at –80 °C.

2.2.6.3.2 Purification of rpUL71_Bac

Using the baculovirus expression system (2.2.3.3) intracellular protein from 3.6 x 10^8 *High5* cells was harvested 48h p.i.. Sedimented cells were lysed in anionic exchange buffer (20mM Bis-Tris, 200mM NaCl, pH 6.5) containing 250µM $MgCl_2$, 200µg DNase I, 200µg RNAse A and 2.5mM sucrose by sonification on ice. Undissolved material was removed by centrifugation (30', 10.000 x *g*, 4°C).

Further as a first purification step supernatant was precipitated with 45% $(NH_4)_2SO_4$ and sediment collected by centrifugation (30', 10.000 x *g*, 4°C). The pellet was taken up in anionic exchange buffer and dialysed against the very same to remove the salt. Secondly, further purification was performed with ÄKTA FPLC system using a Resource Q™ 1ml column (GE Healthcare). The column was washed with three bed volumes anionic exchange buffer prior to loading the proteins. A continuous NaCl gradient (0.2-1M NaCl) was used to elute protein from the column. Again salt was removed by dialysis against anionic exchange buffer. Thirdly, fractions were subjected to gel filtration with a HiPrep 16/60 Sephacryl HR column (GE Healthcare) using ÄKTA FPLC. After equilibration of the column with three bed volumes anionic exchange buffer, the pooled fractions from the previous step were loaded. Forty fractions were collected.

All fractions were analysed by SDS-PAGE (2.2.6.1.1) followed by Coomassie (2.2.6.2) or immunostaining (2.2.7.3) throughout the whole purification procedure.

2.2.7 Immunological Methods

2.2.7.1 Antibody against pUL71 and pUL77

2.2.7.1.1 Synthesising matrix for column affinity chromatography

Purified recombinant protein rpUL71_E.coli or rpUL77_E.coli (see 2.2.6.3.1) was covalently coupled to agarose matrix that was later used for column affinity chromatography to purify specific IgG's from patients' sera.

As a first step protein used as an antigen was dialysed in coupling buffer (0.1M MES pH 6.5, 0.02% NaN_3) for 16h at 4°C. To prepare the matrix 1 Vol. Affi Gel 10 and 2 Vol. Affi Gel 15 (BioRad) were washed with ddH_2O and coupling buffer prior to incubation with antigen for 16h at 4°C. The matrix is collected by centrifugation (15', 2.100 x g, 4°C) and blocked with 1M Ethanolamin-HCl pH 8.0/ 0.02 % NaN_3 for 1h. Further washing with ddH_2O and starting buffer (50mM Tris pH 8.0, 150mM NaCl, 0.02% NaN_3) was performed prior to loading of sera from high titre *HCMV* patients.

2.2.7.1.2 Affinity purified antibodies

HCMV pUL71 specific human polyclonal antibody pAbUL71 or *HCMV* pUL77 specific human polyclonal antibody pAbUL77 were purified from *HCMV* positive patients sera (IgG positive selected by *HCMV* diagnostics, Charité Berlin) by column affinity chromatography. Affinity purification was performed as described previously (77).

Briefly, Sera were diluted 1:4 in starting buffer and incubated with matrix in disposable columns (Econo-Pac 10, BioRad) for 16h at 4°C. After incubation matrix was washed in washing buffer (50mM Tris-HCl pH 8.0, 300mM NaCl, 0.02% NaN_3), in order to remove all unspecific interactions.

Further elution was carried out with acidic elution buffer (0.2M glycine-HCl pH 2.8). The fractions were neutralised with 2.5M Tris-HCl pH 8.0 immediately after collecting. In this manner three fractions were collected. The specificity of the purified fractions was determined using immunoblots loaded with purified rpUL71 or rpUL77, respectively. Immunoblot strips were reacted with Cytotect (Biotest), mAbUL44 and pAbUL71 or pAbUL77, respectively.

2.2.7.2 Immunofluorescence

For immunofluorescence *HFF* cells were grown on cover slips (1 x 10^5). At the appropriate time point cells were fixed with 3% PFA for 20', incubated with 50mM NH_4Cl to block reactive amino groups and permeabilised with 0.2% Triton X-100 for 5'. Detection of specific viral or cellular proteins was carried out using primary antibodies for 45' at RT prior to further incubation for 45' with fluorophore-labelled secondary antibodies (see 2.1.7). Nuclei were

stained using DAPI added to secondary antibody mixture. After staining the samples were mounted in Fluoroprep (bioMerieux) with 2.5% DABCO and examined either under an Olympus BX60 wide field or a Nikon Eclipse A1 laser scanning microscope.

2.2.7.3 Immunostaining following PAGE

2.2.7.3.1 Semi-Dry transfer

All proteins separated on the gel were immobilised onto a nitrocellulose membrane (NC) by electro blotting: Firstly, all materials- Whatmann blotting paper (WM), polyacrylamide gel (gel) and NC- were soaked in blotting buffer (25mM Tris, 200mM glycine, 20% $EtOH_{den.}$).The blot was assembled between the electrodes (-/WM /gel/NC/ WM /+) and transfer was performed in a semi dry blot apparatus under following conditions: 0,8mA/cm^2 blotting area for 60'. The efficiency of protein transfer was analysed by staining NC with a Ponceau S solution (0.5% Ponceau S, 3% TCA).

2.2.7.3.2 Antibody probing

After transfer, NC was blocked with 5% milk powder in PBS/ 0.1% Tween20, 30' at RT or o/n at 4°C. After the blocking, the blot was washed with PBS/ 0.1% Tween20 and probed with the dilution of the primary antibody for 1h at RT or o/n at 4°C. Afterwards, the membrane was washed and incubated with the secondary antibody linked to HRP for 1h. After another washing step the blot was developed using enhanced chemo luminescence (ECL) kit (ECL kit Super Signal, Thermo Scientific) according to the manufacturer and analysed by charge coupled device (CCD) Camera (Vilber-Lourmant).

2.2.7.3.3 Stripping of immunoblots

To remove antibody probing from the immunoblot incubation in stripping buffer (62.5mM Tris-HCl pH 6.8, 2% SDS, 0.7% β-mercaptoethanol) for 30' at 60°C was carried out. The stripping buffer was removed by multiple washing steps in PBS/ 0.1% Tween20 and blocking in 5% milk powder in PBS/ 0.1% Tween20 for 1h at RT. After this procedure the blot could be reused for antibody probing (2.2.7.3.2)

2.2.8 Protein interaction studies

2.2.8.1 Protein-DNA-interactions

2.2.8.1.1 DNA binding assay

In vitro DNA binding analysis was performed as described before (77). Briefly, DNA - cellulose (Sigma-Aldrich) or matrix material from HiTrap™ Heparin HP Columns (GE Healthcare) was loaded with [^{35}S]-labelled pUL77 or MCP diluted 1:10 in DNA binding buffer (50mM Tris-HCl, 10% glycerol, 1mM DTT, 1mM EDTA, pH 8.0). Bound protein was eluted with increasing concentrations of NaCl (200 - 2000mM NaCl gradient). Fractions were subjected to SDS-PAGE (2.2.6.1.1) prior to autoradiography. Radioactive signals were analysed using a Bioimager (Molecular Dynamics Phosphorimager SI, Amersham Pharmacia) and quantified with image processing software ImageJ 1.41o (National Institute of Health, USA).

2.2.8.1.2 Binding to defined double stranded (ds) oligonucleotides.

This assay is modified from the DNA Binding assay described above.

50µl Pierce Avidin Agarose (Thermo Scientific) was equilibrated in DB-buffer (PBS +1% NP-40) for 2h at room temperature. In the following, biotinylated and their complementary oligonucleotides (bio-pac1/pac1_rev) were purified (2.2.5.2.4), combined, denatured and annealed (Figure 3. A**)** for yielding the double stranded 36-mer oligonucleotides bio-pac1. Briefly, denaturating (5' 95°C) and annealing (temperature gradient 80-55°C, 2h) was carried out using a Thermocycler. In addition, a 250-, 500- and 1000-mer biotinylated DNA fragment containing pac1 motif were obtained by PCR using pUC-aseq as a template and either bio-250, bio-500 or bio-1000 together with pUC18-pac as forward and reverse primers (Figure 3. B).

A schematically drawing of the method is depicted in Figure 3.C. Briefly, the biotinylated double-stranded oligonucleotides were bound to the avidin agarose upon incubation for 30' at RT. For removing excess unbound oligonucleotides avidin agarose was washed twice with DB-buffer. The avidin agarose was taken up in 100µl DB-buffer, 20µl of *in vitro* translated protein pUL77, pUL56 or MCP (2.2.5.2.8) were added and incubated o/n at 4°C. After additional washing (50mM Tris-HCl, pH 8.8, 10% glycerol, 1mM DTT, 1mM EDTA, 150mM NaCl) bound DNA-protein complexes were eluted by a NaCl gradient (200-2000mM NaCl) prior to boiling in SDS- loading buffer and analysis by SDS-PAGE followed by autoradiography (see 2.2.8.1.1).

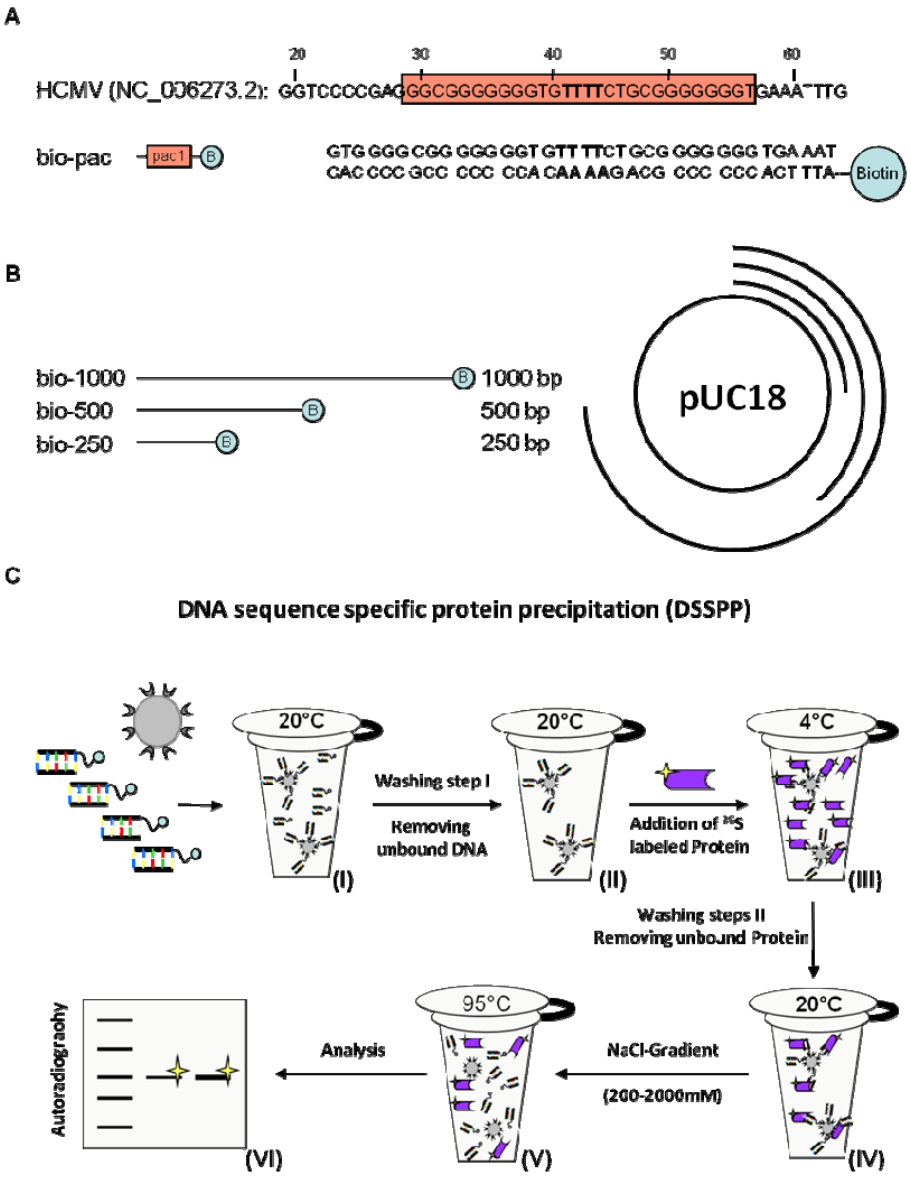

Figure 3: Binding to defined dsDNA. (A) Nucleotide composition of 36-mer bio-pac containing pac1 sequence localised between bp 30-58 in *HCMV* genome (NC_006273.2 (81)). Bio-pac contains nucleotides 30-64, the forward primer is not tagged while the reverse primer is connected to biotin on its 5'-end. (B) Bio-1000, bio-500 and bio-250 are generated by PCR using pUC18-aseq as template. Positions of primers are indicated on the vector map on the right. (C) Schematically drawing of the procedure. (I) Biotinylated dsDNA is incubated with avidin beads at 20°C. (II) Washing step is applied to remove unbound dsDNA prior to (III) addition of *in vitro* translated [^{35}S]-labelled protein. (IV) After serious washing steps (IV) to remove unbound protein a (V) NaCl gradient (200-2000mM) and a boiling step are applied for elution. (V) Samples are analysed by SDS-PAGE and autoradiography.

2.2.8.2 Protein-Protein-interactions

2.2.8.2.1 Biomolecular fluorescence complementation assay (BiFC)

With this method binary protein-interactions were detected using a two-component-fluorophore as reporter. Both parts of the fluorophore did not interact and therefore were not active on their own. In this study citrin (YFP) served as the fluorophore that was fused to the putative interaction partners. It became photo-active upon physical interaction of the fusion proteins by bringing the two fluorophore parts in close proximity.

Hela cells were grown on cover slips to 70% confluence. Prior to transfection cells were arrested for 12h in medium containing 0.1% FCS. For transient expression of fluorophores cells were transfected with three different constructs. Two of them expressing forms of pUL71 fused to the N- or C-terminal part of YFP (pcDNA71_wt-YN and pcDNA71_wt-YC, pcDNA71_L1-YC, pcDNA71_L2-YC; pcDNA71_L3-YC pcDNA71_ΔLZ-YC) and the third construct pcDNA3.1-mCherry expressing mCherry (210, 211, 241). Transfection procedure was carried out as described above (2.2.4.4) and cells were grown for 14h at 37°C and 30' at 32°C prior fixation. Cells were treated according to method described for immunofluorescence (2.2.7.2) with PFA, NH_4Cl and Triton X-100. Nuclei were stained with DAPI and expression of fluorophores analysed using an Axio-Observer.Z1 fluorescence microscope and Axiovision software 4.8 (Carl Zeiss MicroImaging). YFP-Intensity was measured relative to mCherry expression to allow quantitative comparison between different cells (102).

2.2.8.2.2 Co-immunoprecipitation

For co-immunoprecipitation mock-infected or *AD169*-infected cells were harvested 72h p.i. For co-immunoprecipitation in transfected cells *293T* cells were transfected with two putative binding partners cloned into pcDNA3.1/HisB or C (Xpress-tag) and pHM1580 (Myc-tag) and collected 48h after transfection. In detail, (i) pcDNA77-myc was transfected together with pcDNA56, pcDNA89, pcDNA104, pcDNAMCP and pHM123, or (ii) pcDNA71 with pcDNA71-myc, pcDNA71_ΔLZ-myc, pcDNA71_L1-myc, pcDNA71_L2-myc and pcDNA71_L3-myc (iii) or constructs used for BiFC (2.2.8.2.1), respectively. In both cases total cell extracts were prepared by solubilisation in immunoprecipitation buffer (20mM Tris-HCl pH 7.5, 150mM NaCl, 0.5% Tween20, 5mM EDTA, Protease Inhibitor mix Complete Mini) as described for 2.2.4.5. Comparable amounts of extracts and specific antibodies were used for precipitation. Extracts were loaded onto Protein A Sepharose CL-4B (GE Healthcare) and subjected to multiple washing steps in order to remove unspecific binding.

Immunoprecipitates were analysed by SDS-PAGE (2.2.6.1.1) prior to immunostaining (2.2.7.3).

2.2.8.2.3 Yeast two hybrid assay (Y2H)

This screening method was developed to analyse binary protein interactions *in vivo* using yeast as a model organism (84). Two putative interacting proteins are fused as bait and prey to the DNA-binding and activation domain of a transcriptional activator of Gal4-reporter-promoter. Both domains cannot interact independently from binary interactions of the tested proteins. If these proteins directly interact Gal4-reporter-promoter-induced gene products will be detected. In the following, activation of Gal4 reporter promoter was analysed for growth on selective media (2.2.8.2.3.1) and enzymatic activity in a β-galactosidase filter shift assay (2.2.8.2.3.2).

2.2.8.2.3.1 Mating and reporter growth assay

Both prey MAT-a *AH109* and bait Mat-α *Y187* tested positively of accuracy of transfection and negatively for reactivation (2.2.2.2), were spotted on YPD plates for mating and incubated o/n at 30°C. Spotting matrix was stamped on –Leu/-Trp diploid selective and –Leu/-Trp/-Ade/-His reporter selective plates using a replicating block and incubating them for 5 days on 30°C. If growth is observed on –Leu/-Trp/-Ade/-His reporter selective plates this will be due to Gal4 promoter activation through binary protein-protein interaction.

2.2.8.2.3.2 β-Galactosidase filter shift assay

The –Leu/-Trp diploid selective plates prepared in 2.2.8.2.3.1 were used for transferring colonies onto filter paper to generate a cast. The colonies on the filter were lysed in liquid nitrogen 3 x for 30s prior to incubating them on filter paper saturated with β-Gal reaction mix (60mM Na_2HPO_4, 40mM NaH_2PO_4, 10mM KCl, 1mM $MgSO_4$, 10mg X-Gal, 0,18% β-mercaptoethanol) and incubating for 3-5h at 37°C or until blue colour develops.

2.2.9 Electron microscopy (EM)

2.2.9.1 Embedding and thin sectioning

HFF cells (1 x 10^6) were infected at MOI 3 with recombinant viruses *71_ΔLZ-BAC* and *71_L1-BAC*, *71_wt-BAC* and harvested 5 days p.i.. Cells were taken up in 2.5% glutaraldehyde in HEPES buffer (20mM HEPES, 150mM NaCl pH 7.4) and fixed consecutively with 1% osmium tetroxide, 0.1% tannin and 1% Na_2SO_4 all diluted in HEPES buffer. After dehydration with EtOH (50/70/90/100%) and a second staining with 0.2% uranyl acetate, cells were transferred to beam capsules and embedded in 1,2-epoxypropane in glycid ether 100 after addition of hardeners DBA and MNA. Polymerization was induced by heat for 3 days at 65°C. Thin Sections were cut with an ultra microtome (Leica) and sections were transferred to carbon coated cooper grids (Plano, Wetzlar) prior to final staining with 1% uranyl acetate in 40% EtOH and lead citrate. Thin sections were analysed using a TEM Tecnai^{TM} G2 (FEI Company, Eindhoven) electron microscope operated at 120 kV.

2.2.9.2 Staining single particles

Structural details of purified proteins were analysed on carbon coated cooper grids (Plano, Wetzlar) using electron microscopy prior to negatively staining with 2% (w/v) uranyl acetate according to Valentine et al. (238). The carbon coating is produced by firstly coating a matrix of $K_2OAl_2O_3SiO_2$, so-called mica (4) using a Turbo Carbon Coater 208 (Cressington Scientific Instruments Ltd). This carbon–coated mica was loaded with protein by introducing it into the sample suspension at an angle of 30°C for 1´. The carbon film floated off and particles are being adsorbed. The mica was slowly removed, allowing the carbon to fall back in its original position. The same procedure was performed in staining solution whereas a grid was placed on the surface of the carbon film and incubated for 20 s. The grid was lifted up an excess staining solution was drained of by using filter paper.

2.2.10 *In silico* tools

For determination of putative oligomerisation domains and other specific secondary structures e.g. the following prediction programs were used: HeliQuest (http://heliquest.ipmc.cnrs.fr/)(89); Clustalw (http://toolkit.tuebingen.mpg.de/clustalw); p-coils (http://toolkit.tuebingen.mpg.de/pcoils); Quick2d (http://toolkit.tuebingen.mpg.de/quick2_d); Blastclust (http://toolkit.tuebingen.mpg.de/blastclust) (29) and Psi-pred (http://bioinf.cs.ucl.ac.uk/psipred/) (42, 111).

3 Results

3.1 Functional characterisation of *HCMV* pUL77

3.1.1 Identification of the protein pUL77

The antibody purified from patients' sera using column affinity chromatography was tested for monospecificity prior to further usage in this study. To generate pAbUL77 IgGs reactive to pUL77 were purified from sera from high titre *HCMV* patients and tested on immunoblots probed with rpUL77_E.coli.

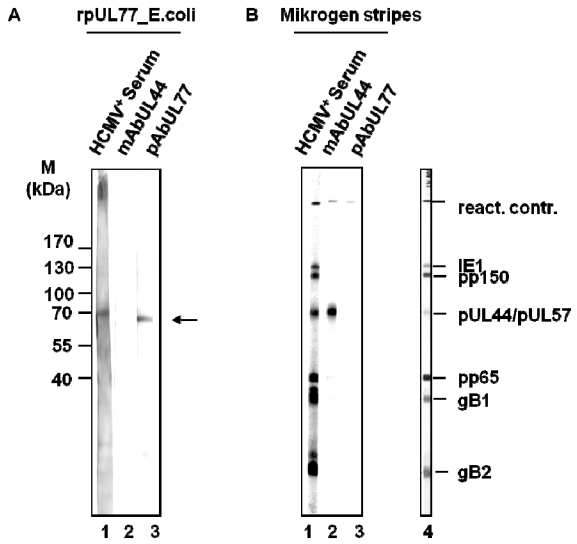

Figure 4: Characterisation of the antibody pAbUL77. (A) Purified rpUL77_E.coli was separated by 10% SDS-PAGE and immunostaining was performed with Cytotect (*HCMV*$^+$ Serum, lane 1), mAbUL44 (lane 2) and pAbUL77 (lane 3). (B) Commercially available immunoblot stripes (Mikrogen Diagnostics, Neuried) containing recombinant immunodominant epitopes of IE1 (53 kDa), pp150 (50 kDa), pUL44/pUL57 (45 kDa), pp65 (31 kDa), gB1 (25 KDa) and gB2 (18 kDa) were reacted with Cytotect (*HCMV*$^+$ Serum, lane 1), mAbUL44 (lane 2) and pAbUL77 (lane 3). Positively reacted control stripe is shown on the right (lane 4). Arrows on the right side indicate the position of pUL77. Molecular weight markers (M) are shown on the left side.

Only Cytotect (Figure 4. A, lane 1) and the purified antibody pAbUL77 (Figure 4. A, lane 3) reacted on strips with purified protein, but not mAbUL44 (Figure 4. A, lane 2). As an additional control for specificity of pAbUL77 immunostaining of different viral proteins was performed. Commercially available immunoblot stripes (Mikrogen Diagnostics, Neuried) containing recombinant polypeptides derived from immediate early protein IE1 (53 kDa), tegument protein pp150 (50 kDa), polymerase co-factor pUL44, single stranded binding protein pUL57 (45 kDa), tegument protein pp65 (31 kDa) and glycoprotein gB (gB1, 25 kDa; gB2, 18 kDa) were used. Only Cytotect (Figure 4. B, lane 1) and mAbUL44 (Figure 4. B., lane 2) but not pAbUL77 (Figure 4. B, lane 3) reacted on the immunoblot, as expected. Thus,

showing that pAbUL77 does not react with other *HCMV* epitops but pUL77 specific ones. Taken together, these results indicate pAbUL77 is a monospecific antibody against pUL77.

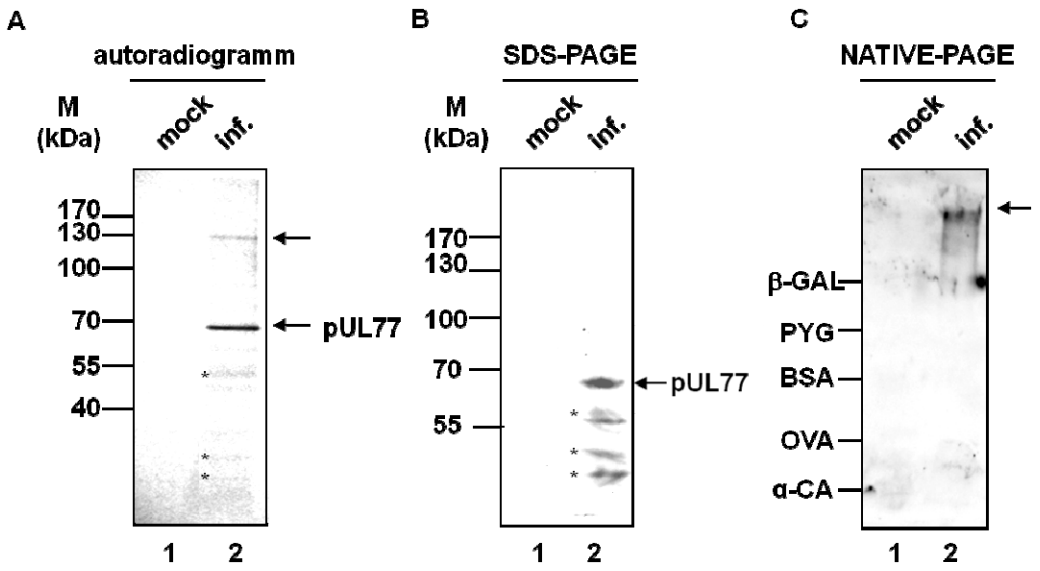

Figure 5: Identification of pUL77. (A) Mock-infected (lane 1) and *AD169*-infected (lane 2) cells were [^{35}S]-labelled 60h p.i.. Cells were harvested and subjected to immunoprecipitation against pAbUL77 prior to 8% SDS-PAGE and autoradiography. (B) Extracts from mock-infected (lane 1) or *AD169*-infected cells (lane 2) were separated by 8% SDS-PAGE prior to immunostaining with pAbUL77. (C) Extracts from mock-infected (lane 1) or *AD169*-infected cells (lane 2) were subjected to 8% NATIVE-PAGE followed by immunostaining with pAbUL77. The asterisks (*) indicates degradation products. Arrows on the right side indicate the positions of the monomer and dimer of pUL77, while molecular weight markers (M) are indicated on the left. Markers for NATIVE-PAGE: β-GAL: β-galactosidase 130kDa; PYG: phosphorylase 100kDa; BSA: bovine serum albumin 68kDa; OVA: Ovalbumine 45kDa; α-CA: carbonic anhydrase 35kDa.

The purified antibody pAbUL77 is used to identify pUL77 in the viral context used for immunoprecipitation in radio-labelled cells and immunostaining after electrophoresis performed under native or denaturating conditions. In immunoprecipitation experiment a band of approximately 70kDA, the calculated molecular size of pUL77 is 73kDa, is prominently detected (Figure 5. A (c.f. 149)). In immunostaining the antibody was used to visualise monomeric and oligomeric forms of pUL77. Under denaturating conditions only the monomeric form and faint bands representing degradation products are visible on the blot (Figure 5. B (SDS-PAGE)). In contrast, higher molecular weight forms were detected under native conditions (Figure 5. C (NATIVE-PAGE)). These results are hinting on an oligomerisation potential of pUL77.

3.1.2 Association of pUL77 with capsids

Extracellular virions were isolated from the supernatant of *AD169*-infected cells 96h p.i and subjected to fragmentation using detergent treatment prior to ultracentrifugation steps. The content of each fraction was analysed by immunostaining and Coomassie staining.

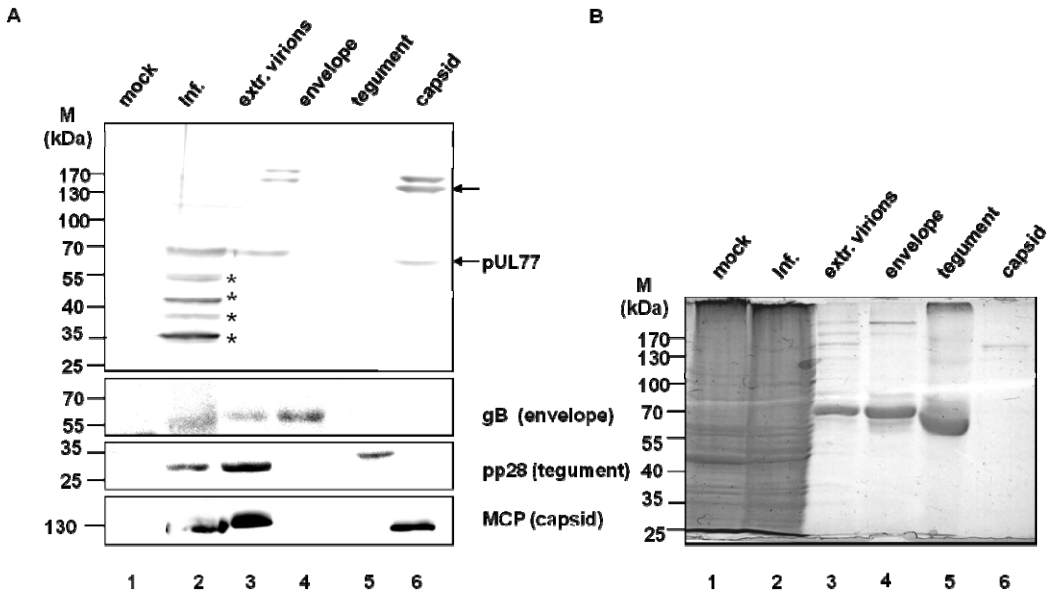

Figure 6: Association of pUL77 with viral capsids. (A) Mock-infected (lane 1) and *AD169*-infected cell extracts (lane 2) as well as extracellular virions (lane 3), purified envelope (lane 4), tegument (lane 5) and capsid (lane 6) fractions were analysed by immunostaining using pAbUL77 (pUL77, upper panel). To control purity of each fraction antibodies against gB for envelope (gB, second panel), pp28 for tegument (pp28, third panel) or MCP for capsid fraction (MCP, lower panel) were reacted as well. (B) To control protein content, samples used for immunoblot in Fig. A were subjected to 8% SDS-PAGE prior to Coomassie staining. The asterisks (*) indicates degradation products. Molecular weight markers (M) are indicated on the left side, putative different weight forms of pUL77 are indicated by arrows.

To analyse the association of pUL77 to the virions specific antibodies against pUL77 (pAbUL77) and marker proteins to test the purity of each fraction (mAbgB for gB, mAbpp28 for pp28, and mAbMCP for MCP) were used. The immunostaining revealed positively for pUL77 in infected cells (Figure 6. A, upper panel, lane 2), extracellular virions (Figure 6. A, upper panel, lane 3) and capsid fraction (Figure 6. A, upper panel, lane 6). We detected monomeric forms of the protein in all three fractions, but oligomeric forms only in the extracellular virions and the capsid fraction that was purified from it. All fractions seem to be free of contaminations, containing only the described protein content, tested by staining against markers gB for envelope (Figure 6. A, second panel (gB)), pp28 for tegument (Figure 6. A, third panel (pp28)) and MCP for capsid (Figure 6. A, lower panel (MCP)) fraction. Figure 6. B shows the overall protein content of each fraction.

Taken together, the results show that pUL77 is a structural capsid-associated *HCMV* protein.

3.1.3 Interaction of *HCMV* pUL77 with DNA packaging proteins

After learning that pUL77 is associated to the capsid as a structural protein we wanted to investigate pUL77's direct interactions to certain other capsid proteins.

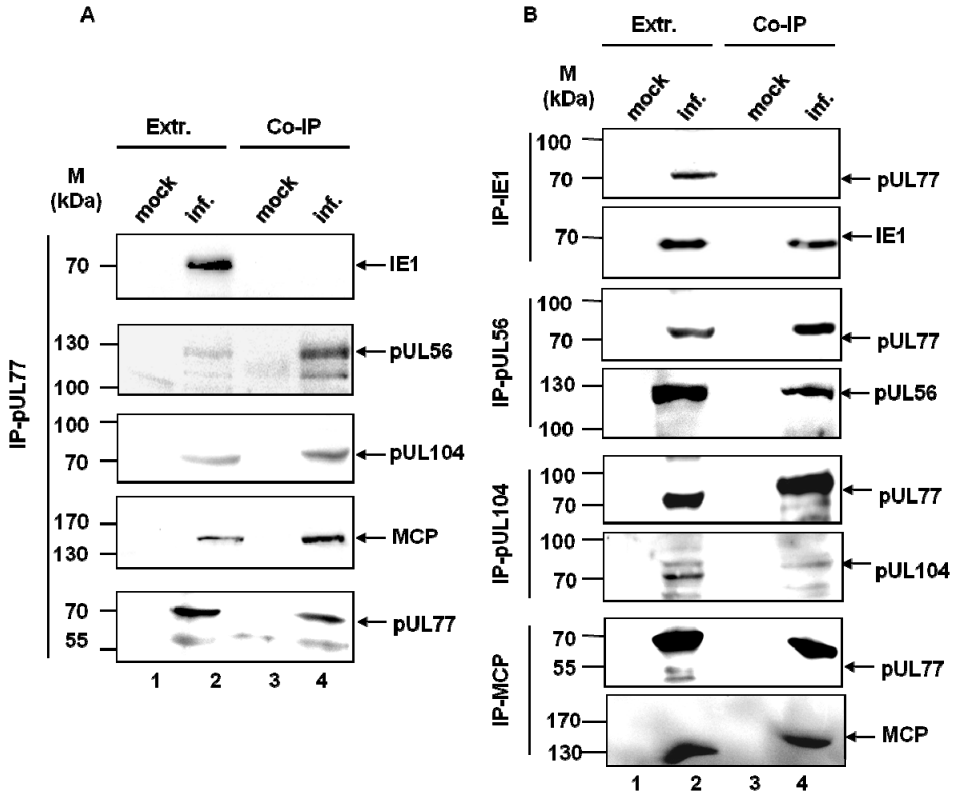

Figure 7: Interaction of pUL77 with DNA packaging proteins. (A) Mock-infected or *AD169*-infected *HFF* lysates at 72h p.i. were precipitated with pAbUL77 and subjected to SDS-PAGE prior to immunostaining using antibodies mAbIE1 (IE1), pAbUL56 (pUL56), pAbUL104 (pUL104), mAbMCP (MCP) and pAbUL77 (pUL77) as control. Extracts (Extr., lane 1-2) as well as precipitates (Co-IP, lane 3-4) from mock-infected (lane 1, 3) and *AD169*-infected (lane 2, 4) cells were analysed. (B) Mock-infected or *AD169*-infected *HFF* lysates at 72h p.i. were precipitated with mAbIE1 (IP-IE1), pAbUL56 (IP-pUL56), pAbUL104 (IP-pUL104 and mAbMCP (IP-MCP) and subjected to SDS-PAGE. Immunostaining was performed using pAbUL77 and as an expression control antibodies that were used for precipitation. Immunostaining was performed using antibodies pUL77 and mAbIE1 (IP-IE1), pAbUL77 and pAbUL56 (IP-pUL56), pAbUL77 and pAbUL104 (IP-pUL104), and pAbUL77and mAbMCP (IP-MCP). Extracts (Extr., lane 1-2) as well as precipitates (Co-IP, lane 3-4) from mock-infected (lane 1, 3) and *AD169*-infected (lane 2, 4) cells were analysed. The arrows indicate the positions of the proteins IE1, pUL56, MCP, pUL104 and pUL77. The molecular weight markers (M) are indicated on the left.

In this study we tested for interactions with MCP that is one of the major components of the capsid (53), pUL104 the portal protein through which the DNA is inserted into the preformed capsids (78, 79), pUL56 the large subunit of the terminase involved in DNA packaging (31,

93) and the non structural viral replication factor immediate early protein IE1 (148) as a negative control.

For that purpose, *HFF*s were mock-infected or *AD169*-infected at a MOI of 2, harvested 72h p.i. and subjected to co-immunoprecipitations (Co-IP). In a first experiment we precipitated against pUL77 (Figure 7. A (IP-pUL77)) and in an alternate experiment against the proteins analysed with immunostaining in the previous experiment, e.g. IE1 (Figure 7. B (IP-IE1)), pUL56 (Figure 7. B (IP-pUL56)), pUL104 (Figure 7. B (IP-pUL104)) and MCP (Figure 7. B (IP-MCP)).

In other words, either the monospecific antibody pAbUL77 (Figure 7. A) or mAbIE1 against IE1, pAbUL56 against pUL56, pAbUL104 against pUL104 and mAbMCP against MCP (Figure 7. B) were used for precipitation. The following immunostaining using the antibodies mentioned above detected pUL56 (Figure 7. A (pUL56)), MCP (Figure 7. A (MCP)), the pUL104 (Figure 7. A (pUL104)) and pUL77, to analyse the presence of both precipitated proteins (Figure 7. A (pUL77)) in *HCMV*-infected cell extracts and precipitates. No band was detected in mock-infected cell extracts or precipitates (Figure 7. A and B, lanes 1, 3) using virus specific antibodies mAbIE1, pAbUL77, pAbUL56, pAbUL104 and mAbMCP. Immunostaining against IE1 was used as a negative control (Figure 7. A (IE)). In addition, using antibodies specific for pUL56, pUL104, MCP and IE1 for precipitation, pUL77 was detected in the corresponding manner, thus confirming the interactions (Figure 7. B).

To further examine whether interactions between pUL77 and packaging proteins are direct, without other viral proteins involved, co-immunoprecipitations in *293T*-transfected cells were performed. Briefly, cells were co-transfected with pcDNA77-myc and pcDNA3.1/HisC (Figure 8, lanes 3-4 (vector**)**), pcDNA77-myc and pHM123 encoding IE1 (Figure 8, lanes 5-6 (IE1)), pcDNA77-myc and pcDNA56 (Figure 8, lanes 7-8 (pUL56)), pcDNA77-myc and pcDNA104 (Figure 8, lanes 9-10 (pUL104)) or pcDNA77-myc and pcDNAMCP (Figure 8, lanes 11-12 (MCP)). Cell extracts were harvested 48h after transfection. For precipitation a specific antibody against the Myc-tag (E-Q-K-L-I-S-E-E-D-L) of pUL77 prior to immunostaining against Xpress-tag (D-L-Y-D-D-D-D-K) of IE1, pUL56, pUL104 and MCP was used. In precipitates monomers of pUL56, pUL104 and MCP were detected (Figure 8, lanes 8, 10, 12). In precipitates of mock, vector-transfected as well as IE1-transfected cells no specific proteins were observed (Figure 8, lane 2, 4, 6).

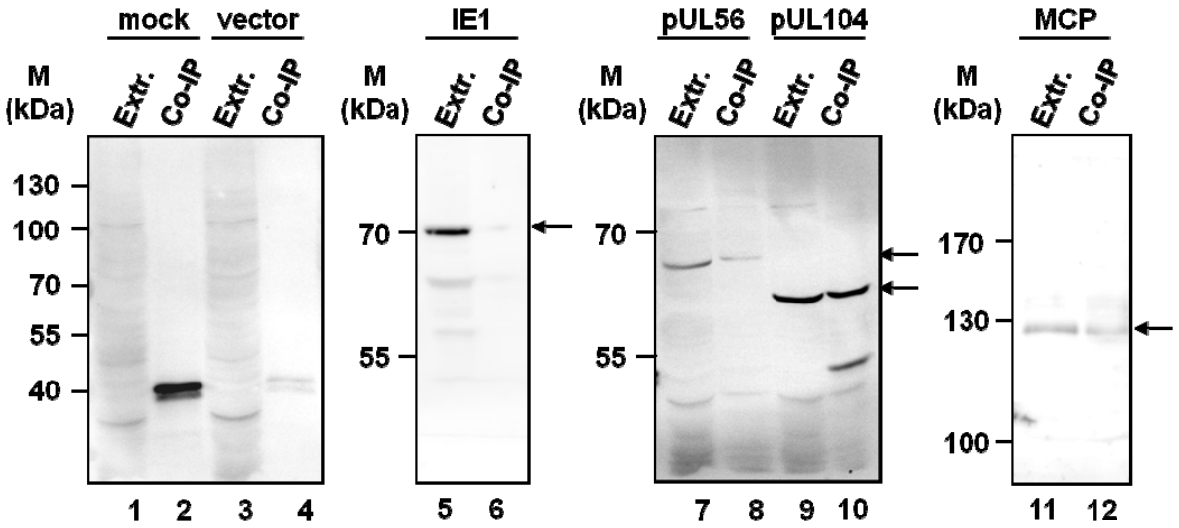

Figure 8: Analysing direct interactions. *293T* cells were either transfected with pcDNA77-myc alone (mock, lane 1-2) or co-transfected with a combination of pcDNA77-myc and pcDNA3.1/HisC (vector, lanes 3-4), pcDNA77-myc and pHM123 (IE1, lanes 5-6), pcDNA77-myc and pcDNA56 (pUL56, lanes 7-8), pcDNA77-myc and pcDNA104 (pUL104, lanes 9-10) or pcDNA77-myc and pcDNAMCP (MCP, lanes 11-12). Co-immunoprecipitation was performed 48h after transfection with pcDNA77-myc specific mAbMyc_m. Lysates were subjected to SDS-PAGE prior to immunostaining using mAbXpress specific for Xpress-tag (D-L-Y-D-D-D-D-K) of pcDNA56, pcDNA104 and pcDNAMCP or pHM123. Extract (Extr. Lane 1, 3, 5, 7, 9, 11) and precipitate (Co-IP lane 2, 4, 6, 8, 10, 12) fractions are analysed. The arrows indicate the positions of the proteins IE1, pUL56, MCP, pUL104 and pUL77. The molecular weight markers (M) are indicated on the left.

These data implicate physical interactions between the capsid-associated pUL77 and the structural proteins of the *HCMV* capsid, in more detail: (i) the large terminase subunit pUL56, (ii) the portal protein pUL104 and (iii) MCP.

Therefore we hypothesise that interactions between pUL77 and the capsid proteins tested are a hint for a function of pUL77 in events connected to capsid assembly and/or DNA packaging.

3.1.4 DNA binding of *HCMV* pUL77

To further analyse whether pUL77 might be connected to DNA packaging its ability to bind dsDNA was examined. Therefore, *in vitro* binding studies were performed. [^{35}S]-labelled pUL77 was loaded on a dsDNA cellulose column or heparin-sepharose which is used as a dsDNA analogue (18, 46, 162, 208). Scott et al. (208) described immobilised heparin to have two main modes of interaction with proteins; (i) it can operate as an affinity ligand, e.g. in its interaction with coagulation factors; or (ii) heparin functions as a high capacity cation exchanger, due to its anionic sulphate groups. The negative charge mimics the electrostatic

characteristics of dsDNA and therefore heparin-sepharose is used to bind DNA-binding proteins.

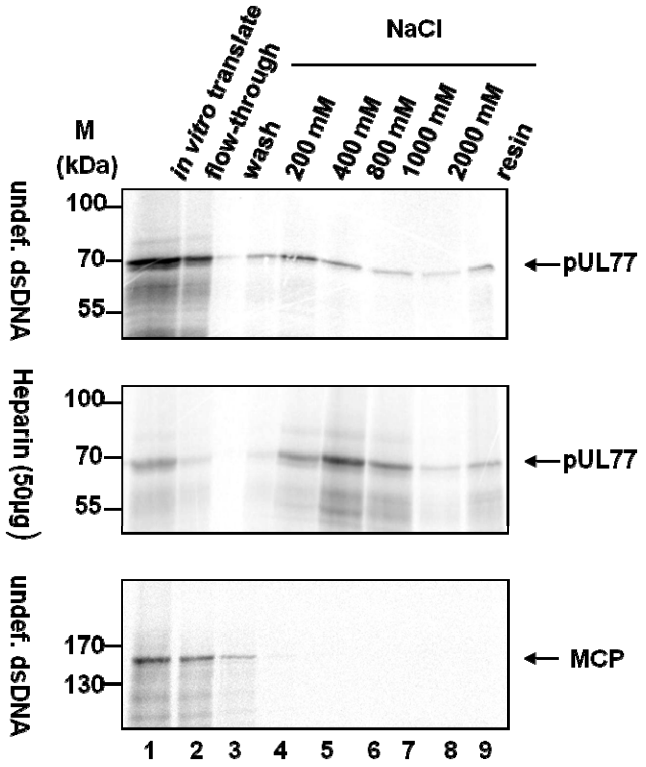

Figure 9: Interaction of pUL77 with dsDNA. (upper panel) *In vitro* translated [^{35}S]-labelled pUL77 (*in vitro* translate, lane 1) was applied to a dsDNA-cellulose column. After the column was washed (wash, lane3), pUL77 was eluted with increasing NaCl concentrations (200-2000mM NaCl, lanes 4-8) and an additional boiling step (resin, lane 9). (middle panel) *In vitro* translated [^{35}S]-labelled pUL77 (*in vitro* translate, lane 1) was applied to a heparin-sepharose column. After the column was washed (wash, lane3), pUL77 was eluted with increasing NaCl concentrations (200-2000mM NaCl, lanes 4-8) and an additional boiling step (resin, lane 9). (lower panel) To control specificity of the method in *vitro* translated [^{35}S]-labelled MCP (*in vitro* translate, lane 1) was loaded onto dsDNA-cellulose column. The column was washed (wash, lane3) prior to elution with increasing NaCl concentrations (200-2000mM NaCl, 4-8) an additional boiling step (resin, lane 9) (cf. 149). Molecular weight markers (M) are indicated on the left; the positions of the proteins are indicated on the right.

After serious washing steps bound proteins were eluted with a NaCl-gradient (200-2000mM NaCl). Eluates were analysed by SDS-PAGE and autoradiography. The protein pUL77 could be detected in all eluted fractions in both experiments binding to dsDNA-cellulose as well as to heparin-sepharose columns (Figure 9. upper and middle panel). Still we detect a peak in elution at 400-800mM NaCl for the undefined dsDNA (Figure 9. upper panel, lane 5-6) and at 400-1000mM NaCl for heparin (Figure 9. middle panel, lane 5-7). Thus, the results are implying an interaction of pUL77 with dsDNA. In contrast to this observation, there is no

significant signal for MCP, used as a negative control, detected (Figure 9. lower panel, lanes 4-9(cf. 149)). These results indicate that pUL77 has the ability to bind dsDNA.

3.1.5 *HCMV* pUL77 binds to dsDNA of at least 500bp in length

To further analyse pUL77 binding to dsDNA the assay described above was adapted. To answer the question whether the DNA has to be specially designed to allow binding of pUL77, defined species of DNA were used.

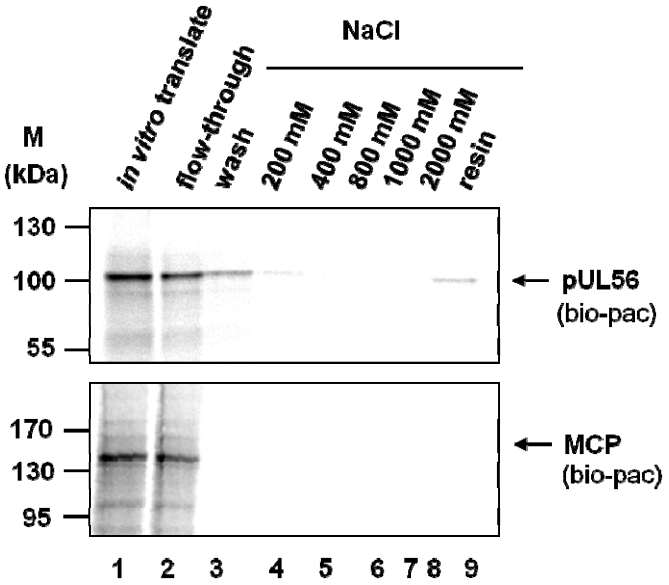

Figure 10: Testing known interactions. To oligonucleotides bio-pac *in vitro* translated [^{35}S]-labelled pUL56 (upper panel, lane 1) or MCP (lower panel, lane 1) were added as positive and negative control. Column was subjected a serious washing step (lane 3) and to elution with increasing NaCl concentrations (lanes 4-8, (200-2000mM NaCl)) and an additional boiling step (lane 9 (resin)). Samples were analysed by 8% SDS-PAGE and autoradiography. Molecular weight markers (M) are indicated on the left, the positions of the proteins on the right.

Either small fragments containing specific motifs by oligonucleotide synthesis (bio-pac) or longer ones by PCR (bio-250, bio-500, bio-1000) were obtained. The bio-pac oligonucleotide corresponds to the pac1 sequence (163). The motif is described as the recognition motif of the terminase complex (31). Bogner et al. used the very same specific 36-mer to analyse the interaction between pUL56 and pac1 in an electro mobility shift assay (31). As proof of principal and for testing specificity of the method the experiment described in the paper was reconstituted using the method optimised in this study.

For pUL56 we detect binding to bio-pac. In detail, for pUL56 (Figure 10, upper panel, lane 3 (wash)**)** we see an excess of protein being washed away while the rest of the protein binds so

tight to the sequence that it cannot be removed by elution with 200-2000mM NaCl (Figure 10, upper panel, lane 4-8 (200-2000mM NaCl)) alone. Only after an additional boiling step (Figure 10, upper panel, lane 9 (resin)) pUL56 is completely removed from the beads. In the case of MCP, that is known not to bind dsDNA, we detect no specific bands in the elution or resin fractions (Figure 10, lower panel, lanes 3-9). In addition, experiments using bead material alone does not show interactions with the proteins applied (data not shown, cf. 149).

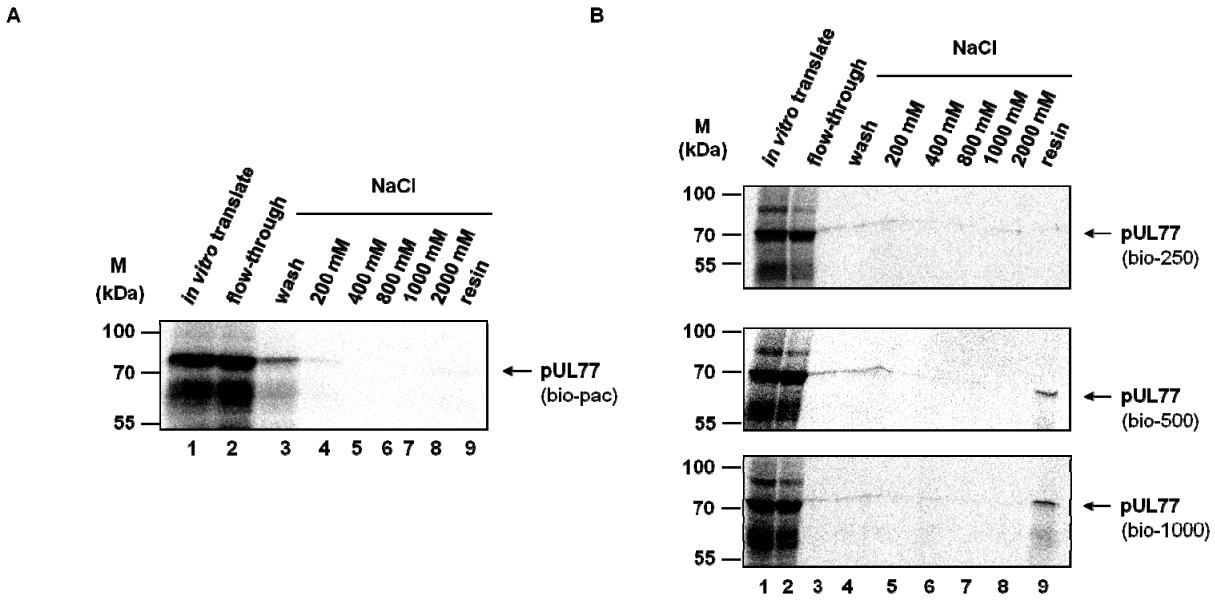

Figure 11: *HCMV* pUL77 binds to defined dsDNA. (A) The binding reaction was carried out by incubation of dsDNA oligonucleotide 36-mer bio-pac containing pac1 motif (lanes 1-9) with avidin-agarose resin followed by addition of *in vitro* translated [^{35}S]-labelled pUL77. Washing and elution steps were carried out as described previously. Briefly, column was subjected a serious washing step (lane 3), to elution with increasing NaCl concentrations (lanes 4-8, (200-2000mM NaCl)) and an additional boiling step (lane 9 (resin)). (B) The binding reaction was carried out by incubation of dsDNA oligonucleotides 250-mer bio-250 (upper panel, lanes 1-9), 500-mer bio-500 (medium panel, lanes 1-9), 1000-mer bio-1000 (lower panel, lanes 1-9), respectively. Washing and elution steps were carried out as described in A. Samples were analysed by 8% SDS-PAGE and autoradiography. Molecular weight markers (M) are shown on the left; the positions of the proteins are indicated on the right.

Since it is possible to detect specific interactions between proteins and rather short dsDNA fragments (36-mer bio-pac) on bead material, this method was used in further experiments.

Because the pac-sequences are the only motifs on the *HCMV* genome described so far to facilitate specific interactions to viral proteins involved in packaging, we were testing whether pac-sequences might mediate binding of pUL77 to dsDNA. In contrast to pUL56 (Figure 10, upper panel) we did not find any specific binding for pUL77 to bio-pac (Figure 11. A). Therefore we hypothesise that not a specific motif but the DNA itself being a negatively

charged species facilitates the interaction. The amount of charge provided from the 36-mer is not sufficient to facilitate an interaction.

Hence, we constructed longer DNA-species resulting in higher negative charge and applied them to this assay. Figure 11. B shows that only after applying an oligonucleotide of 500bp or longer a specific binding similar to pUL56/bio-pac could be detected. In other words, a specific band for pUL77 is detected in the resin fraction of bio-500 (Figure 11. B, middle panel, lane 9) and bio-1000 (Figure 11. B, lower panel, lane 9).

To draw further conclusions from these findings a quantification of the results is necessary. Therefore a factor needs to be defined that reflects the relative strength of the interaction between protein and DNA. In our study we defined the band intensity detected by Bioimager in resin (Figure 9, Figure 10 and Figure 11, lane 9) relative to the input (Figure 9, Figure 10 and Figure 11, lane 1) as binding efficiency (BE). This number has nothing to do with global binding constants measured by physicochemical methods like stop-flow or Biacore but serves to help us setting the results of this assay in ratio. In other words, the quantification allows us to analyse differences in the binding between different proteins and DNA species tested in this assay. The results of this quantification are summarised in Table 1.

Table 1: Quantification of DNA-binding. Using the binding efficiency (BE) defined by the formula on the left hand side DNA-binding reactions were quantified. BE is defined 10 for binding between pUL56 and bio-pac1. BE < 1 is defined as no binding. Values were obtained in three independent experiments and standard deviations are calculated.

$$BE = \frac{I_{resin}}{I_{IT}} \times 100$$

BE ...binding efficiency

I_{resin}...Intensity of 100% resin

I_{IT} ...Intensity of 100% *in vitro* translate

protein	oligonucleotide	binding efficiency (BE)
pUL56	bio-pac1	10±0.53
MCP	bio-pac1	0.2±0.40
pUL77	bio-pac1	0.2±0.03
pUL77	bio-250	0.5±0.45
pUL77	bio-500	2.2±0.41
pUL77	bio-1000	4.9±0.72
pUL77	genom. DNA (Sigma)	8.6±1.67

We defined the interaction between pUL56 and pac1 as BE=10, for the interaction is known from literature to be specific, long-lived and strong enough to allow the terminase to perform its specific cut to separate one unique length genome from the other (31). In contrast to that all interaction BE<1 were defined as not specific, e.g. for the interaction between MCP and pac1, pUL77 and pac1 as well as pUL77 and bio-250. In comparison to pUL56 and pac1, BE

from the interaction between pUL77 and bio-500 is 80% reduced, whereas with bio-1000 only 50% and with the genomic DNA approximately 20%. This findings show that the interaction between pUL77 and dsDNA seems to get stronger with longer interacting DNA fragments, thereby strengthening the hypothesis that we are analysing an electrostatic effect. Taken together, we could show that we designed a method that can be used to quantitatively analyse binding between proteins and specifically designed DNA species. Applying this method to further analyse the DNA binding abilities of pUL77 we could show that this interaction is dependent upon a certain length of the provided DNA.

3.2 Functional characterisation of *HCMV* pUL71

3.2.1 Identification of the protein pUL71

To generate a specific antibody against pUL71 a similar approach as described for generation of pAbUL77 was used. Since Beghetto et al. published that pUL71 causes a strong immunogenic response in *HCMV* patients (27), the sera of high titre *HCMV* positive individuals was applied to column affinity chromatography against rpUL71_Ecoli. The purified fractions were tested for monospecificity prior to further usage in this study.

Figure 12. A shows blots probed with rpUL71_Ecoli and stained with either purified antibody pAbUL71 (Figure 12. A, lane 1 (pUL71)), Cytotect (Figure 12. A, lane 2 (*HCMV*$^{+}$ Serum)) or mAbUL44 (Figure 12. A, lane3 (pUL44)). Only pAbUL71 and the positive control Cytotect reacted with the recombinant protein. Using the commercial strips containing for different immunogens (Mikrogen Diagnostics, Neuried, cf. pAbUL77 purification 3.1.1) we found Cytotect (Figure 12. B, lane 2 (*HCMV*$^{+}$ Serum)) and mAbUL44 (Figure 12. B, lane 3 (pUL44)) but not pAbUL71 (Figure 12. B, lane 1 (pUL71)) reacting. This finding is hinting towards the specificity of the antibody against its target. To further analyse specificity we transfected a 6x His-tagged (H-H-H-H-H-H) pUL71 expressed from pcDNA71 in *293T*s and reacted the blot with either mAbHis or pAbUL71. Both antibodies visualised a single band at approximately 55kDa further hinting on the monospecificity of the antibody (Figure 12. C).

Further the antibody was used to detect pUL71 in mock-infected and *AD169*–infected *HFF*s separated by either SDS-PAGE or NATIVE-PAGE. In SDS-PAGE we detected a single band at 55kDA in infected cells (Figure 12. D, lane 1). Whereas, in NATIVE-PAGE a higher molecular weight species was detected (Figure 12. E, lane 1) hinting on a possible oligomerisation tendency of the protein that will be further discussed in this study (3.2.8). No specific band was detected in the mock fractions under both conditions (Figure 12. D and Figure 12. E., lane 2).

Taken together we conclude that (i) with pAbUL71 we generated a monospecific antibody against pUL71 that (ii) reacts in infected and transfected cells in one band of approximately 55kDa under denaturating conditions and (iii) a higher molecular weight band that might represent an oligomer, under native conditions.

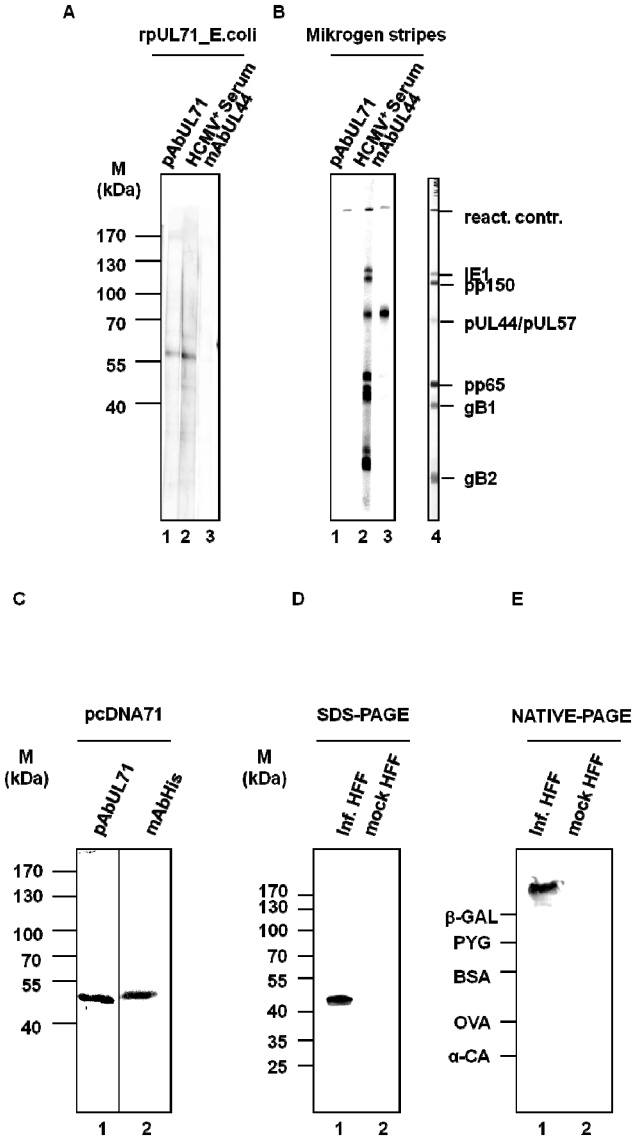

Figure 12: Identification of the pUL71. (A) The generated antibody pAbUL71 was tested for specificity. Purified rpUL71_Ecoli was separated by 10% SDS-PAGE and subjected to immunostaining using pAbUL71 (pUL71, lane 1), Cytotect (*HCMV*$^+$ Serum, lane 2) and mAbUL44 (pUL44, lane 3). (B) Commercially available immunoblot stripes (Mikrogen Diagnostics, Neuried) containing immunodominant epitopes of IE1 (53 kDa), pp150 (50 kDa), pUL44/pUL57 (45 kDa), pp65 (31 kDa), gB1 (25 KDa) and gB2 (18 kDa) were reacted with pAbUL71 (lane 1), Cytotect (*HCMV*$^+$ Serum, lane 2) and mAbUL44 (lane 3). Positively reacted control stripe is shown on the right. (C) Cell extracts of transiently expressed pUL71 fused to a 6x His-tag (H-H-H-H-H-H) was analysed using specific antibodies against pUL71 (pAbUL71, lane1) and 6x His-tag (mAbHis, lane2). (D) Extracts from *AD169*-infected (lane 1) or mock-infected cells (lane 2) were separated by 8% SDS-PAGE prior to immunostaining with pAbUL71. (E) Extracts from *AD169*-infected (lane 1) or mock-infected cells (lane 2) were subjected to 8% NATIVE-PAGE followed by immunostaining with pAbUL71.Molecular weight markers (M) are indicated on the left. Markers for NATIVE-PAGE: β-GAL: β-galactosidase 130kDa; PYG: phosphorylase 100kDa; BSA: bovine serum albumin 68kDa; OVA: Ovalbumine 45kDa; α-CA: carbonic anhydrase 35kDa.

3.2.2 Association of pUL71 with tegument fraction

Extracellular virions were isolated from the supernatant of *AD169*-infected cells 96h p.i and subjected to fragmentation using detergent treatment prior to multiple ultracentrifugation steps. The content of each fraction was analysed by immunostaining and Coomassie staining.

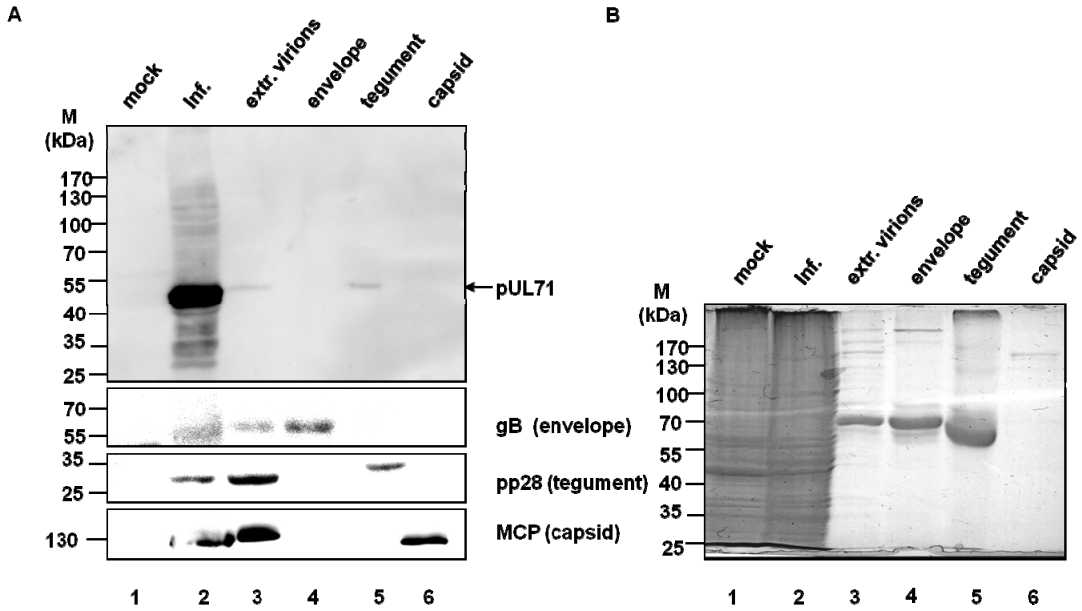

Figure 13: Association of pUL71 with the tegument. (A) Mock-infected (mock, lane 1) and *AD169*-infected cell extracts (Inf., lane 2) as well as extracellular virions (lane 3), purified envelope (lane 4), tegument (lane 5) and capsid (lane 6) fractions were analysed by immunostaining using pAbUL71 (pUL71, upper panel) and antibodies mAbgB for envelope (gB, second panel), mAbpp28 for tegument (pp28, third panel) or mAbMCP for capsid fraction (MCP, lower panel). (B) As a control for protein content, samples used for the immunoblot in A were subjected to 8% SDS-PAGE prior to Coomassie staining. Molecular weight markers (M) are indicated on the left side, the proteins are indicated by arrows.

To analyse the association of pUL71 to the virions the specific antibody pAbUL71 (Figure 13. A, upper panel (pUL71)) and marker proteins for each fraction were used similar to 3.1.2, e.g. antibodies mAbgB for envelope (Figure 13. A, second panel (gB)), mAbpp28 for tegument (Figure 13. A., third panel (pp28)) or mAbMCP for capsid fraction (Figure 13. A, lower panel (MCP)).

Immunostaining shows pUL71 to be found in *AD169*-infected cells (Figure 13. A, upper panel, lane 2 (pUL71)) as well as in extracellular virions (Figure 13. A, upper panel, lane 3 (pUL71)). After fractionating of extracellular virions, pUL71 is exclusively detected in the tegument fraction (Figure 13. A, upper panel, lane 5 (pUL71)). It was tested by staining against specific markers whether all fractions containing the proposed protein content. All marker proteins were detected in infected cells (Figure 13. A, all panels, lane 2) and

extracellular virions (Figure 13. A, all panels, lane 3) and gB exclusively in envelope (Figure 13. A, second panel, lane 4 (gB)), pp28 exclusively in tegument (Figure 13. A, third panel, lane 5 (pp28)) and MCP exclusively in capsid fraction (Figure 13. A, lower panel, lane 6 (MCP)). Taken together, this experiment shows that pUL71 is a structural protein associated to the tegument fraction of extracellular virions.

3.2.3 Expression of pUL71 within the viral life cycle

For a further functional characterisation of the protein it is important to know its temporal and spatial expression pattern. An expression kinetic study was performed analysing samples at specific time points throughout the infection. The samples were subjected to immunofluorescence and immunostaining. To assay growth the expression of several marker proteins for specific time points in the viral life cycle was tested in parallel. IE1, the major immediate early protein is expressed as one of the first proteins, pUL44 a member of the DNA polymerase machinery and MCP the major capsid protein expressed at a late stage in infection were chosen as markers. These proteins represent immediate-early, early-late and late expression kinetics.

In the control section of Fig A (Figure 14. A, controls) the expression pattern of marker proteins are shown. IE1 (Figure 14. A, controls, lane IE1) is expressed from the earliest time point, 6h p.i., tested onwards throughout the whole experiment in the nucleus of *AD169*-infected cells. Expression of pUL44 (Figure 14. A, controls, lane pUL44) starts in a few cells at 24h p.i but more pronounced from 48h p.i onwards in distinct replication centre like areas in the nucleus, whereas expression of MCP (Figure 14. A, controls, lane MCP) starts at 72h p.i in similar patterns.

From 96h p.i. extracellular virions (91) can be detected in the supernatant therefore the replication cycle is thought to be completed. Experiment was continued until 168h p.i. when almost all cells were lysed. Expression of pUL71 (Figure 14. A, pUL71) is detected first in cells at 24h p.i. but generally from 48h p.i. onwards getting more pronounced over time in the cytosol showing a peak at 72h p.i.. The expression pattern is very distinct, forming a junxtanuclear round shaped complex that in some cells seems to rearrange the nucleus around it into a kidney-shaped form.

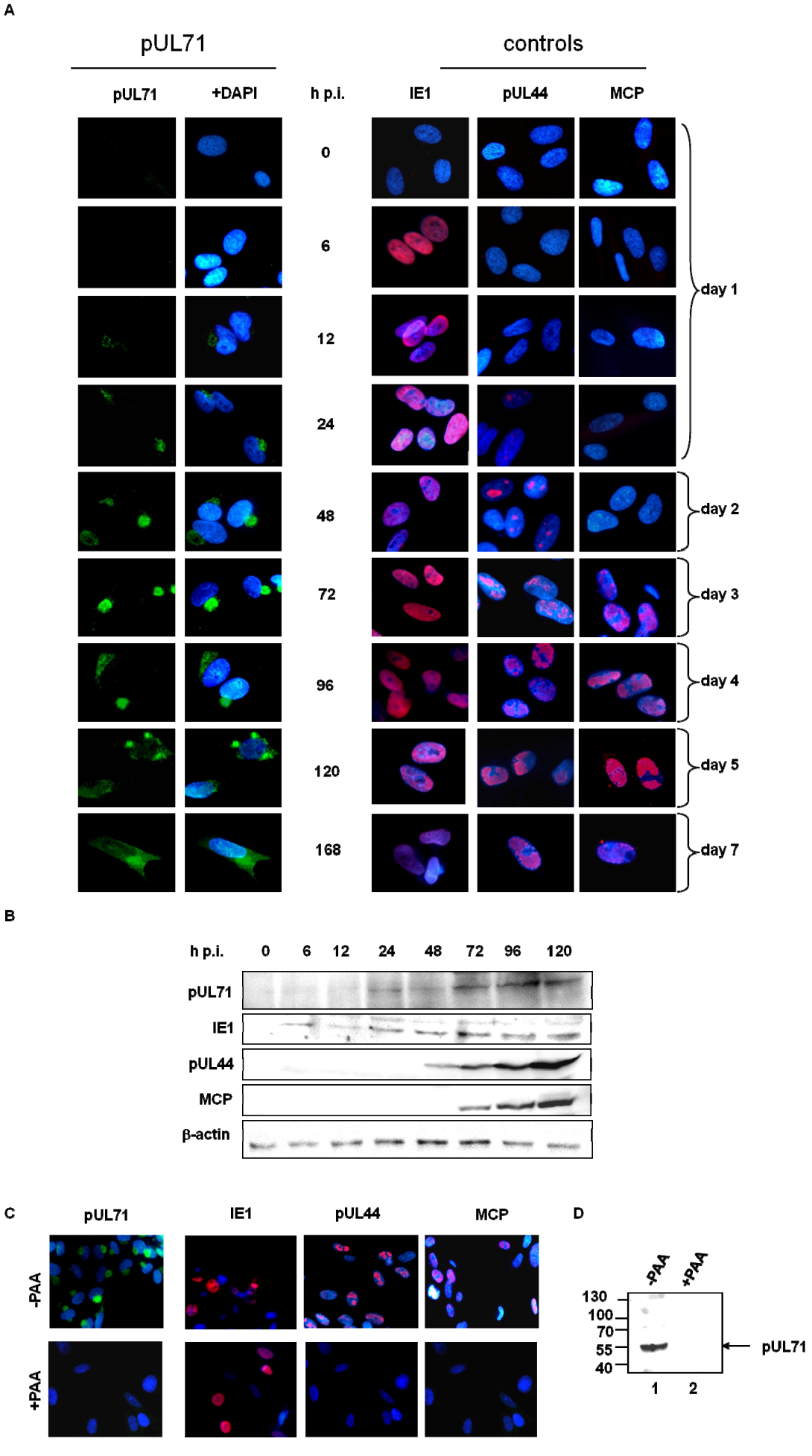
A
pUL71
controls
pUL71
+DAPI
h p.i.
IE1
pUL44
MCP
0
6
12
24
48
72
96
120
168
day 1
day 2
day 3
day 4
day 5
day 7
B
h p.i.
0
6
12
24
48
72
96
120
pUL71
IE1
pUL44
MCP
β-actin
C
pUL71
IE1
pUL44
MCP
-PAA
+PAA
D
-PAA
+PAA
130
100
70
55
40
pUL71
1
2

Figure 14: Expression of pUL71 within the viral life cycle. (A) *HFF*s were infected with a MOI of 2 and fixed at indicated time points (0, 6, 12, 24, 48, 72, 96, 120, 168h p.i.) for immunofluorescence analysis. Cells were reacted wit DAPI and specific antibodies. Expression kinetic was obtained for pUL71 using pAbUL71 (green, pUL71) as well as for IE1 using mAbIE1 (red, controls lane IE1), pUL44 using mAbUL44 (red, controls lane pUL44) and MCP using mAbMCP (red, controls lane MCP). (B) *HFF*s were infected with a MOI of 2 and cells were harvested at indicated time points (0, 6, 12, 24, 48, 72, 96, 120h p.i.), separated by 8% SDS-PAGE and analysed by immunostaining. Immunoblots were reacted with pUL71 (upper panel, pUL71), mAbIE1 (2nd panel IE1), mAbUL44 (third, panel pUL44), mAbMCP (fourth, panel MCP) and pAbβ-actin (lowest panel β-actin). (C) Influence of inhibitor substance PAA on pUL71 expression was analysed by immunofluorescence in MOI 2 infected *HFF*s at 72h p.i.. Cells were grown in the absence (upper panel) and presence (lower panel) of PAA. Protein expression was analysed using pAbUL71 (green, lane pUL71) mAbIE1 (red, lane IE1), mAbUL44 (red, lane pUL44) and mAbMCP (red, lane MCP). (D) The effect of PAA on pUL71 was further analysed using immunostaining. *HFF*s were infected with a MOI of 2 grown in the absence (lane1) and presence (lane2) of PAA, harvested 72h p.i., separated by 8% SDS-PAGE and analysed with pAbUL71. Arrows on the right side indicate the position of pUL71. Molecular weight markers (M) are shown on the left.

For immunostaining a similar expression kinetic as in immunofluorescence studies is detected for all proteins tested, e.g. pUL71 (Figure 14. B, upper panel (pUL71)) IE1 (Figure 14. B, second panel (IE1)), pUL44 (Figure 14. B, third panel (pUL44)) and MCP (Figure 14. B, lower panel (MCP)). Expression of pUL71 (Figure 14. B, upper panel (pUL71)) is detected from 48h p.i. onwards increasing over time.

To further determine the time of pUL71 expression within the programmed cascade of *HCMV* translation, a chemical compound phosphonoacetic acid (PAA) was applied that inhibits the expression of proteins dependent upon expression of the viral polymerase gene (UL54) (220). The expression of pUL71 (Figure 14. C, lane pUL71), IE1 (Figure 14. C, lane IE1), pUL44 (Figure 14. C, pUL44) and MCP (Figure 14. C, MCP) at 72h p.i. was analysed in the absences (Figure 14. C, upper panel) and presence (Figure 14. C, lower panel) of PAA. Addition of PAA resulted in inhibition of expression of pUL71, pUL44 and MCP. Since pUL71 is expressed from 48 h p.i onwards but dependent on expression of viral DNA polymerase it is supposed to have an early late expression kinetic. These findings were further verified by immunostaining. Again pUL71 expression at 72h p.i. was analysed in the absence (Figure 14. D, lane 1) and presence (Figure 14. D, lane 2) of pUL71. In line with the previous observation, pUL71 was only detected in the absence of the inhibitor. Taken together, pUL71 is expressed with an early-late kinetic in a distinct junxtanuclear expression pattern in the cytosol.

3.2.4 pUL71 and the assembly complex (AC)

As shown in the previous immunofluorescence study (e.g. Figure 14. A, pUL71, 72h p.i.) pUL71 shows a very specific cytosolic expression pattern. Similar patterns are described in literature for pp28 (203, 209) and other proteins (202) involved in egress of viral particles as well as for cellular components of the endoplasmatic reticulum (ER) and Golgi apparatus (Golgi) (47, 70, 71, 101) in *HCMV* infected cells. To analyse if pUL71 is arranged or even directly interacting with these structures termed assembly complex (AC) (70) confocal immunofluorescence microscopy will be used.

*HFF*s were mock-infected or *AD169*-infected and fixed 72h p.i prior to antibody staining against cellular (GM130, p230) and viral markers for AC (pp28). The localisation of the Golgi was analysed using mAbGM130 to stain for marker protein GM130 and of the trans-Golgi network (TGN) using mAbp230 for p230. In Figure 15. A, C these structures were analysed in mock-infected cells, whereas in Figure 15. B, D the reorganisation of those structures upon viral infection is shown. Fig. E and F shows the localisation of pp28- a large tegument protein- both in mock-infected or *AD169*-infected cellss using mAbpp28. All markers of the AC are stained in red; pUL71 is always stained in green. On the micrograph B we detect a similar distribution but not a spatial co-localisation between Golgi-markers and pUL71, the same is seen for the TGN-marker (Figure 15. D) and pp28 (Figure 15. F). Although some proteins spatially co-localise the overall distribution pattern shows no hint on a direct interaction. Taken together, we conclude that the junxtanuclear localisation of pUL71 is similar in shape and localisation to the AC. Still no direct interaction between pUL71 and the AC was observed with the three markers tested in this study.

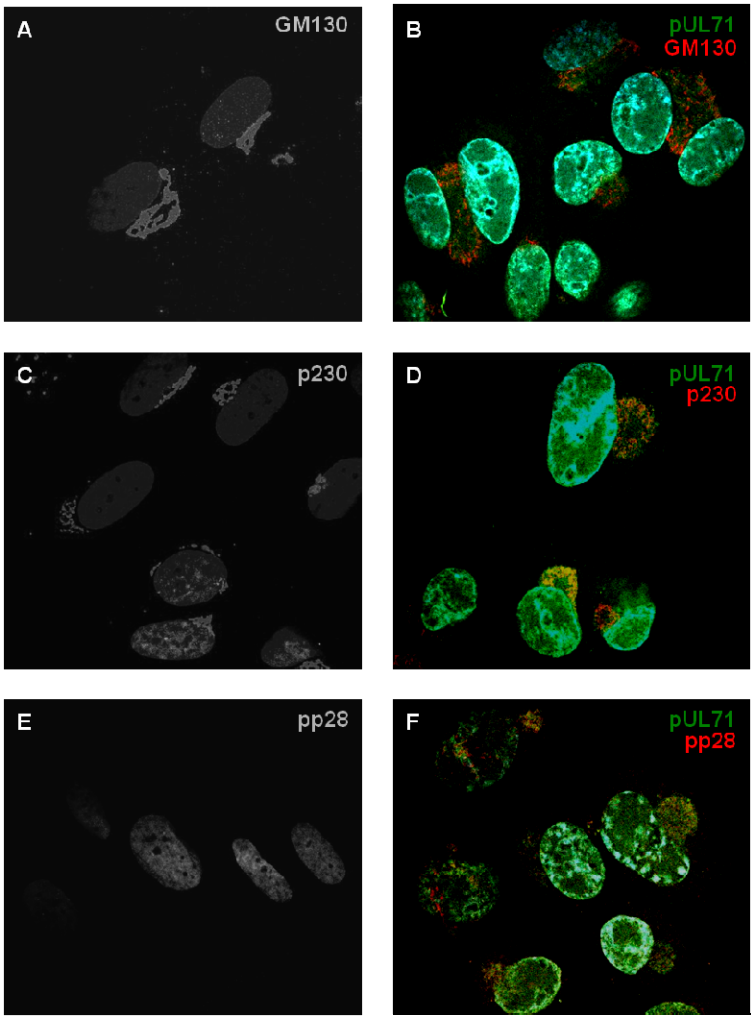

Figure 15: Spatial localisation to the assembly complex (AC). *HFF*s were mock-infected or *AD169*-infected at a MOI of 2, fixed 72h p.i. and subjected to immunofluorescence. (A) Expression pattern of Golgi-marker GM130 in mock-infected cells. Nuclei were stained with DAPI and marker protein with mAbGM130. Micrograph represented as grey scale. (B) Expression pattern of GM130 in *AD169*-infected cells. Nuclei are stained with DAPI (blue), mAbGM130 (red GM130) and pAbUL71 (green pUL71). Micrograph represents merge image. Spatial co-localisation is indicated by yellow fluorescence. (C) Expression pattern of TGN-marker p230 in mock-infected cells. Nuclei were stained with DAPI and marker protein with mAbp230. Micrograph represented as grey scale. (D) Expression pattern of p230 in *AD169*-infected cells. Nuclei are stained with DAPI (blue), mAbp230 (red p230) and pAbUL71 (green pUL71). Micrograph represents merge image. Spatial co-localisation is indicated by yellow fluorescence. (E) Negative control of viral marker pp28 in mock-infected cells. Nuclei were stained with DAPI and marker protein with mAbpp28. Micrograph represented as grey scale. (F) Expression pattern of pp28 in *AD169*-infected cells. Nuclei are stained with DAPI (blue), mAbpp28 (red pp280) and pAbUL71 (green pUL71). Micrograph represents merge image. Spatial co-localisation is indicated by yellow fluorescence.

3.2.5 Screening pUL71 against a cellular library

To test whether pUL71 might bind to cellular factors that play a role in egress of *HCMV* virions, a Yeast-two-hybrid (Y2H) screen against a cellular library was performed. Used as a bait pGBUL71 was transfected into *Y187* strain and mated with the cellular library (MEF:

Mouse Embryonic Fibroblasts in pACT2, Clontech) that was transfected into *AH109* previously. The mated colonies were applied to selective plates and analysed for growth and β- galactosidase activity. Unfortunately all clones selected in this screen turned out to be false positive after repeating the selectivity assays. A similar experiment was carried out in the group of Dr. Jens von Einem that resulted in not detecting any interaction partners of pUL71 as well (Dr. Jens von Einem, *personal communication*).

Therefore we conclude that, (i) either there are no interactions between pUL71 and cellular proteins occurring, which is rather unlikely taking the confocal images into consideration; or (ii) more likely, that the method is not applicable to detect those interactions. This could be either because of using a mouse library instead of a human derived one or the detection limit of the method is not sensitive enough to detect viral-host interactions of pUL71.

3.2.6 Screening pUL71 against a viral library

Since no interaction partners of pUL71 were found in the previous Y2H screen against the cellular library, an in-house library containing several viral proteins was constructed. This library was used in further screens.

Table 2: Screening for viral interaction partners- Summary of results of Y2H screen against the in –house library. Briefly, pUL71 as bait or prey was screened against pUL56, pUL89, pUL77, MCP, pUL104 and empty vector controls in appropriate form (bait/prey). As a read-out either using β-Gal filter activity (β-Gal) or selective growth (-His, -Ade) was analysed. Positive readout is represented by +, negative by -.

bait	prey	β-Gal	-His	-Ade
pUL56	pUL71	-	-	-
pUL89	pUL71	-	+	-
pUL77	pUL71	+	+	-
MCP	pUL71	-	+	+
pUL104	pUL71	+	-	+
Vector	pUL71	-	-	-
pUL71	pUL56	-	-	-
pUL71	pUL89	-	+	+
pUL71	pUL77	-	+	-
pUL71	MCP	-	+	-
pUL71	pUL104	-	-	+
pUL71	Vector	-	-	-

Again bait constructs were transfected into *Y187*, prey constructs into *AH109* yeast strain and analysed upon reactivation. The constructs that were negative for reactivation were combined upon mating both strains. The mated, diploid yeast colonies were applied to selective plates and analysed for growth and β- galactosidase activity in a β-galactosidase filter shift assay. Table 2 outlines the results of 5 independent experiments. Not all interactions were detected in all readouts, but Sanderson et al. (10) introduced a method defining combinations of these results as trustworthy indicators for positive interactions. Growth on selective media deficient for adenine (–Ade) as well a combination of two or more other readout methods are good indication for positive interactions. According to that only interactions between bait pUL71 and pUL77, MCP and 104 as prey, as well as pUL89 as bait and pUL71 as prey are trustworthy candidates for positive interactions.

Therefore, we can conclude that the Y2H screen gives us hints on interactions between pUL71 and the capsid and capsid-associated proteins tested. We detected interactions between pUL71 and structural proteins pUL77, pUL104 and MCP that need to be further verified by another protein-protein interaction assay.

The interaction between pUL71, that localises in the cytoplasm (3.2.3) and pUL89 that is exclusively found in the nucleus (228), is considered to have no biological relevance. Therefore, it was not further analysed in this study.

3.2.7 Confirming interactions found in the Y2H screen

In this experiment we tried to confirm interactions found in the Y2H screen between pUL71 and the subset of proteins by co-immunoprecipitation in infected cells. *HFF*s were mock-infected or *AD169*-infected. Cells were harvested 72h p.i. and extracts subjected to co-immunoprecipitation against pAbUL71.

The interaction partners were analysed by immunostaining against pUL104 (Figure 16. A), MCP (Figure 16. B), pUL77 (Figure 16. C), pUL56 (Figure 16. D) and IE1 (Figure 16. E) that served as a negative control.

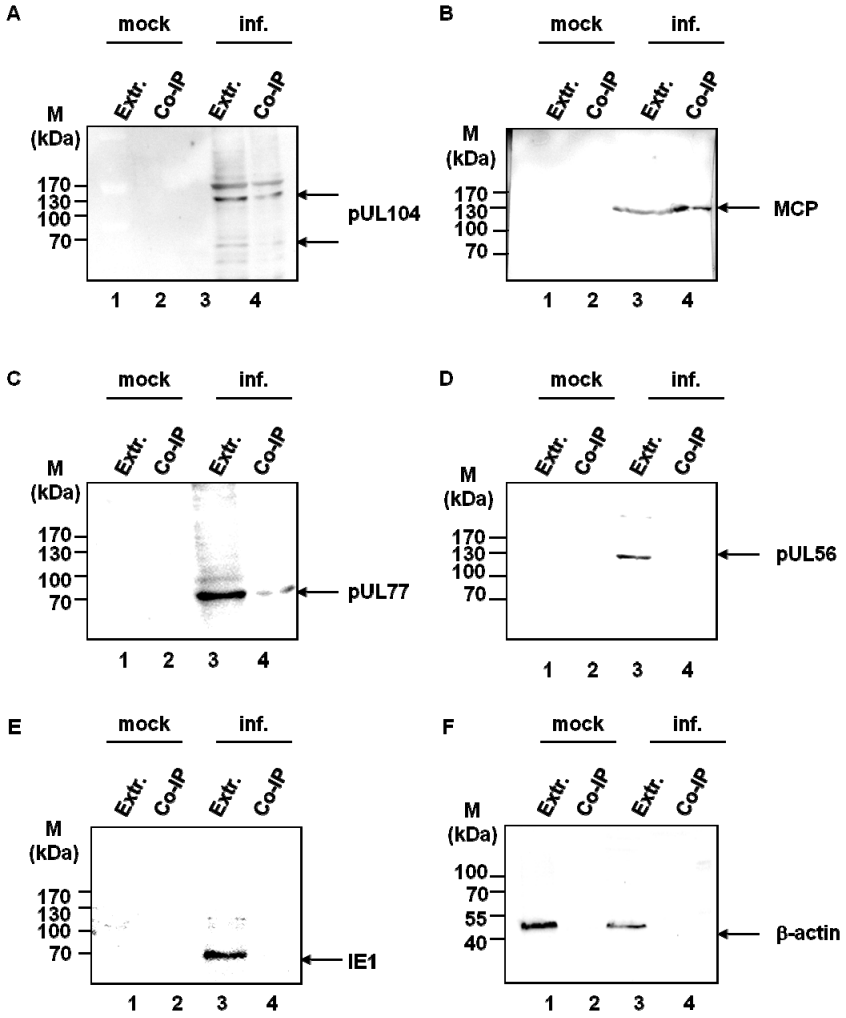

Figure 16: Verifying interaction found in Y2H screen. Mock-infected or *AD169*-infected *HFF* lysates at 72h p.i. precipitated with pAbUL77 and subjected to 8% SDS-PAGE prior to immunostaining. Mock-infected cell extracts (Extract, lane 1) and precipitates (Co-IP, lane 2) as well as *AD169*-infected cell extracts (Extract, lane 3) and precipitates (Co-IP, lane 4) were analysed. Immunostaining was performed using antibodies (A) mAbUL104, (B) mAbMCP, (C) pAbUL77, (D) pAbUL56, (E) mAbIE1 and (F) pAbβ-actin. Arrows on the right side indicate the position of proteins. Molecular weight markers (M) are shown on the left side.

The presence of pUL71 in the extract and precipitate was verified (Figure 16. F, lane 3-4) by staining with pAbUL71. No signal was detected in extract and precipitates of mock-infected cells (Figure 16. A-F, lane 1-2). In *AD169*-infected cells the extract fraction always contained pUL71 (Figure 16. F, lane 3) and the appropriated protein tested (Figure 16. A-E, lane 3). Only if the protein is detected in the precipitate as well, we will analyse a direct interaction. In this study pUL104 (Figure 16. A, lane 4), MCP (Figure 16. B, lane 4) and pUL77 (Figure 16. C, lane 4) was found in the precipitate but not pUL56 (Figure 16. D, lane 4) and IE1 (Figure 16. E, lane 4). Thus, further verifying the interactions found in Y2H screen between pUL71 and pUL104, MCP and pUL77.

3.2.8 Oligomerisation of pUL71

The detection of the higher molecular weight band in the NATIVE-PAGE using pAbUL71 (Figure 12. E) gave a hint on the putative oligomerisation tendency of pUL71. To further verify this finding baculovirus expressed recombinant protein rpUL71-Bac was purified by a combination of anionic exchange chromatography and gel filtration.

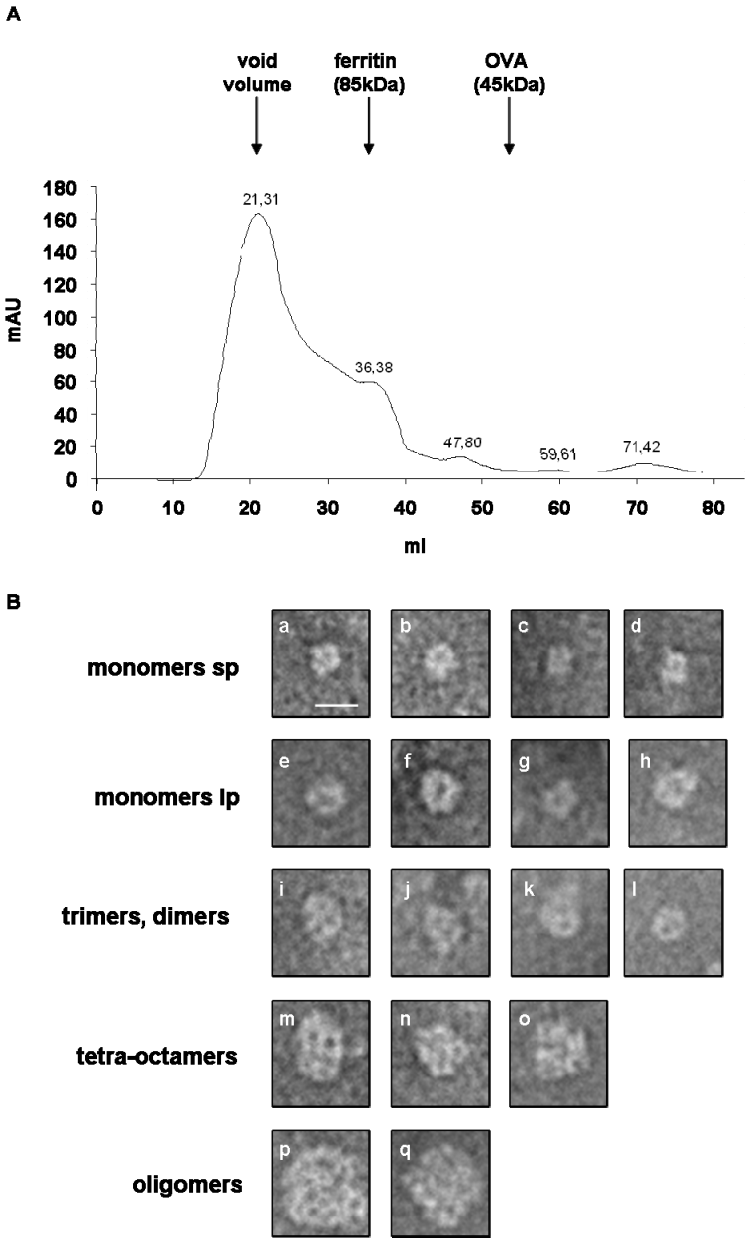

Figure 17: Oligomerisation potential of rpUL71-Bac. (A) Chromatogram of gel filtration. Peak at 35ml represents the dead volume. Marker proteins are indicated below to connect elution volume with protein size. Void Volume (= 25 ml); Ferritin (85kDa = 38ml); OVA (45kDa = 55ml). (B) Negative stained particles from sample taken at 47.8ml analysed by EM. Molecular weight (kDa) can be calculated from size of the particles (77). Different oligomers formed from the sample. Monomeric forms (a-h), dimers or trimers (i-l) and higher oligomeric forms (m-q). Bar size =200nm.

In the gel filtration fraction at 47.8 ml was taken (Figure 17. A), later on used for electron microscopy (EM) analysis. The purified protein was negative stained and subjected to EM analysis. Species of different size were detected that were calculated to be monomeric (Figure 17. B, a-h) as well as higher molecular weight forms of the protein (Figure 17. B, i-q) (cf. 77). These result hints on the ability of recombinantly expressed rpUL71-Bac to form higher ordered structures on its own.

To further test the oligomerisation ability of pUL71, samples were analysed under different SDS-PAGE condition as described by Seo et al. (209). For pp28 dimerisation studies mock-infected and *AD169*-infected *HFF* cells were harvested 72h pi. and treated under denaturating (2%SDS, 5% b-mercaptoethanol, 5' 95°C) or non denaturating (0.1%SDS, RT) conditions prior to separation by SDS-PAGE and immunostaining. The experiment described by Seo et al. was repeated to test the functionality of the method under conditions in our lab (c.f. Figure 18. A). As expected, we do not find any specific bands for pp28 in mock-infected cells (Figure 18. A, lane 1-2). Whereas we detect several bands reflecting the monomeric form of the protein at 28kDa as well as higher molecular forms at 55kDa and above 170kDa in *AD169*-infected cells under non-denaturating conditions (Figure 18. A, lane 3). On the other hand we could only detect a single band reflecting the monomeric form of pp28 in *AD169*-infected cells under denaturating conditions (Figure 18. A, lane 4). Therefore, we state that this method is suitable to test oligomerisation tendencies of *HCMV* proteins.

In Figure 18. B the method was applied to test for oligomerisation of pUL71. Again no specific bands were found in mock-infected cells (Figure 18. B, lane 1-2). In contrast diverse bands were detected applying pAbUL71 to *AD169*-infected cells treated under non-denaturating conditions. Thereby we detected a band at 55kDa that might represent the monomer, a faint band at 130kDa and a very prominent band above 170kDa representing a higher order oligomeric form of pUL71 (Figure 18. B, lane 3). In extracts treated under denaturating conditions only one specific band at 55kDa was detected (Figure 18. B, lane 4). These results further indicate the ability of pUL71 to form higher ordered structures in infection.

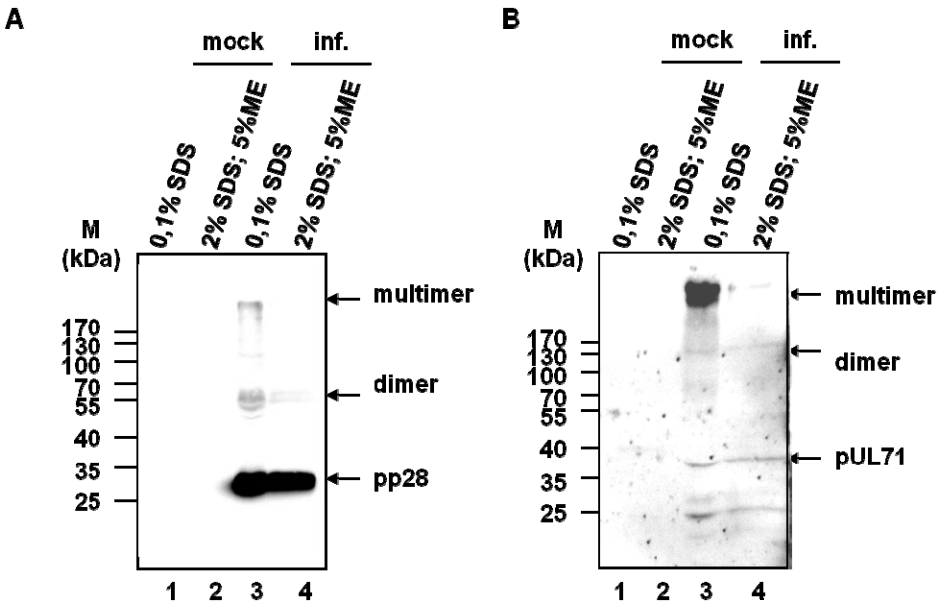

Figure 18: Oligomerisation under different SDS-PAGE conditions. Mock-infected and *AD169*-infected *HFF*s were harvested 72h p.i. and equivalent samples were analysed by 8% SDS-PAGE prior to immunostaining. Samples were prepared under different conditions. (A) Immunostaining against pp28 to analyse the oligomeric forms of pp28 in mock-infected (lane 1-2) and *AD169*-infected (lane 3-4) cells treated under non-denaturating (0.1% SDS, lane 1,3) or denaturating (2% SDS, 5% ME, lane 2,4) conditions. (B) Immunostaining against pUL71 to analyse the oligomeric form of pUL71 in mock-infected (lane 1-2) and *AD169*-infected (lane 3-4) under non-denaturating (0.1% SDS, lane 1,3) or under denaturating (2% SDS, 5% ME, lane 2,4) conditions. Molecular weight markers (M) are indicated on the left. Arrows indicate molecular weight forms of analysed proteins.

3.2.9 The leucine zipper motif

Since oligomerisation seems to be a characteristic of pUL71, we were interested in elucidating motifs in the amino acid (aa) sequence itself that serve as interaction domains.

Therefore, several *in silico* analyses using programs Motif Runner Version 1.0 (http://www.generunner.net/) and motif scan (http://myhits.isb-sib.ch/cgi-bin/motif_scan) scanning HAMAP profiles, PROSITE patterns, SMART, PFAM and FT-lines virtual motifs databases were performed.

The results of those *in silico* motif scans are summarised in Table **3**. The only motif with a potential to influence oligomerisation is the leucine zipper motif or also called bZip domain that was first described by Landschulz et al. (130) as an interaction domain in DNA binding protein GCN4 in yeast. O'Shea et al. (173, 174) described the motif to be composed of at least four heptads with hydrophobic amino acids at position 1 and 4 forming a hydrophobic core. In other words the leucine zipper motif facilitates dimerisation through parallel coiled-coil motifs and binds DNA through its hydrophobic domain. This domain is unstructured in the

absence of DNA and adopts a helical structure upon binding, thereby describing a class of DNA binding proteins (19, 45, 94, 121, 237). In more recent publication this motif is no longer restricted to DNA binding but generally accepted as a protein-protein interaction domain (141, 189).

Table 3: Conserved motifs of pUL71. Table summarises the conserved motifs calculated by *in silico* analysis using Motif Runner Version 1.0 (http://www.generunner.net/) and motif scan (http://myhits.isb-sib.ch/cgi-bin/motif_scan) with HAMAP profiles, PROSITE patterns, SMART, PFAM and FT-lines virtual motifs databases. Resulted motif type and amino acid positions are indicated.

Motifs	Position (aa)
Phosphorilation sites	
cAMP- and cGMP-dependent kinase	350-353
Casein kinase II	51-54, 130-133, 148-151, 210-213, 301-304, 340-343
Protein kinase C	108-110, 285-287, 340-342
Leucine zipper motif	34-55
N-myristoylation site	173-178
Herpes virus U44 protein (140)	21-166 (E-value = $4.6\ 10^{-19}$)

To illustrate the domain in pUL71 aa 34-55 were represented in an alpha-helical wheel (Figure 19. A) and analysed its physicochemical properties using HeliQuest software (Figure 19. B) (89). The classical leucine zipper motif is disturbed by asparagin (N44) on position 4 (35). Though, we find a rather large hydrophobic face (L55, L37, L48, L41, L34, P52, F45) consisting of the leucines on position 1 and some other hydrophobic aa on positions 4 and 5 of the heptads (Figure 19. A and B). Therefore we conclude that this motif although not being a classical leucine zipper motif, still has potential to mediate hydrophobic interactions resulting in oligomerisation of pUL71. Therefore we will further refer to the motif as a leucine zipper-like motif.

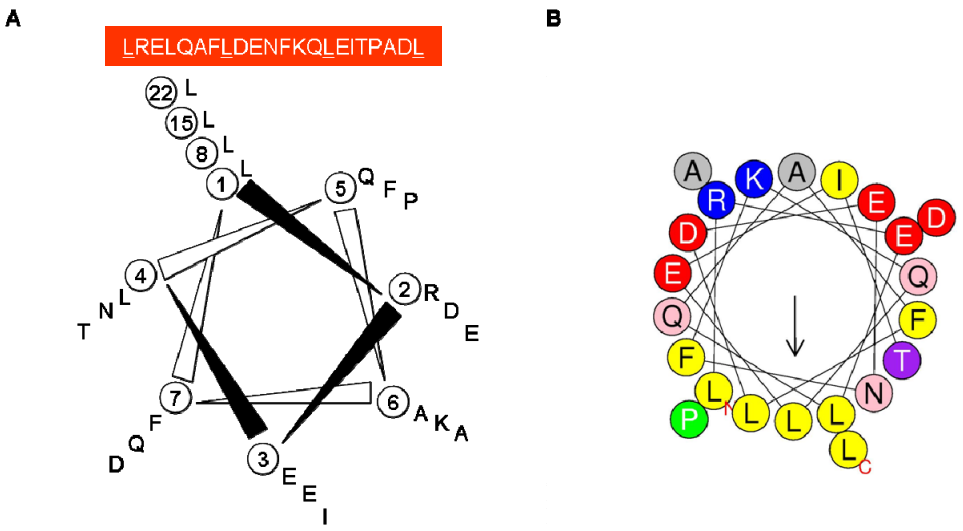

Figure 19: Analysing physicochemical properties of the putative leucine zipper motif. (A) Representation of amino acids 34-55 in an alpha-helical wheel. Positions on the heptad are indicated by numbers 1-7. The important positions 1, 8, 15 and 22 are specially indicated. (B) Representation of physicochemical properties in an alpha-helical wheel using HeliQuest. Polar amino acids are represented in red (D, E: - charge) and blue (R, K: + charge); Polar amino acids in pink/ violet (Q, N, T); Hydrophobic in yellow (F, L, I) and such that are not disturbing hydrophobicity are marked in grey (A) or in green (P) for their aromatic side-chain. The hydrophobic core spans from L-L-L-L-L-P-F.

In a *HCMV* genome wide scan we analysed the abundance of such leucine zipper motifs. Out of 162 proteins expressed from *HCMV* (82, 239), in sequence NC_006273.2 (81) we detected only 11 proteins containing one or more leucine zippers. In other words, leucine zippers are found in 7% of all protein content reflecting a not highly abundant motif. (Figure 20). Most of these proteins, like pUL14, pUL50 (43, 200, 157, 158), pUS14 (70), pUS17 (69, 70), pUS20 (160), pUS29 (160) are membrane associated. Some are related to DNA packaging like pUL51 (36), pUL104 (77, 78, 79) and for some the function is not fully elucidated yet (pUL48 (120, 254), pUL88 (23)). Since the exact function of the motif is not elucidated in any of those proteins one has to speculate that they serve different purposes within the proposed protein function by facilitating protein-lipid, protein-DNA and protein-protein interactions.

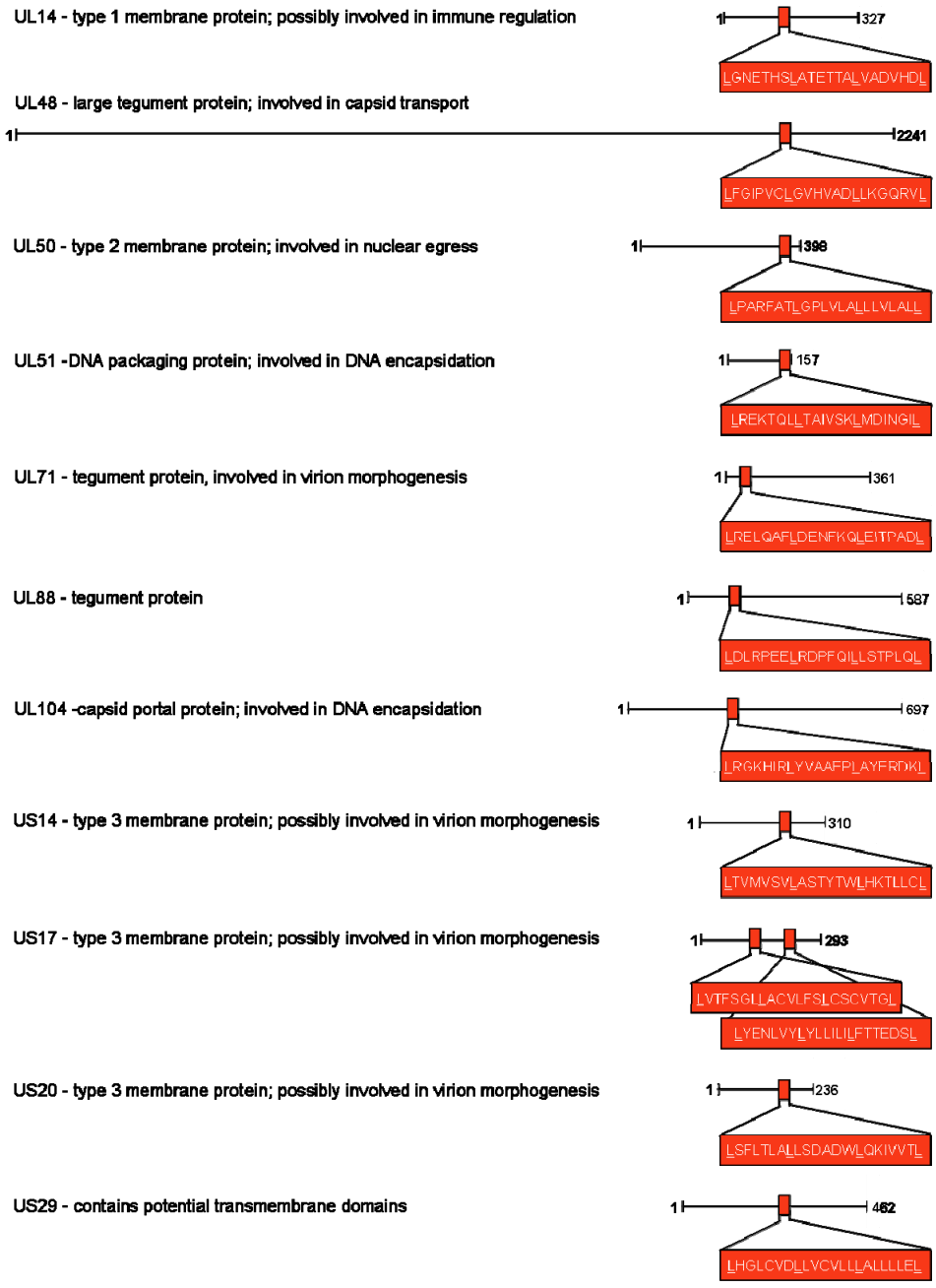

Figure 20: Abundance of leucine zipper motifs in the *HCMV* proteome. Schematically representation summarises results from *HCMV* proteome-wide leucine zipper motif scan. For *in silico* analysis motif scan (http://myhits.isb-sib.ch/cgi-bin/motif_scan) software was used. Resulting proteins are indicated. Name and function is marked on the left, sequence and position of leucine zipper motifs within the amino acid sequences are represented by a red squares shown on the right.

Taken together, we conclude that such a leucine zipper motif is not completely unknown but not very abundant in *HCMV* proteins. Thus, hinting that the *in silico* prediction has resulted in a motif potentially present in the actual protein.

To identify whether the leucine zipper-like motif functions as an oligomerisation domain of pUL71 *in vitro*, different mutants as well as the full length protein were *in silico* analysed prior to applying it to protein-protein interaction studies.

First a subset of alterations was introduced into UL71 affecting either individual amino acids or the whole motif. Five different constructs the wt UL71 71_wt, the three point single nucleotide change mutations L1 (L34A/L41A), L2 (L34A/L41A/L55A), L3 (L34A/L41A/L48A/L55A) and deletion mutant ΔLZ (Figure 21. A, 1-5) were analysed. Prior to subjection to *in vitro* studies constructs were analysed using secondary structure prediction software p-coils, coils, psi-pred and quick2_d. (29). In Figure 21. B we see the results of p-coils analyses. The exchange of two leucines into alanine at amino acids 34 and 44 resulted in loss of the predicted coiled-coil domain in the leucine zipper-like motif. While we see a peak of 0.2 on the probability scale [window 14] in 71_wt (Figure 21. B, 71_wt), none is detected in prediction for L1 (Figure 21. B, 71_L1). A loss of the predicted coiled-coil structure is observed as well for the more invasive mutations 71_L2, 71_L3 and 71_ΔLZ (Figure 21. B, 71_L2, 71_L3 and 71_ΔLZ).

The loss of the coiled-coil structure through the amino acid exchange hints on a corresponding loss in interacting ability of those mutants. To test this hypothesis the constructs were applied to *in vitro* assays.

Figure 21: Mutational analysis of the leucine zipper-like motif in pUL71. (A) Schematically representation of leucine zipper-like motif (red bar). Exchanged amino acids are indicated in white. Constructs 71_wt (L R E L Q A F L D E N F K Q L E I T P A D L), 71_L1 (A R E L Q A F A D E N F K Q L E I T P A D L), 71_L2 (A R E L Q A F A D E N F K Q L E I T P A D A), 71_L3 (A R E L Q A F A D E N F K Q A E I T P A D A) are carrying two or more single nucleotide exchanges on heptad positions 1. Complete deletion of leucine zipper motif is constructed in 71_ΔLZ. (B) Analysis of coiled-coil structures using p-coils software. Result for 71_wt is depicted on the left, result for 71_L1 on the right. Position of leucine zipper-like motif within the amino acid sequence is indicated by the red square. p-coils uses sliding windows of 14 (green), 21 (blue), and 28 (red).

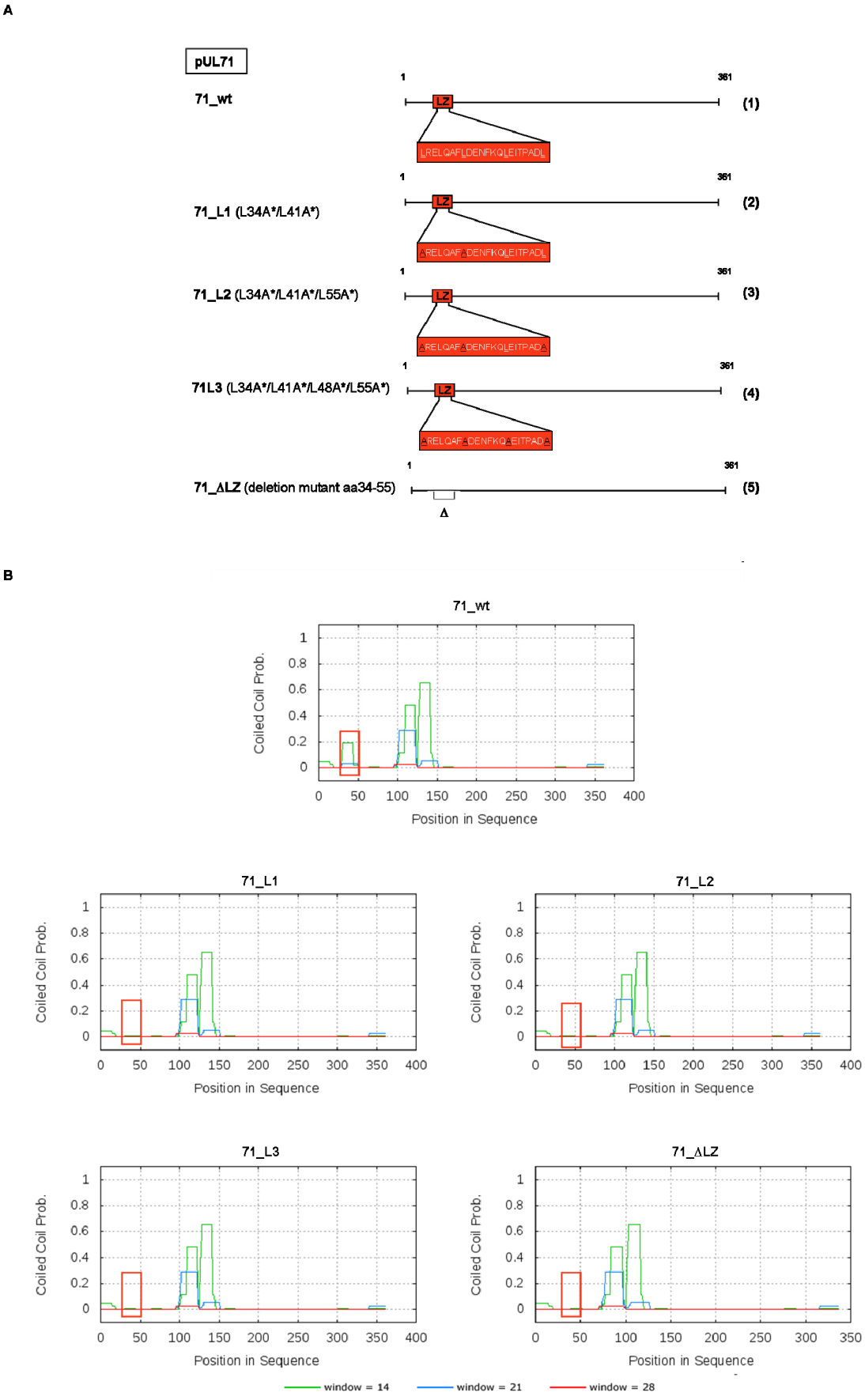

Figure legend for Figure 21 on page 94.

3.2.10 Analysis of the leucine zipper-like motif *in vitro*

To test the predicted interaction domain the *in silico* analysed constructs (cf. Figure 21) were cloned into vectors expressing proteins fused to fluorophores and later on used in biomolecular fluorescence complementation (BiFC) assays.

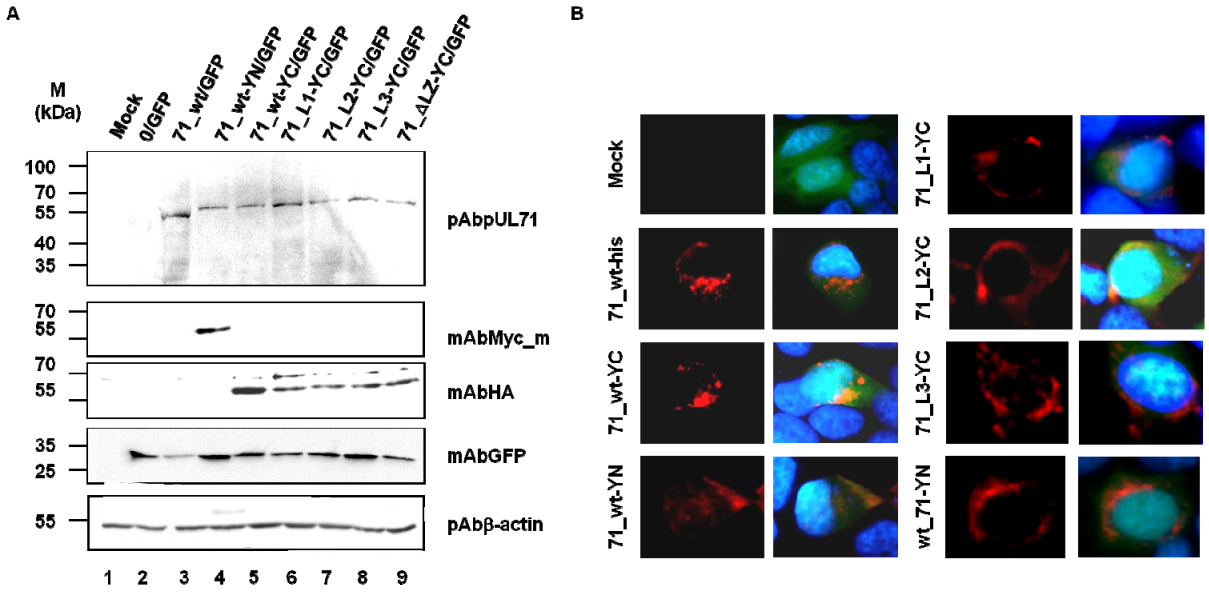

Figure 22: Optimising the BiFC-system. *Hela* cells were transfected with constructs later on used for BiFC: none- tagged pcDNA71 (71_wt), YN- tagged pcDNA71_wt-YN (71_wt-YN) and YC-tagged (i) pcDNA71_wt-YC (71_wt-YC), (ii) pcDNA71_L1-YC (71_L1-YC), (iii) pcDNA71_L2-YC (71_L2-YC), (iv) pcDNA71_L3-YC (71_L3-YC), and (v) pcDNA71_ΔLZ-YC (71_ΔLZ-YC) together with expression control pcDNA3.1-GFP (GFP). (A) Cells were harvested 24h after transfection and analysed by immunostaining using specific antibodies against pUL71 (pAbUL71, upper panel), against the tags (mAbMyc_m, second panel; pAbHA, third panel), against GFP (mAbGFP, fourth panel) and to control equal protein amounts against β-actin (pAbβ-actin, lower panel). (B) Cells were fixed 24h after transfection and analysed by immunofluorescence. Transiently expressed pUL71 forms 71_wt, 71_wt-YN, 71_wt-YC, 71_L1-YC, 71_L2-YC, 71_L-YC and 71_ΔLZ–YC were stained with pAbUL71 in red, GFP-expression is detected in green and nuclei were stained with DAPI.

Firstly, conditions were tested further used in BiFCs. To verify that I_{BiFC} values measured later on are dependent upon interacting proteins, the level of transient protein expression was tested. Constructs were transfected together with a GFP-construct to assay the expression efficiency of the cells. The best results were obtained using following conditions: *Hela* cells at 70% confluence were starved prior to transfection and grown 16h at 37°C follow by 30' at 32°C. Protein expression was analysed using immunostaining and immunofluorescence. Immunostaining shows that YN-tag on 71_wt-YN (Figure 22. A, lane 4) and YC-tags on 71_wt-YC, 71_L1-YC, 71_L2-YC, 71_L3-YC and 71_ΔLZ-YC (Figure 22. A, lane 5-9) do not interfere with protein-expression compared to the none-tagged wild type form (Figure 22. A, lane 3). In line with that also mutations in the leucine zipper-like motif do not interfere

with protein-expression. Amounts of protein are comparable to 71_wt-YC (Figure 22. A, comparing lane 5 with lanes 6-9). In line with the immunostaining data intracellular localisation is not disturbed through tags or mutations (Figure 22. B) Therefore, we conclude that the conditions tested are applicable for BiFCs.

Cells were grown on cover slips prior to transfection with both transient expression constructs fused to one half of the fluorophores YFP. Briefly, a combination 71_wt-YN fused to the N-terminal and various species of pUL71 fused to the C-terminal part of YFP were expressed (71_wt-YC, 71_L1-YC, 71_L2-YC, 71_L3-YC and 71_ΔLZ-YC). In addition, a construct expressing mCherry was co-transfected. Cells were grown under conditions determined above, prior to fixation for immunofluorescence.

Examples for raw data (Figure 23. A, upper panel left to right: vector-YC: pcDNA*71_wt-YN/* pcDNA-YC + *pcDNA3.1-mCherry;* 71_wt-YC: pcDNA*71_wt-YN/pcDNA71_wt-YC* + *pcDNA3.1-mCherry*; 71_L1-YC: pcDNA*71_wt-YN/* pcDNA*71_L1-YC* + *pcDNA3.1-mCherry*; lower panel left to right: 71_L2-YC: pcDNA*71_wt-YN/* pcDNA*71_L2-YC* + *pcDNA3.1-mCherry*; 71_L3-YC: pcDNA*71_wt-YN/pcDNA71_L3-YC* + *pcDNA3.1-mCherry;* 71_ *ΔLZ* -YC: pcDNA*71_wt-YN/pcDNA71_ΔLZ-YC* + *pcDNA3.1-mCherry)* are given. Expression of YFP is indicated by arrows. The YFP-Intensity (I_{YFP}) of each acquired micrograph was measured relatively to mCherry expression ($I_{mCherry}$) according to this formula $I_{BiFC} = \frac{I_{YFP}}{I_{mCherry}}$ using Axiovision software 4.8 to allow quantitative comparison of I_{BiFC} between different cells. Results are represented in a histogram (Figure 23. B). I_{BiFC} was set to 100% for 71_wt-YN/71_wt-YC. In comparison to the interaction between both wild type forms I_{BiFC} was reduced to approximately 40% for all other interactions. This numbers are comparable to I_{BiFc} detected for empty vector. Data is highly significant since between 47 and 153 cells were analysed for each form and p-values were calculated. Thus, indicting that an alteration in the leucine zipper motif results in a loss of interaction between the two proteins and therefore in a decrease in YFP expression.

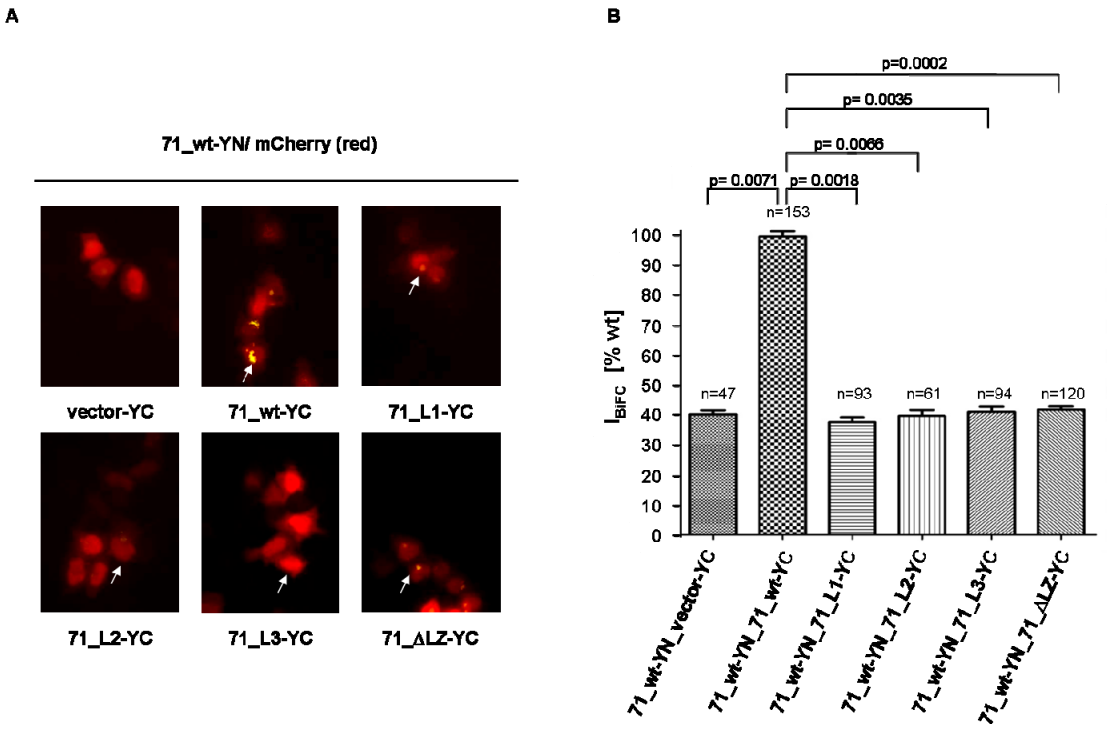

Figure 23: Analysing oligomerisation potential of pUL71 using BiFC. Cells were grown on cover slips prior to transfection with a combination of pcDNA71_wt-YN (71_wt-YN) and constructs pcDNA-YC (Vector-YC), pcDNA71_wt-YC (71_wt-YC), pcDNA71_L1-YC (71_L1-YC), pcDNA71_L2-YC (71_L2-YC), pcDNA71_L3-YC (71_L3-YC) or pcDNA71_ΔLZ-YC (71_ΔLZ-YC). Additionally a construct expressing mCherry was transfected. Cells were fixed 24h after transfection and analysed using immunofluorescence. (A) Immunofluorescence data. Expression of YFP (YC+YN) is detected in yellow, mCherry in red. (B) Quantification of BiFC results. I_{BiFC} is set to 100% for interaction 71_wt-YN/71_wt-YC. Other interactions are set in ratio. Error bars on the histogram are ± standard deviation from three independent experiments. Statistical analysis was performed and p-values were calculated using paired Student's t-test. Significance is indicated by p-value; n: number of analysed cells.

To further verify those results, a different *in vitro* method was applied to analyse whether the leucine zipper motif serves as the oligomerisation domain in pUL71. For co-immunoprecipitations pUL71 species previously tested by *in silico* analysis and further by BiFCs were inserted into pcDNA3.1HisC and pHM1580 and transfected into *293T* cells. The cell type is changed because in contrast to BiFCs a strong protein over-expression is needed to produce sufficient protein amounts for co-immunoprecipitation.

For precipitation a specific antibody against the Myc-tag (mAbMyc_r) of 71_wt^{myc} or 71_L1^{myc}, 71_L2^{myc}, 71_L3^{myc} and 71_ΔLZ^{myc} was used prior to immunostaining against Xpress-tag of 71_wt^{xpress}. Empty vectors pHM1580 (Vector^{myc}) or pcDNA3.1+ (Vector^{xpress}) were transfected additionally. The extract fractions were stained with both antibodies to test the expression of Myc-tagged and Xpress-tagged proteins. Using mAbMyc_r we detected protein directly bound to the beads in precipitates (Figure 24. A, lane 3, mAbMyc_r).

Whereas if mAbXpress was used, a band representing 71_wt^{xpress} would only be detected in the precipitate in the sample in which 71_wt^{myc} was co-expressed (Figure 24. A, right panel, mAbXpress, 71_wt^{myc}/ 71_wt^{xpress}), thus confirming an interaction only between wild type proteins. In precipitates of vector-transfected as well as mock-infected cell extracts no specific proteins were precipitated.

Further we analysed whether the YFP-tagged constructs used in BiFCs could be directly applied to co-immunoprecipitations.

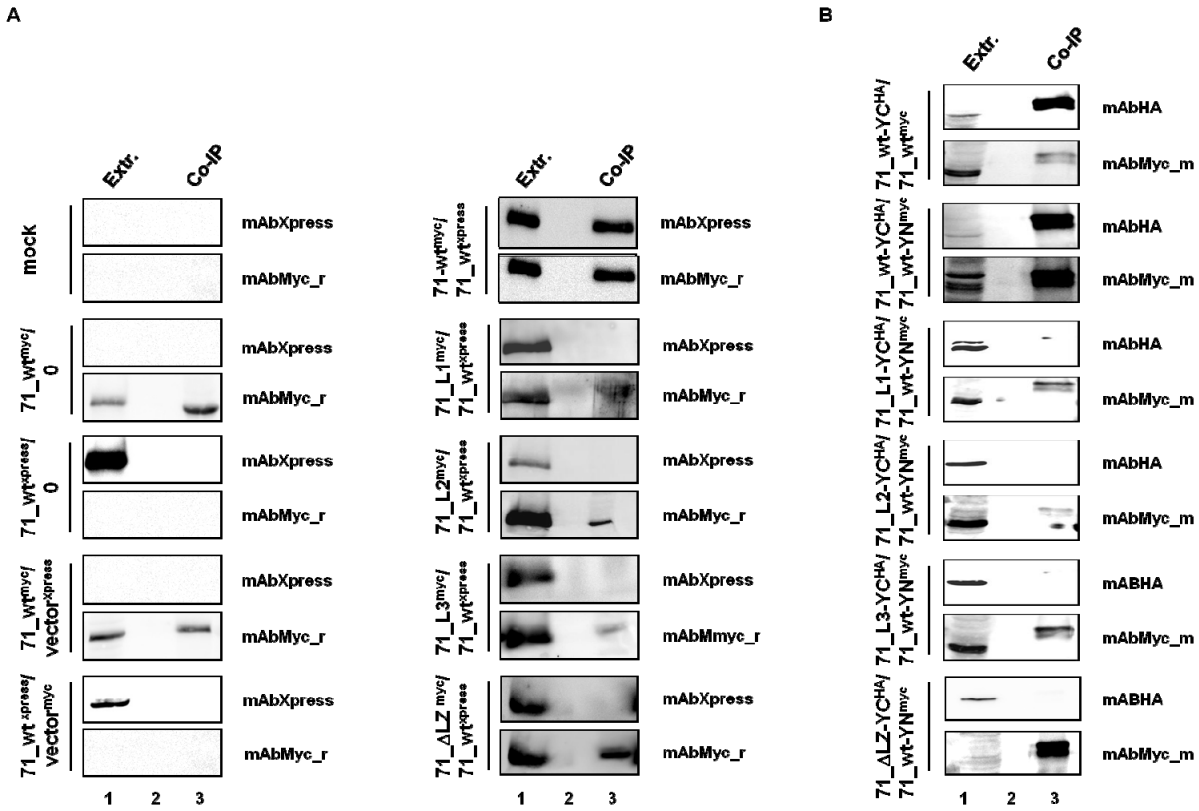

Figure 24: Analysing oligomerisation potential of pUL71 using Co-IPs. (A) *293T* cells were transfected with a combination of pcDNA71 (71-wt^{xpress}) and pcDNA71-myc (71-wt^{myc}), pcDNA71_L1-myc (71-L1^{myc}), pcDNA71_L2-myc (71-L2^{myc}), pcDNA71_L3-myc (71-L3^{myc}) or pcDNA71_ΔLZ-myc (71-ΔLZ^{myc}). As controls pcDNA71 or pcDNA71-myc were transfected alone or together with the empty vectors pHM1580 (Vector^{myc}) or pcDNA3.1+ (Vector^{xpress}). Cells were harvested 48h after transfection and subjected to precipitation against mAbMyc_r. Extract (Extr., lane 1) and precipitate (Co-IP, lane 3) fractions were analysed using mAbXpress (upper panel) and mAbMyc_r (lower panel). Lane 2 was left empty to prevent contamination upon loading. (B) *293T*s cells were transfected with constructs used for BiFCs. A combination of pcDNA71_wt-YC (71_wt-YC^{HA}) and pcDNA71-myc (71-wt^{myc}) as well as pcDNA71_wt-YN (71_wt-YN^{myc}) was transfected, respectively Further, pcDNA71_wt-YN (71_wt-YN^{myc}) was combined with pcDNA71_wt-YC (71_wt-YC^{HA}), pcDNA71_L1-YC (71_L1-YC^{HA}), pcDNA71_L2-YC (71_L2-YC^{HA}), pcDNA71_L3-YC (71_L3-YC^{HA}) or pcDNA71_ΔLZ-YC (71_ΔLZ-YC^{HA}). Cells were harvested 48h after transfection and subjected to precipitation against mAbMyc_m. Extract (Extr., lane 1) and precipitate (Co-IP, lane 3) fractions were analysed using mAbHA (upper panel) and mAbMyc_m (lower panel). Again lane 2 was left empty to prevent contamination upon loading.

Hence, mAbMyc-m against 71_wt^{myc} or 71_wt-YN^{myc} was used for precipitation, respectively. For immunostaining mAbHA against the HA-Tag (Y-P-Y-D-V-P-D-Y-A) of YC-tagged pUL71 was used. Similar results are obtained by subjecting constructs used for BiFCs to co-immunoprecipitations, in comparison to the not YFP-tagged proteins (Figure 24. B). Only pUL71 that is not altered in its leucine zipper-like motif can interact, e.g. between 71_wt-YC^{HA}and 71_wt^{myc} as well as between 71_wt-YC^{HA}and 71_wt-YN^{myc} (Figure 24. B. 71_wt-YC^{HA}/ 71_wt^{myc}; 71_wt-YC^{HA}/ 71_wt^{myc}): The C-terminal fused fluorophores YC or YN do not seem to interfere with the precipitation reaction by covering the interacting domains.

These data implicates physical interactions, which are a prerequisite for oligomerisation, are only present between two wild type pUL71. If alterations in this motif like an exchange of two hydrophobic amino acids (L1) or more invasive ones (L2, L3, ΔLZ) are caused, this function is lost. Thus, confirming the leucine zipper-like motif to facilitate direct protein-protein interaction.

3.2.11 The leucine zipper motif is associated with pUL71 function

The previous *in vitro* studies revealed that pUL71 has an oligomerisation tendency dependent upon an intact leucine zipper-like motif. Further we wanted to know whether the abolishing of oligomerisation influences viral replication. Therefore, mutations were introduced into recombinant *HCMV 71_wt-BAC* by BAC-Mutagenesis (231) resulting in the deletion mutant *71_ΔLZ-BAC* or in the single nucleotide exchange mutant *71_L1-BAC*, analogous to constructs pcDNA71_ΔLZ or pcDNA71_ΔLZ-YC and pcDNA71_L1 or pcDNA71_L1-YC both tested *in vitro*.

First, the influences of such mutations on viral replication were determined. *HFF*s were infected at MOI of 1.5 with the three viruses *71_wt-BAC, 71_ΔLZ-BAC* and *71_L1-BAC*. At indicated time points (0-168h p.i.) supernatants were harvested and titres were determined. The shedding of virus started 48h p.i. for all three viruses confirmed by an increased detection of infectious particles. Though in the following, a decreased shedding between 72h p.i. and 120h p.i of about two log phases for mutant viruses *71_ΔLZ-BAC* and *71_L1-BAC* (titre:~10^5) is observed compared to *71_wt-BAC* (titre: ~10^7). Still both mutant viruses can overcome this inhibition from 120h p.i onwards. This effect results in a growth deficiency between 72h p.i. and 120h p.i, comparing the three growth kinetics (Figure 25, *71_wt-BAC, 71_ΔLZ-BAC, 71_L1-BAC*). Therefore the results indicate that alterations in the leucine zipper motif influence the replication of the virus.

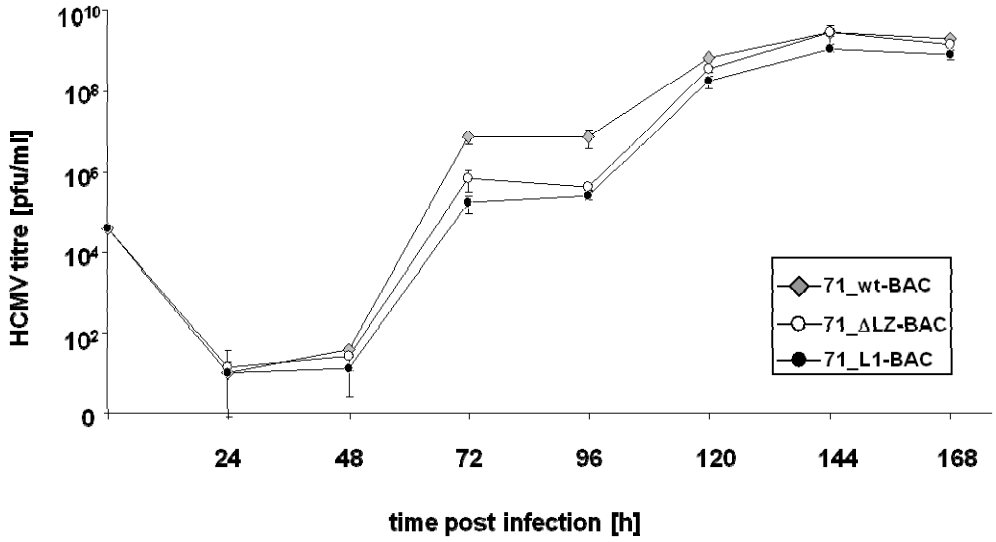

Figure 25: Growth kinetics of wt and mutant viruses. *HFF*s were infected at MOI of 1.5 with *71_wt-BAC, 71_ΔLZ-BAC* and *71_L1-BAC* for growth kinetics. Supernatants were harvested at indicated time point and progeny virus titres were determined. Error bars in the histogram indicate the standard deviation from three independent experiments. Growth of *71_wt-BAC* is represented by grey diamonds, *71_ΔLZ-BAC* by open and *71_L1-BAC* by the closed circle. pfu: plaque forming units.

While performing the plaque assays for the growth kinetic, we observed that the plaques of mutant viruses *71_ΔLZ-BAC* and *71_L1-BAC* are significantly smaller than the ones produced by *71_wt-BAC*. Therefore, we decided to analyse this observation in more detail. We infected *HFF*s on cover slips with one of the three viruses *71_wt-BAC, 71_ΔLZ-BAC* and *71_L1-BAC* at a MOI of 1.5 and grown 216h p.i. in viscous medium containing methocel. The cells were fixed, probed with specific antibody against IE1 (mAbIE1) and analysed using immunofluorescence. By analysing the plaque size we get hints about the cell-to-cell spread activity of the virus (212).

Size of the plaques is dependent on number of neighbouring cells infected via direct cell-to-cell spread. In case of the mutated viruses *71_ΔLZ-BAC* and *71_L1-BAC* this cell-to-cell spread seems to be reduced in comparison to *71_wt-BAC* (Figure 26. A)

In order to analyse this phenotype of reduced cell-to-cell spread more precisely, the effect was quantified by counting mean numbers of infected cells from each plaque. The results are represented in the histogram (Figure 26. B). Plaque size decreases about 80% comparing both *71_ΔLZ-BAC* (mean number 5 cells per plaque) and *71_L1-BAC* (mean number 8 cells per plaque) to *71_wt-BAC* (mean number 35 cells per plaque).

These results indicate that the reduced growth of mutant viruses *71_ΔLZ-BAC* as well as *71_L1-BAC* compared to *71_wt-BAC* observed in the growth kinetics is detected more pronounced in the cell-to-cell spread assay. Particularly, the reduction in viral growth seems to be even stronger when exclusively analysing cell-to-cell spread.

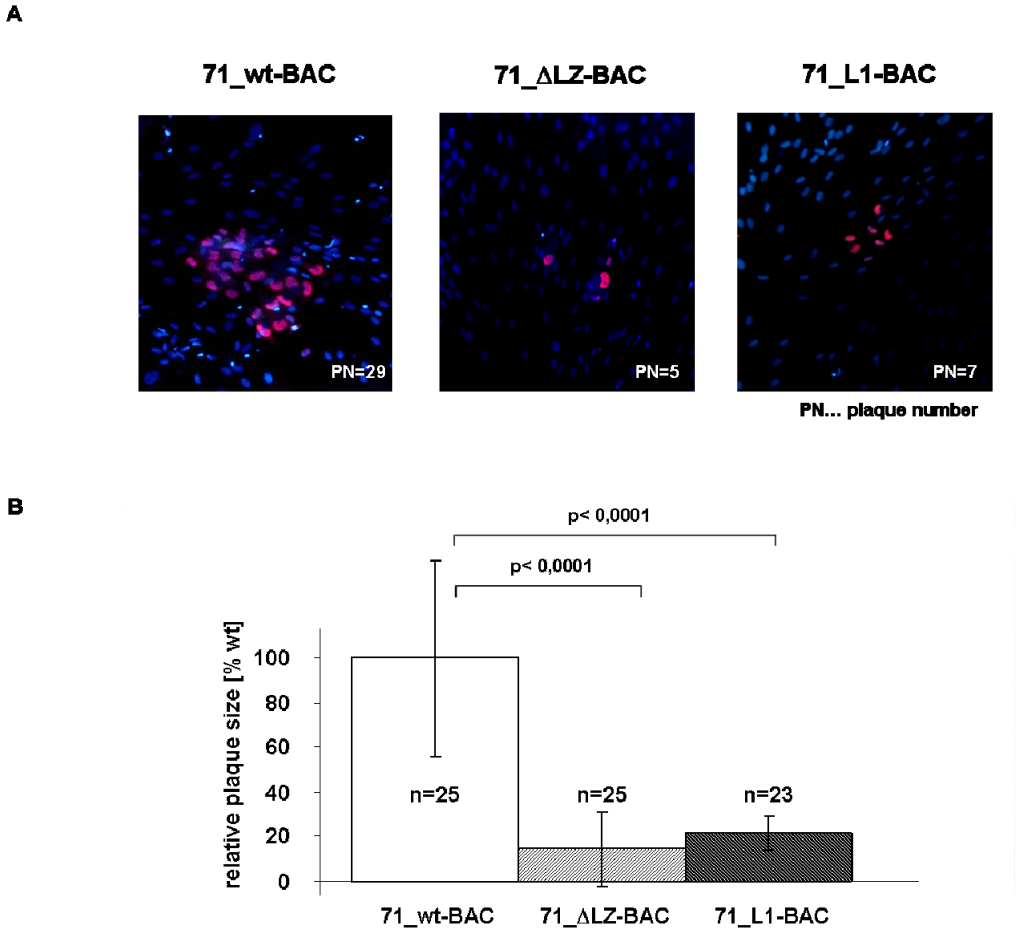

Figure 26: Analysis of cell-to-cell spread. (A) *HFF*s were infected with *71_wt-B*AC (left), *71_ΔLZ-BAC* (middle) and *71_L1-BAC* (right) at a MOI of 1.5 and grown on cover slips 216h p.i. in viscous medium containing methocel. The cells were fixed and subjected to immunofluorescence. Nuclei were stained with DAPI, infected cells with mAbIE1 (red) against IE1. A group of five or more neighbouring infected cells is defined as one plaque. Representative micrographs of plaques produced by *71_wt-BAC* (left), *71_ΔLZ-BAC* (middle) and *71_L1-BAC* (right). (B) Numbers of infected cells from each plaque of corresponding virus *71_wt-BAC, 71_ΔLZ-BAC* and 71_L1-BAC were quantified. Relative plaque size was analysed by setting mean plaque number of *71_wt-BAC* to 100% and the others in ratio. Error bars on the histogram are ± standard deviation from three independent experiments. Significance of the results was determined by using paired Student´s t-test (p-values).

To shed further light onto these observations the intracellular distribution of pUL71 in relationship to the localisation of other viral proteins was analysed using confocal microscopy.

*HFF*s were infected with viruses *71_wt-BAC, 71_ΔLZ-BAC* and *71_L1-BAC* at a MOI of 3 until fixed for immunofluorescence at 120h p.i.. In all micrographs pUL71 was stained in green, while the tegument protein pp150 (109), representing maturing virions in the cytoplasm was stained in red (Figure 27. A).

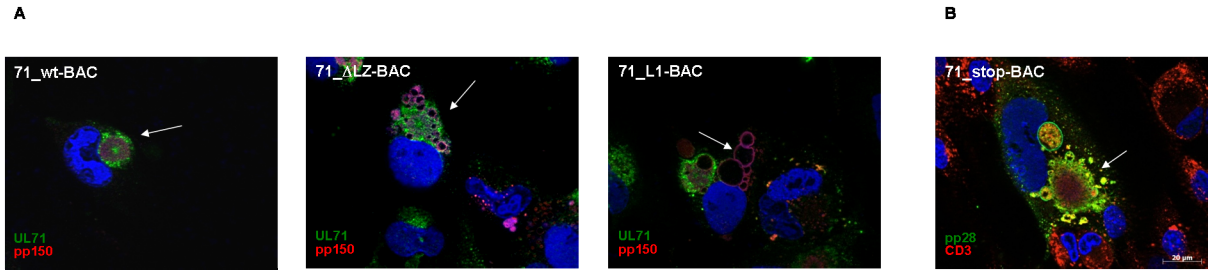

Figure 27: Intracellular localisation of pUL71 and other tegument proteins in mutants with alterations in the leucine zipper-like motif. (A) *HFF*s were infected with a MOI of 3 with one of the three viruses *71_wt-BAC* (left), *71_ΔLZ-BAC* (middle) and *71_L1-BAC* (right), respectively. Spatial distribution of viral proteins was analysed 120h p.i. by confocal microscopy using antibodies pAbUL71 against pUL71 (green) and mAbpp150 against tegument protein pp150 as a marker for maturing virions (red). Arrows indicate distribution of maturing virions in contrast to pUL71 in micrographs *71_wt-BAC* (left), *71_ΔLZ-BAC* (middle) and *71_L1-BAC* (right), respectively. (B) In comparison to A micrograph of a virus lacking the whole UL71 (*71_stop-BAC*) is reproduced from the paper Schauflinger et al. (205) with permission. To mark distribution of maturing virions in the infected cell an antibody against tegument protein pp28 was used. Vesicular structures were marked by an antibody against endosomal protein CD3.

In the micrograph *71_wt-BAC* both pUL71 and the virions (pp150) are localised to the AC in the typical junxtanuclear pattern (Figure 27. A, left, *71_wt-BAC*). Virions localise in a brood cycle (donut shape) within the spherical pUL71 pattern. In both mutant viruses *71_ΔLZ-BAC* (Figure 27. A, middle, *71_ ΔLZ –BAC*) and *71_L1-BAC* (Figure 27. A, right, *71_L1-BAC)* we see a disruption of this pattern. However, pUL71 somewhat localises in the junxtanuclear sphere whereas pp150 lost its typical distribution. A similar phenotype is described for viruses deficient for the whole UL71 open reading frame (*71_stop-BAC*) constructed on an *AD169* (248) or *TB40E* (205) backbone.

Figure 27. B is a representation of the 71-stop mutant described by Schauflinger et al. (205) that shows a similar phenotype in immunofluorescence as *71_ΔLZ-BAC* and *71_L1-BAC*. In this micrograph localisation of virions is represented by pp28 (203), tegument protein encoded at UL99, stained in green. Endosomal markers CD3 are represented in red.

In both cases virions seem to be stuck inside cellular structures that might represent vesicles if the leucine zipper motif is altered. This observation is in line with the deficiencies in growth. Therefore, we hypothesise that the function of pUL71 in the viral life cycle is dependent on intact oligomerisation that is facilitated through this motif.

To further analyse whether the observed growth defect of mutant viruses is based on a defect in virus morphogenesis ultrastructural investigations by electron microscopy were performed. Hence, *HFF*s were infected with one of the three viruses *71_wt-BAC, 71_ΔLZ-BAC* or *71_L1-BAC* at a MOI of 3. Cells were harvested 120h p.i., fixed and embedded for EM-analysis to analyse secondary envelopment (cf. 205).

We analysed 50 cells of each mutant virus on average and counted between 250 and 630 virions in the cytoplasm. Virions in the nuclei were counted as well, but no significant differences between distribution of A-, B- and C- capsids could be detected between *71_wt-BAC, 71_ΔLZ-BAC* or *71_L1-BAC*. Therefore we concentrated on the quantification of cytosolic particles and sub-classified them into five forms that were counted independently: (i) dense bodies, an accumulation of viral proteins enveloped by lipid membrane (=DB) (83, 204), (ii) non-infectious enveloped particles (NIEPs), derived from B-capsids that have lost their DNA upon packaging but undergo morphogenesis (=NP) (108), (iii) and virions prior (naked) (=N), (iv) during (=E) or (v) that completed envelopment (=V) (152, 154) (Figure 28. J). Upon general inspection we find about 50-60% less cytosolic viral products in the mutant viruses *71_ΔLZ-BAC* (Figure 28. D-F) or *71_L1-BAC* (Figure 28. G-I) compared to *71_wt-BAC* (Figure 28. A-C). This might be due to the growth defect or simply due to the selection of cells since we do not detect differences in the number of capsids produced in the nucleus. The only striking finding is the accumulation of vacuoles in *71_L1-BAC* (Figure 28. G-I) compared to the other viruses where we do not detect such an effect.

Though we detect that infected cells are increasing in size due to the assimilation of virions and other viral products, we cannot detect any structure that might represent the AC found in immunofluorescence studies with EM analysis.

Taking a closer look, we quantified different virion forms and detected that the ratio between enveloped virions and such that are prior or in the state of envelopment differ between *71_wt-BAC* and *71_ΔLZ-BAC* or *71_L1-BAC* (Table 4). This effect is obvious comparing percentages and as well as counted numbers. We detect 3 to 6 folds more mature enveloped virions in *71_wt-BAC* than in the mutant viruses *71_ΔLZ-BAC* or *71_L1-BAC*. Comparing the ratio N:E:V in one population we find 1:1:5 in other words five times more mature virions in *71_wt-BAC*. In contrast, the ratio N:E:V is 2:2:1 for *71_ΔLZ-BAC* or 2:1:2 for *71_L1-BAC* showing a tendency of towards non-enveloped particles. Hence we hypothesise, that alterations in the leucine zipper-like motif lead to viruses with less efficient secondary envelopment of *HCMV* particles.

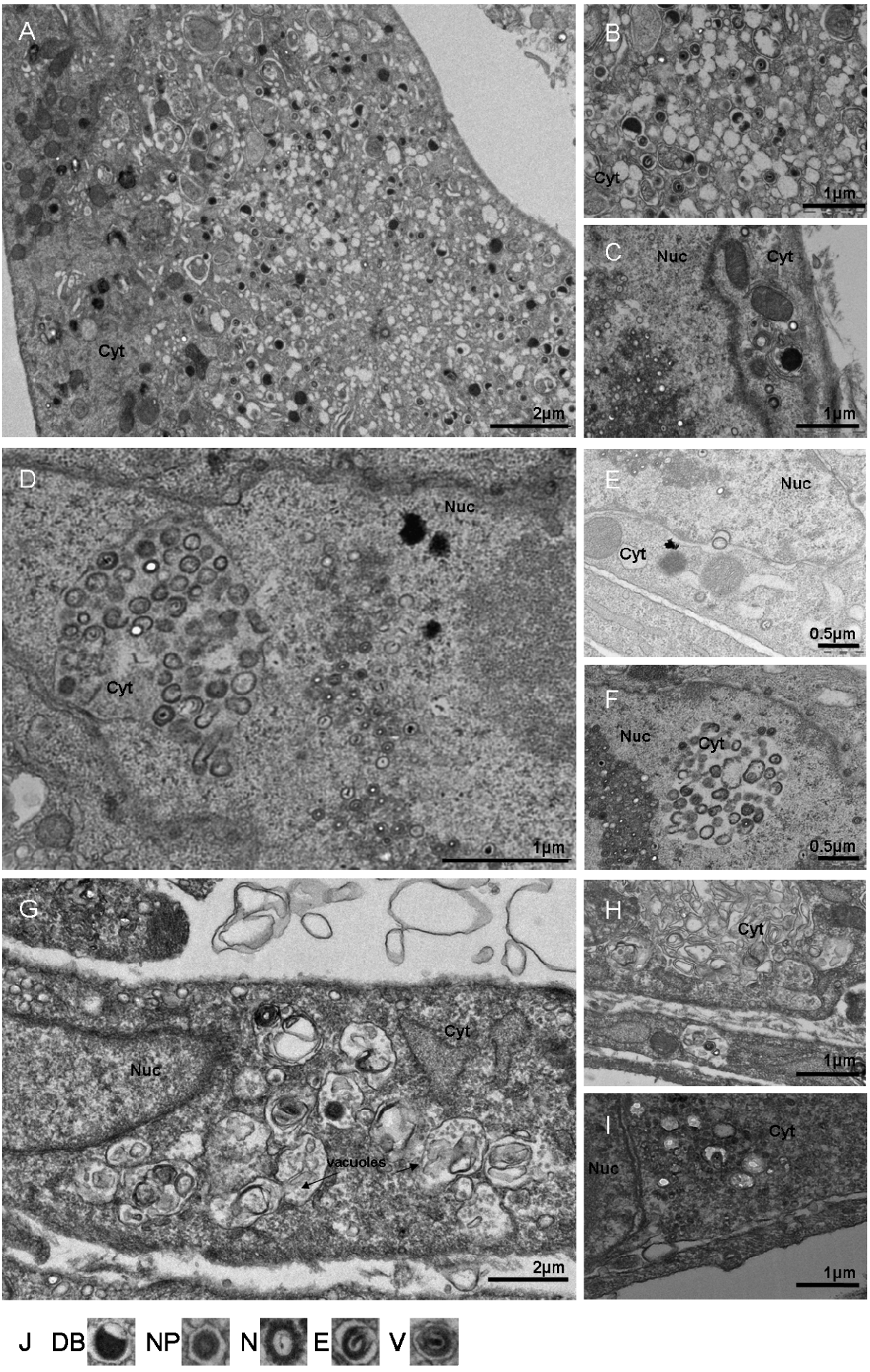
A
Cyt
2μm
B
Cyt
1μm
C
Nuc
Cyt
1μm
D
Nuc
Cyt
1μm
E
Nuc
Cyt
0.5μm
F
Nuc
Cyt
0.5μm
G
Cyt
Nuc
vacuoles
2μm
H
Cyt
1μm
I
Cyt
Nuc
1μm
J DB NP N E V

Figure 28: Localisation of virions by transmission electron microscopy (TEM) of ultra thin sections. (A-C) Selection of electron micrographs from *HFF* infected with *71_wt-BAC* 120h p.i. Overview pictures are showing cytoplasm (Cyt) and partially nucleus (Nuc) to verify that the cells are infected. (D-F) Selection of electron micrographs from *HFF* infected with *71_ΔLZ-BAC* 120h p.i. Overview pictures that show cytoplasm (Cyt) and partially nucleus (Nuc) to verify that the cells are infected. (G-I) Selection of electron micrographs from *HFF* infected with *71_L1-BAC* 120h p.i.. Overview pictures that show cytoplasm (Cyt) and partially nucleus (Nuc) to verify that the cells are infected. Striking morphological changes like vacuoles are indicated by arrows. (J) Key of viral products in the cytoplasm: DB: dense bodies; NP: non-infectious particles; N: naked virions; E: virions during envelopment; V: enveloped virions. The scale bars correspond to the indicated magnifications.

Additionally there might be a difference in protein production levels since we detect different percentages of dense bodies as well. In detail, while the number of dense bodies found in *71_wt-BAC* is around 45% of total viral products in the cytoplasm, the numbers decrease in *71_ΔLZ-BAC* to 14% and in *71_L1-BAC* even to 2% (Table 4). In addition, the reduced number of viral particles detected could be an explanation for the growth deficiency in the mutant viruses.

Taken together, in our ultrastructural investigations we observed that alterations in the leucine zipper-like motif cause a growth deficient phenotype that is dependent on insufficient secondary envelopment.

Table 4: Quantification of viral content in the cytoplasm. Counted particle numbers and percentages of each fraction relative to the total number of viral products in the cytoplasm are obtained to allow comparisons between the three viruses *71_wt-BAC, 71_ΔLZ-BAC* and *71_L1-BAC*. Values represent means ± standard deviation from three independent experiments.

	Dense bodies (=DB)	non-infectious particles (=NP)	naked virions (=N)	virions during envelopment (=E)	enveloped virions (=V)	total number of viral products in cytoplasm
71_wt-BAC	286±17.3 (45.7%)	105±22 (16.8%)	37±2.1 (5.9%)	37±5.7 (5.9%)	161±12.5 (25.7%)	626 ±80.4 (100%)
71_ΔLZ-BAC	41.8±3.3 (14.7%)	125±21.3 (44.0)	53.2±16 (18.7%)	38±11.6 (13.3%)	26.6±8.4 (9.3%)	284.6±26.9 (100%)
71_L1-BAC	4.6±4.2 (1.8%)	115±19.9 (45.5%)	55.2±12.7 (21.8%)	32.2±11.6 (12.7%)	46±12.4 (18.2%)	253±44 (100%)

To summarise the findings of the functional characterisation of pUL71 in the viral context we detected that the function of the protein is dependent upon a non altered leucine zipper-like motif. Since we verified previously that leucine zipper-like motif causes oligomerisation in *in vitro* studies, we conclude that protein function is dependent upon oligomerisation of pUL71.

If function of pUL71 is destroyed due to mutations in the leucine zipper-like motif we detect a phenotype for viruses *71_ΔLZ-BAC* and *71_L1-BAC* that is characterised by (i) a general deficiency in viral replication detected by growth kinetics assay, (ii) a diminished cell-to-cell spread, (iii) a spatial de-localisation of the virion marker pp150 from pUL71 towards vesicular structures in immunofluorescence and (iii) by insufficient secondary envelopment of viral particles ultrastructural analysis.

4 Discussion

4.1 Functional characterisation of *HCMV* pUL77

One of the crucial steps of *HCMV* maturation and a potential drug target are all processes involved in DNA packaging into preformed capsids (30, 106, 107). Therefore a deepening of our understanding of this processes are necessary. So far we understand that viral packaging is a multifunctional process in which several gene products are involved. In the case of *HSV-1* it is known that at least seven proteins, the gene products of UL6 (128, 166, 176), UL15 (20, 253), UL17 (199, 230), UL25 (144, 222), UL28 (226, 253), UL32 (50) and UL33 (16), are required for DNA cleavage and packaging. Homologous proteins pUL104, pUL89, pUL93, pUL77, pUL56, pUL52 und pUL51 (52) are found in *HCMV* but the exact mode of action of each protein and the interplay between each other is not elucidated to date.

In the present study the *HCMV* protein UL77 (pUL77), the structural homolog to *α-Herpesvirinae* pUL25, was characterised. Analyses were performed using an antibody against pUL77, pAbUL77, generated in this study. The antibody was purified from patients' sera using column affinity chromatography. This is possible since pUL77 is present in sufficient amounts in infected individuals to cause host-dependent immune response. Furthermore pAbUL77 was successfully tested for monospecificity. On the one hand a subset of monospecific antibodies was reacted against the used antigen and on the other hand pAbUL77 was reacted against commercially available immunoblot stripes containing recombinant polypeptides of the most abundant *HCMV* immunogens.

In *HCMV* infected cells pAbUL77 precipitated a protein with a molecular mass of approximately 70 kDa. The same protein size was found in infected cells separated by SDS-PAGE prior using pAbUL77 for immunostaining. For comparisons the calculated molecular mass of pUL77 is ~73kDa.

The tendency of pUL77 to form oligomers was observed in NATIVE-PAGE as well as in SDS-PAGE for extracellular virions. Since the binding seems to be rather strong, not completely lost under denaturating conditions, it is likely that the oligomer formation occurs via covalent binding. Such strong interactions are not unlikely for proteins that have to face severe pressure or other harsh environmental conditions like structural proteins of viruses as well as archeal proteins. Peters et al (180) reported that tetramers of tetrabrachion, an archeal surface protein forms a very stable complex held together by covalent binding, could only be denatured by 70% sulphuric acid or heating to 130°C for 30 min in 6 M guanidine hydrochloride. Therefore we suggest that the stability of the pUL77 oligomer under

denaturing/reducing conditions is due to a coiled-coil structure. A coiled-coil motif was identified by *in silico* prediction and further analysed by *in vitro* protein-protein interactions studies by other members of this group and combined with data of this study for the publication by Meissner et al. (149)

Further the subviral localisation of pUL77 was examined by ultracentrifugational separation steps of the virion fractions prior to immunostaining. Again pUL77 oligomers were detected in purified extracellular virions and capsids. Thus, demonstrating that pUL77 is a capsid-associated structural protein. This is in agreement with several observations with the homologous proteins of *α-Herpesvirinae* (118, 124, 229). The *HSV-1* homologue has been analysed by ultrastructural methods and was found to be located at the vertexes of the capsid (64, 165). This localisation of pUL25 was described to play a role in stabilisation of capsids during DNA packaging against the pressure that is acting upon the capsids while DNA insertion (60, 171, 235). We are hypothesising that this is a function of *HCMV* pUL77 as well.

In order to test our hypothesis, studies concerning interactions with DNA packaging motor components and structural capsid proteins were performed. Co-immunoprecitations in infected as well as transfected cells were carried out. In infected cells experiments were conducted vice versa to further verify the findings. Co-immunoprecipitations in transfected cells were performed to show that the interactions found in infected cells were direct and not dependent upon other viral proteins, that might facilitate the interaction of pUL77 to any given capsid or capsid-associated protein. In all three experiments we detected interactions between pUL77 and the major capsid protein (MCP) as well as the large terminase subunit pUL56, in contrast to all other known terminase subunits a structural component associated with the capsid, and the portal protein pUL104. The direct interactions with the DNA packaging motor components pUL56 and pUL104 support the proposed function of pUL77 during DNA packaging (33, 78, 206).

Recent findings indicate that the homologous proteins in *α-Herpesvirinae* do not interfere with DNA cleavage but are involved in later stages of packaging like generating a headfull signal to stop the packaging process or providing a cap to seal the portal and hold DNA within packaged capsids (15, 119, 144, 171, 222, 235). For *HSV-1* pUL25 it has been shown that a UL25 null virus causes an accumulation of A-capsids because of deficient DNA packaging (144). Even more recent data implicates an additional function of *HSV-1* pUL25 in entry (175, 193). In these studies direct interactions between pUL25 and the nuclear pore were demonstrated that implicate that the protein facilitates the step of DNA release from the capsids into the nucleus (193).

Anyhow, short time DNA binding would be a prerequisite for both proposed functions.

Therefore the DNA-binding ability of *HCMV* pUL77 was tested in several assays. Firstly binding to non-defined genomic DNA-cellulose was tested in an assay described previously (77) and in an optimised version using heparin-sepharose as target. Scott et al. (208) described the negative charge of immobilised heparin to mimic the electrostatic characteristics of dsDNA. Therefore heparin-sepharose can be used to bind DNA-binding proteins. Further different targets were supplied to pUL77 to answer the question whether the DNA has to be specially designed to allow binding. Either small fragments containing specific motifs by oligonucleotide synthesis (bio-pac) or longer ones by PCR (bio-250, bio-500, bio-1000) were obtained, labelled with biotin and covalently bound to avidin- sepharose beads. The bio-pac oligonucleotide corresponds to the pac1 sequence (163) and is used, because it is the only to date known motif to facilitate DNA-protein interactions in the process of packaging in *HCMV*. The motif is described as the recognition motif of the terminase complex (31). Bogner et al. used the very same specific 36-mer to analyse the interaction between pUL56 and pac1 in an electrophoretic mobility shift assay (31). We verified that it is possible to detect specific interactions between proteins and rather short dsDNA fragments (36-mer bio-pac) by applying pUL56 and therefore used the assay for further experiments.

In the case of pUL77 we found that the protein binds dsDNA but in contrast to pUL56 in a sequence-independent manner though dependent on length of applied DNA. Our results are in line with the report of Ogasawara (171) showing that *HSV-1* pUL25 binds to genomic DNA. In contrast to the terminase subunit pUL56 that only needs a 36-mer encoding pac1 the binding was only observed with the 500- and 1000-meric dsDNA. Possible explanation for this observation could be the different functions of both proteins. While the sequence specific DNA-binding of pUL56 is required to detect unique length genomes, subject them to endonuclease activity and insert them into the capsid, the association of pUL77 with DNA is more likely a temporary stabilisation. In addition, one could hypothesise that the observed effect is due to a different characteristic of the DNA. In our study we defined the relative band intensity detected on the blots by Bioimager as binding efficiency (BE) and used this for quantitative comparisons. Therefore we detected that binding between pUL77 and DNA seems to gets more pronounced with longer DNA fragments are applied. Since the enlargement of DNA fragments results in increasing negative charges we are hypothesizing to analyse an electrostatic effect. Now we wanted to know whether this effect is unspecific due to physico-chemical properties of the whole protein or a real effect.

Therefore we consider the isoelectric point (pI) of pUL77 that is 5.73, indicating the protein is negatively charged at the used physiological pH 7.3. Therefore the observed effect is not unspecific due to a positive charged protein.

Taken together all observed functions of *HCMV* pUL77 like association to the virions as a structural capsid-associated protein, that directly binds to components of the DNA packaging motor and its DNA binding ability indicate a potential function during packaging or DNA release. Up to now, further studies will need to be performed aimed at deepening of our understanding concerning the role of *HCMV* pUL77 in the viral life cycle. To further investigate whether pUL77 plays a role in entry or processes related to DNA packaging it would be interesting to analyse the ultrastructural phenotype of a recombinant virus that is deficient for pUL77. Further it would be interesting to identify the DNA binding site and generate a mutant virus with alterations in this domain. To analyse the phenotype of both recombinant virus can give us information whether the function of the protein is exclusively connected to DNA-binding.

4.2 Functional characterisation of *HCMV* pUL71

As mentioned previously in this study (cf. 1.2.4.) DNA-packaged capsids have to leave the nucleus and undergo further steps of morphogenesis in the cytoplasm before being released from the cell as mature infectious virions. Several viral proteins are described to facilitate assembly and egress of the virions among them a number of tegument proteins (91). Thereby the virus interacts with cellular proteins of the endoplasmic reticulum (43), Golgi apparatus (101), endosomal recycling complex (123), multivesicular body (47, 87) and ESCRT (endosomal sorting complex required for transport) (225) to make use of cellular trafficking pathways for virus transport and morphogenesis.

One potential candidate that might be involved in such processes is the *HCMV* protein UL71 (pUL71), the homolog of *α-Herpesvirinae* pUL51 (25, 131). In contrast to *HCMV* pUL77 and *HSV-1* pUL25 we are not analysing a structural but a positional homologue. This means that both proteins do not share significant homology at the nucleotide or amino acid level. However, *HCMV* pUL71 and *HSV-1* pUL51 are both members of the *Herpesvirus* U44 superfamily, containing a conserved functionally unclassified U44 domain (140).

Members of U44 superfamily can be found in all *Herpesvirinae*. While there is not much known about the function of *HCMV* pUL71, *HSV-1* UL51 has been shown to be a palmitylated (169) tegument-associated, late protein (67) with putative involvement in egress.

To further characterise the protein an antibody against pUL71, pAbUL71, was generated similar to specific antibody pAbUL77, generated in the first part. The antibody was tested for monospecificity prior for further usage. A protein of 55kDa was detected in the monospecificity assay, in transfected and *AD169*–infected cells separated by SDS-PAGE. By analysing NATIVE-PAGE a higher molecular weight species was detected indicating oligomerisation potential of the protein.

In *α-Herpesvirinae*, UL51 has been identified as a viral protein incorporated into viral particles (67, 119). *HCMV* pUL71 has also been characterized as part of the tegument of viral particles by mass spectronomy analysis (239). To further verify whether *HCMV* pUL71 is connected to virions, extracellular virions were isolated and subjected to fragmentation by ultracentrifugation. In this assay, pUL71 was detected both in extracellular as well as in the tegument fraction. This finding shows that pUL71 is a structural protein associated to the tegument fraction of extracellular virions and is in line with findings described for *α-Herpesvirinae* (67, 119).

For further functional characterisation it is important to know the temporal and spatial expression pattern of *HCMV* pUL71 since previous genome analyses failed to result in a clear expression kinetics of pUL71 (49).

We analysed the growth kinetics of *HCMV* pUL71 by several methods including, a time experiment and inhibitor studies by immunostaining and immunofluorescence, respectively. Our data show that pUL71 is expressed in the cytoplasm accumulating over time with an early-late kinetic. Hence, the protein is expressed from 48h p.i. onwards but dependent upon presence of viral inhibitor phosphonoacetic acid (PAA) and thereby the expression of the viral DNA-polymerase. A similar experiment was carried by another group defining the protein to be expressed with early kinetics, by applying the antiviral drug Foscarnet another inhibitor of the viral DNA-polymerase (205). Those inconsistent results are possible because both substances inhibit the viral DNA-polymerase using different modes of action; moreover pUL71 might use different promoters in our strain *AD169* compared to *TB40E* used by this group (205). Therefore, these results might not be contradictory caused by minor inconsistencies of the experimental set up instead.

In addition, our experiment showed that pUL71 is expressed in a very specific cytosolic expression pattern. A spherical rather large junxtanuclear structure is detected in the cytoplasm that seems to cause morphological changes such as a redistribution of the nucleus in a kidney –shaped form. Accumulation in comparable structures is described for a number of viral proteins (70, 99, 101, 129, 138, 202, 209, 227) during infection. These structures are

termed “assembly compartment” or “assembly complex” (AC) (101, 202). The AC was described to contain many vesicles derived from the *trans*-Golgi network, secretory, and endosomal pathway (66, 71, 87, 202, 233) because it combines all structures required for morphogenesis and final envelopment. In our confocal microscopy studies we could link *HCMV* pUL71 to distribution patterns of viral (pp28) and the cellular (GM130, p280) marker proteins for the AC. In line with our observations both *PrV* UL51 and *HSV-1* UL51 are localized at Golgi membranes in transfected cells (169). The same is true for transfected pUL71 (this study, data not shown; Dr. Jens von Einem, *personal communication*). Since *HCMV* infection induces changes in the cellular membrane system such as a spatial reorganisation of the endosomal pathway components we can conclude that homologues in all three viruses might be involved in egress (71).

This study in line with others (205, 248) showed that pUL71 is one of the viral proteins that localises in the AC. Still our data only reveals similar distribution pattern with the proteins tested; hence, it is not convincing to indicate any direct protein-protein interactions. Although some proteins spatially co-localise the overall distribution pattern shows no hint on a direct binding. This is likely since we only tested the three most prominent proteins described for the AC (71).

To test whether pUL71 might bind to cellular or viral factors that play a role in egress of *HCMV* virions, Yeast-two-hybrid (Y2H) screens against different libraries were performed. Similar studies were performed by others as well using a cellular library (236) and a subset of viral libraries (181, 232). Our screen against the cellular library gave no positive interactions. This observation is in line with unpublished experiments carried out using a library described by Uetz et al. (236) that resulted in not detecting any interaction partners of pUL71 (Dr. Jens von Einem, *personal communication*). Therefore we conclude that, (i) either there are no interaction between pUL71 and cellular proteins occurring, which is rather unlikely taking the confocal images into consideration; (ii) or more likely, that the method is not applicable to detect those interactions. This could be either because of using a mouse library instead of a human derived one or the detection limit of the method is not sensitive enough to detect viral-host interactions of pUL71 with cellular proteins. In a further study pUL71 will be screened again against a human derived library to elucidate whether the negative results have been caused by choosing the wrong library.

Our library screen against our “in house” viral library resulted in detection interactions between pUL71 and pUL77, MCP, pUL89 and pUL104 according to the identification method for trustworthy positive interactions described by Sanderson et al. (10).

The interaction potential of pUL71 was also tested against different viral libraries by other groups. Phillips et al and To et al. performed two independent Y2H screens against different subsets of viral proteins (181, 232). However, Phillips et al. was not successful identifying interactions of pUL71 with a subset of capsid or tegument proteins because of difficulties with reactivation (181). In contrast, To et al. identified interactions between pUL71 and pUL26, a transcription factor, and pUL51, DNA packaging protein. Furthermore, the interaction between pUL71 and pUL89 was verified. In addition also the self-interaction of pUL71 was detected by Y2H (232). This finding is further hinting towards our hypothesis that pUL71 has a potential for oligomerisation. Interaction between pUL71, which localises in the cytoplasm, (3.2.3) and pUL89, pUL26 and pUL51, which are exclusively localised in the nucleus, are considered to have no biological relevance. Unfortunately Y2H screens prepare an artificial system that allows proteins to be expressed in Yeast nuclei independent of their natural distribution, folding, or abundance. This leads to high numbers of detected false positive interactions, observed unlikely to associate *in vivo* (246). Therefore all results need to be further verified by methods better reflecting *in vivo* conditions.

The interactions that were considered to likely occur *in vivo* were analysed in co-immunoprecipitations in infected cells. Y2H establishes a method of analysing direct interactions, without other viral proteins involved, apart from the ones transfected. Hence, we performed co-immunoprecipitations in infected cells under conditions in the viral context. Thus, verifying interactions between pUL71 and pUL104, MCP and pUL77. These proteins are components of the capsid and partially involved in DNA packaging. Since there were no interactions detected between pUL71 and pUL56 and because of pUL71's cytosolic distribution we can exclude any influence of pUL71 in processes connected to DNA packaging that occur in the nucleus. Therefore it is more likely that pUL71 as a tegument protein is connected to the capsids at an early stage of morphogenesis. This observation might also be in line with the rather early expression in *HCMV* life-cycle (48h p.i.). The protein is present when egress starts 24h later at 72h p.i..

The oligomerisation tendency of pUL71 was discussed earlier by analysing the bands detected in NATIVE-PAGE. There we detected a band of higher molecular weight that could occur due to interactions with the virions or because of oligomerisation of the protein. In addition, the Y2H screen described by To et al. (232) provided evidence that pUL71 has a self-interacting and therefore oligomerisation potential. To further investigate that finding baculovirus expressed recombinant protein rpUL71-Bac was purified by a combination of anionic exchange chromatography and gel filtration prior to EM analysis of negative stained single particles.

Derived from a gel filtration fraction representing the monomeric form, the purified protein has the tendency to self-assemble. We detected several particles calculated to represent monomeric as well as higher molecular weight forms of the protein derived from this fraction. These result implicated that the recombinantly expressed rpUL71-Bac has the ability to form higher ordered structures without additional viral proteins involved.

To verify those findings, more closely situated to *in vivo* conditions, studies under denaturating or non denaturating SDS-PAGE conditions were performed in infected cells. Thereby we detect that presence of pUL71 oligomeric forms is dependent upon non denaturating SDS-PAGE a finding that goes in line with observations for pp28 oligomerisation (209). Since oligomerisation tendency of pUL71 was indicated by several independent methods analysing the protein alone as well as in the viral context, results can be considered to be applicable *in vivo*.

To further analyse the oligomerisation potential of pUL71 first *in silico* analysis was performed. Scanning of a subset of frequent motif databases predicted a leucine zipper motif situated between aa 34-55 of the protein. Leucine zipper motifs are composed of at least four heptads of amino acids with hydrophobic ones at position 1 and 4 forming a hydrophobic core. (130, 173, 174). This motif was predominately described in DNA binding proteins but in more recent publication it is generally accepted as a protein-protein interaction domain (19, 45, 94, 121, 141, 189, 237).

Further investigations of the physico-chemical properties (89) revealed that we are not analysing a classical leucine-zipper motif rather a large hydrophobic face (L55, L37, L48, L41, L34, P52, F45) spanning over this area, termed leucine zipper like motif in this study. Still we hypothesise that this domain has potential to mediate hydrophobic interactions resulting in oligomerisation of pUL71. Such leucine zipper-like motifs are not conserved throughout UL71 homologues in the *Herpesvirinae. In silico* analysis of *HSV-1* UL51 predicted no such domain; still a large hydrophobic domain was predicted in the N-terminal part of the protein (p. 138). Further analysis in *HSV-1* need to be preformed before any conclusions could be drawn from this *in silico* prediction. In both proteins we detect hydrophobic cores at comparable positions. However, continuative investigations need to be carried out to elucidate whether this is due to coincidence or a conserved region in all U44 proteins.

In silico analysis of the *HCMV* proteome predicted in the following proteins- pUL14, pUL48, pUL50, pUL51, pUL104, pUS17 and pUS29 – to contain similar leucine zipper motifs. In *α-Herpesvirinae* the only characterised predicted leucine motif zipper is the one in portal protein

of *HSV-1* pUL6 the homologue of *HCMV* pUL104. This motif was described not to be involved in dimerisation of the protein and hypothesised to stabilise DNA during packaging (139) and more recently to facilitate binding to terminase subunits of *HSV-1* (250). Those findings show that such a leucine zipper or other hydrophobic cores such as the leucine zipper-like motif of *HCMV* pUL71 mediate many functions. The function is not restricted to facilitate oligomerisation although in most cases such an interaction is a prerequisite for the actual function of the protein. Since the presence of such a motif is not a guarantee on having identified the oligomerisation domain of the protein, additional studies were performed to elucidate its function in pUL71. Therefore a series of *in silico* and *in vitro* experiments were performed. Coiled-coil motif analysis predicted that an alteration of the motif by single nucleotide exchanges (71_L1, 71_L2, 71_L3) or deletion (71_ ΔLZ) will result in a loss of the coiled-coil domain between aa 27-51. Since we are hypothesising that the leucine zipper-like motif is the oligomerisation domain of pUL71, a loss of the coiled-coil structure in this region would result in a corresponding loss in interacting ability of those mutants. Furthermore, biomolecular fluorescence complementation (BiFC) assays (116) and co-immunoprecipitations were used to verify these predictions *in vitro*. Both assays indicated that alterations in the leucine zipper-like motif results in a loss of interaction between two pUL71 proteins. Previously, Hu et al. analysed interactions between cellular bZip transcription factors in living cells using BiFC (102). Therefore we choose this method to help us solve our question concerning characterisation of leucine zipper- like motif in pUL71. BiFC data was quantified analysing relative YFP signal of at least >47 cells per experiment, to ensure producing statistical relevant data. The decrease in YFP signals of about 60% for mutated forms (71_L1, 71_L2, 71_L3 and 71_ ΔLZ) in comparison to 71_wt is comparable to experiments carried out applying 71_wt to the vector alone. The finding indicates that even exchange of 2 L to A at crucial position 1 of the heptads results in loss of interaction ability. The YFP signal will not be completely abolished due to several reasons: (i) the laser might cause cross-excitation of YC or YN though they should not emit light on their own resulting in background fluorescence or (ii) BiFC visualises not direct binding but spatial proximity therefore all tagged proteins that localise in close proximity will cause background fluorescence.

For example all forms of pUL71 still co-localise because their localisation signal to AC (aa 1-16, Dr. Jens von Einem, *personal communication*) was not altered in the constructs. Anyhow even empty vectors that express YC alone cause comparable background fluorescence. This could be due to the close proximity between protein factory of ER and pUL71 localisation. Because a 60% decrease in light intensity can be seen as significant enough no further

experiments with pUL71 lacking the cytosolic localisation domain (aa 1-16) were performed. However, vector experiments revealed that even proteins that have no co-localisation with pUL71 in proximity of Golgi/ER are causing comparable background signals.

To verify those results with a method that detects physical binding co-immunoprecipitation experiments were carried out analysing none YFP-tagged as well as YFP-tagged constructs. These two subsets of experiments were performed, first to verify the BiFC results and further to ensure that the tags used in BiFC do not physically interfere with the binding domains. Both subsets of experiments gave comparable results. Still expression of none YFP-tagged proteins was more sufficient in *293T*s resulting in qualitatively better immunostainings. The oligomerisation of pUL71 was analysed as well by To et al. in their Y2H screen followed by verification in immunoprecipitations (232). In contrast to our experiments To et al. could not verify their results by co-precipitation using the Y2H constructs in *U373* cells. This is likely because sufficient protein amounts might not be produced in this system using vectors constructed for expression in another species. Preliminary experiments in our lab using *U373* instead of *293T*s together with pcDNA3.1 constructs failed as well to detect interactions between pUL71 and capsid proteins because of insufficient protein expression levels (this study, data not shown). Taken together data of *in vitro* assays implicate physical interactions, which are a prerequisite for oligomerisation, are only present between two wild type pUL71. If alterations in this motif like an exchange of two hydrophobic amino acids (L1) or more invasive ones (L2, L3, ΔLZ) are caused, this function is lost. Thus, confirming the leucine zipper-like motif to facilitate direct protein-protein interaction.

To analyse whether this loss of oligomerisation caused by alterations in the leucine zipper-like motif has any influence on viral maturation, similar mutations were induced into recombinant *HCMV*. Those mutations resulted in the deletion mutant *71_ΔLZ-BAC* and in the single nucleotide exchange mutant *71_L1-BAC*. Growth kinetic experiments were performed relative to wild type virus *71_wt-BAC*. The recombinant viruses were constructed in cooperation with Dr. Jens von Einem. Revertant viruses were constructed and tested for all mutations induced but could not be implied in our experiments due to our cooperation requirements. Therefore all characterisation experiments of recombinant viruses were performed in parallel in our and in the lab of Dr. Jens von Einem.

We characterised our viruses for growth, cell-to-cell spread, intracellular distribution of pUL71 in comparison to other tegument proteins and ultrastructural investigations by electron microscopy.

Growth kinetics were performed for the three viruses *71_wt-BAC, 71_ΔLZ-BAC* and *71_L1-BAC* for 168h (7 days) at MOI 1.5. Additional experiments were performed using *71_wt-BAC, 71_ΔLZ-BAC* and *71_L1-BAC* together with both revertants at high MOI (5) and low MOI (0.1) analysing shedded virus in the supernatant as well as cell associated virus (Dr Jens von Einem, *personal communication*). In all experiments growth impairments from 48-72h p.i. were observed indicated by reduced viral titres of about 2 to 3 log phases. Furthermore, we detected up to 80% reduced plaque size in *71_ΔLZ-BAC* and *71_L1-BAC* in comparison to wild-type. This observation indicates an impaired cell-to-cell spread activity.

In line with our results, the phenotype of a *HCMV* mutant carrying a transposon insertion in UL71 is characterized by a small plaque phenotype and impaired viral growth (251). In addition, a *HSV-1* UL51-null mutant is described with impaired viral growth reflected by reduced plaque sizes and a nearly 100-fold reduction in virus yield compared to wild-type virus (202). A similar phenotype was detected recently analysing *HCMV* 71-null mutants in strains *AD169* and *TB40E* (205, 248). Comparing those published results from 71-null mutants to our phenotype caused by mutations in the leucine zipper-like motif of pUL71 we detect many parallels.

Intracellular observations using immunofluorescence revealed that mutations in the leucine zipper like motif of pUL71 in *71_ΔLZ-BAC* and *71_L1-BAC* cause a reorganisation of other tegument proteins in infected cells compared to wild-type. While localisation of pUL71 does not seem to be altered, tegument protein pp150, used as markers for maturing virions, assembles on vesicular structures. This phenotype is comparable to phenotype described for viruses deficient for the whole UL71 open reading frame (*HCMV* 71-null mutants) constructed on an *AD169* (248) or *TB40E* (*71_stop-BAC*, 205) backbone. Schauflinger et al. described those vesicles as multivesicular bodies and further identified them by ultrastructural analysis using EM (205).

In line with literature we performed ultrastructural investigations by EM. Accordingly, *HFF*s were infected with one of the three viruses *71_wt-BAC, 71_ΔLZ-BAC* or *71_L1-BAC*. Cytoplasmic viral particles were quantified resulting in an accumulation of virions in a stage prior or during secondary envelopment. This effect is highly significant. We detect 3 to 6 folds more mature enveloped virions in *71_wt-BAC* than in the mutant viruses *71_ΔLZ-BAC* or *71_L1-BAC*. Therefore, we hypothesise, that alterations in the leucine zipper-like motif lead to viruses with less efficient secondary envelopment of *HCMV* particles. A similar growth defect has been reported for a UL51-deficient *PrV* (119). Large numbers of intracellular capsids in the cytoplasm lacking the envelope or at various stages of envelopment were found,

suggesting that envelopmental processes were affected in absence of *PrV* UL51 (119). A UL51-deficient *HSV-1* has been shown to exhibit a 100-fold growth defect and to be defective for nuclear egress (170).

Schauflinger et al. (205) argued that in their UL71-null mutant pUL71 is dispensable for events before cytoplasmic envelopment but required for correct morphogenesis of the AC (71, 202, 203) and its associated vesicular system (248). A comparable phenotype is likely for our mutants because of similar results occurring for both in all experiments performed. Still we do not detect the multivesicular bodies in which the capsids accumulate described by Schauflinger et al. (205). Formation of these structures is maybe cell-type dependent. Schauflinger et al. (205) used *HFF*s for all described experiments but ultrastructural analysis was performed in *MRC-5* (Human diploid fibroblasts) (59). In contrast we always used *HFF*s in all our experiments. Therefore it is possible that in *MRC-5* it is more likely that those multivesicular bodies establish. The same is true for detection of the AC in ultrastructural analysis. We could never detect such accumulations in *HFF*s were they are highly abundant in *MRC-5* (Dr. Jens von Einem, *personal communication*).

None the less, an accumulation was found of capsids lacking the envelope or at various stages of envelopment in all those experiments. In experiments performed by Schauflinger et al. (205) this effect was easily detected upon sight, whereas in our experiments after statistical quantification.

Therefore we conclude that the function of pUL71 in the viral context is dependent upon a non altered leucine zipper-like motif. Since we verified that leucine zipper-like motif causes oligomerisation in *in vitro* studies, we conclude that protein function is dependent upon oligomerisation of pUL71. In other words if the protein cannot oligomerise it cannot facilitate processes involved in secondary envelopment. Involvement in secondary envelopment brings the proteins into close contact with membranes composed from lipids. Since it is published that leucine zipper motifs facilitate protein-protein (141, 189), protein-DNA (19, 45, 94, 121, 237) as well as protein-lipid interactions (240) through hydrophobic interactions, it would be interesting to elucidate whether pUL71 has the ability to bind lipid-bilayers by its hydrophobic core produced by the leucine zipper-like motif dependent oligomers. Taking this thought into consideration it would be interesting to investigate whether the function of pUL71 is to stabilise the process of envelopment by binding both the virions (by binding capsid proteins pUL77, pUL104 and MCP) and cellular membrane structures in its oligomeric form.

Literature

Textbooks and Manuals:

1. Boppana S. B., Fowler K. B. (2007). Persistence in the population: epidemiology and transmisson. In Arvin A., Campadelli-Fiume G., Mocarski E., Moore P. S., Roizman B., Whitley R., Yamanishi K.(eds.). Human Herpesviruses; Cambridge University Press, Cambridge.; Chapter 44

2. Davison A. J. (2007) Overview of classification. In Arvin A., Campadelli-Fiume G., Mocarski E., Moore P. S., Roizman B., Whitley R., Yamanishi K. (eds.) Human Herpesviruses; Cambridge University Press. Cambridge.; Chapter 1

3. Hayat, M. A. (1986). Basic techniques for transmission electron microscopy. Academic Press

4. Hoppert, M., Holzenburg, A. (1998). Electron Microscopy in Microbiology. Bios Scientific Publishers Ltd.

5. Kornberg, A., Baker, T., A. (1992). DNA Replication. W. H. Freeman and Company, New York.

6. Mocarski, E. S., Courcelle, Howley, D. M. K. A. P. M. (2001). Cytomegaloviruses and their replication. In: Fields B. N, Knipe D. M. (eds.): Virology., 4nd Edition, Raven Press, New York.; 2629–2673.

7. Pass, R. F. **(**2001**).** Cytomegalvirus. In: Fields B. N, Knipe D. M. (eds.): Virology., 4nd Edition, Raven Press, New York., 2675-2705.

8. Radsak K., Kern H., Reis B., Reschke M., Mockenhaupt T., Eickmann M. **(**1995**).** Aspects of viral morphogenesis and of processing and transport of viral glycoproteins. in: Friedman, H. and Barbanti-Brodano, G. (eds.): DNA Tumor Viruses: Oncogenic Mechanisms., Plenum Press, New York.; 295-312.

9. Sambrook, J.; Maniatis, T.; Russel, D.W. (2001). Molecular cloning: a laboratory manual. Cold Spring Harbor Laboratory Press.

10. Sanderson C. M., Charalabous P. (2009). Using yeast two-hybrid methods to investigate large numbers of binary protein interactions.. In: Elaswarapu R and M..(eds.) Methods Express., Scion Publishing Limited. Oxford, UK.

11. Stinski M. F.**,** Thomson D. R.**,** Wathen M. N. **(**1981**).** Structure and Function of the cytomegalovirus genome. In Nahamias S. J., Dowle W. R., Schinazi R. F.(eds.): The Human Herpesviruses- An interdisciplinary perspective; Elsevier, New York.

12. Clontech Ltd. (2007). Matchmaker^{TM} GAL4 Two-Hybrid System 3 & Libraries User Manual.

13. Clontech Ltd. (2008). Yeast Protocols Handbook.

Research articles:

14. Akter P., Cunningham C., McSharry B. P., Dolan A., Addison C., Dargan D. J., Hassan-Walker A. F., Emery V. C., Griffiths P. D. (2003). Two novel spliced genes in human cytomegalovirus. J. Gen. Virol.; *84*: 1117–1122.

15. Ali M. A.**,** Forghani B.**,** Cantin E. M. **(**1996). Characterization of an essential HSV-1 protein encoded by the UL25 gene reported to be involved in virus penetration and capsid assembly. Virology.; *216***:** 278–283.

16. Al-Kobaisi M. F.**,** Rixon F. J.**,** McDougall I.**,** Preston V. G. **(**1991). The herpes simplex virus UL33 gene product is required for the assembly of full capsids. Virology.; *180*: 380-388.

17. Anders D. G.**,** McCue L. A. **(**1996**).** The human cytomegalovirus genes and proteins required for DNA synthesis. Intervirology.; *39*: 378-388.

18. Augustin M. A., Huber R., Kaiser J.T. (2001). Crystal structure of a DNA-dependent RNA polymerase (DNA primase). Nat. Struct. Biol.; *8*: 57-61.

19. Asada R., Kanemoto S., Kondo S., Saito A., Imaizumi K. (2011). The signalling from endoplasmic reticulum-resident bZIP transcription factors involved in diverse cellular physiology. J. Biochem.; *149*: 507-518.

20. Baines J. D., Cunningham C., Nalwanga D., Davison A. J. (1997). The UL15 gene of herpes simplex virus type 1 contains within its second exon a novel open reading frame that is translated in frame with the uL15 gene product. J. Virol.; *71*: 2666-2673.

21. Baker M. L.**,** Jiang W.**,** Rixon F. J.**,** Chiu W. **(**2005**).** Common ancestry of herpesviruses and tailed DNA bacteriophages. J. Virol.; *79*: 14967-14970.

22. Baldick C. J. Jr., Marchini A., Patterson C. E., Shenk T. (1997). Human cytomegalovirus tegument protein pp71 (ppUL82) enhances the infectivity of viral DNA and accelerates the infectious cycle. J. Virol.; *71*: 4400-4408.

23. Baldick C. J. Jr., Shenk T. (1996). Proteins associated with purified human cytomegalovirus particles. J. Virol.; *70*: 6097–6105.

24. Bankier A. T., Beck S., Bohni R., Brown C. M., Cerny R., Chee M. S., Hutchison C. A. 3rd., Kouzarides T., Martignetti J. A., Preddie E. **(**1991**).** The DNA sequence of the human cytomegalovirus genome. DNA Seq.; *2*: 1-12.

25. Baumeister J.**,** Klupp B. G.**,** Mettenleiter T. C. (1995). Pseudorabies virus and equine herpesvirus 1 share a nonessential gene which is absent in other herpesviruses and located adjacent to a highly conserved gene cluster. J. Virol.; *69*: 5560-5567.

26. Baxter M. K.**,** Gibson G. **(**2001**).** Cytomegalovirus basic phosphoprotein (pUL32) binds to capsids in vitro through its amino one-third. J. Virol.; *75*: 6865-6873.

27. Beghetto E., Paolis F. D., Spadoni A., Del Porto P., Buffolano W., and Gargano N. (2008). Molecular dissection of the human B cell response against cytomegalovirus infection by lambda display. J. Virol. Methods.; *151*: 7–14.

28. Bello C., Whittle H. **(**1991**).** Cytomegalovirus infection in gambian mothers and their babies. J. Clin. Pathol.; *44*: 366-369.

29. Biegert A., Mayer C., Remmert M., Söding J., Lupas A. (2006) The MPI Toolkit for protein sequence analysis. Nucleic. Acids. Res.; *34*, W335-339.

30. Bogner E. **(**2002**).** Human cytomegalovirus terminase as a target for antiviral chemotherapy. Rev. Med. Virol.*; 12*: 115-127.

31. Bogner E., Radsak K., Stinski M. F. (1998). The gene product of human cytomegalovirus open reading frame UL56 binds the pac motif and has specific nuclease activity. J. Virol.; *72*: 2259-2264.

32. Bogner E., Reschke M., Reis B., Mockenhaupt T., Radsak K. **(**1993**).** Identification of the gene product encoded by ORF UL56 of the human cytomegalovirus genome. Virology.; *196*: 290-293.

33. Bogner E., Reschke M, Reis B., Reis E., Britt W., Radsak K. **(**1992**).** Recognition of compartmentalized intracellular analogs of glycoprotein H of human cytomegalovirus. Arch. Virol.; *126*: 67-80.

34. Bold S., Ohlin M., Garten W., Radsak K. **(**1996**).** Structural domains involved in human cytomegalovirus glycoprotein B- mediated cell-cell fusion. J. Gen. Virol.; *77*: 2297-2302.

35. Bornberg-Bauer E., Rivals E., Vingron M. (1998). Computational approaches to identify leucine zippers. Nucleic. Acids. Res.; *26*: 2740-2746.

36. Borst E. M., Wagner K., Binz A., Sodeik B., Messerle M. (2008). The Essential Human Cytomegalovirus Gene UL52 Is Required for Cleavage-Packaging of the Viral Genome. J. Virol.; *82*: 2065-2078.

37. Britt W. J. (1984). Neutralizing antibodies detect a disulfide-linked glycoprotein complex within the envelope of human cytomegalovirus. Virology.; *135*: 369-378.

38. Britt W. J., Auger D. (1985). Identification of a 65 000 dalton virion envelope protein of human cytomegalovirus. Virus. Res.; *4*: 31-36.

39. Britt W. J., Mach M. (1996) Human cytomegalovirus glycoproteins. Intervirology.; *39*: 401-412.

40. Britt W. J., Pass R. F., Stagno S., Alford C. A. **(**1991**).** Pediatric Cytomegalovirus infection. Transplant. Proc.; *23*: 115-117.

41. Browne E. P.**,** Shenk. T. (2003). Human cytomegalovirus UL83-coded pp65 virion protein inhibits antiviral gene expression in infected cells. PNAS.; *100***:** 11439-11444.

42. Bryson K., McGuffin L. J., Marsden R. L., Ward J. J., Sodhi J. S., Jones D. T. (2005). Protein structure prediction servers at University College London. Nucl. Acids. Res.; *33*: W36-38.

43. Buchkovich N. J., Maguire T. G., Alwine J.C. (2010). Role of the Endoplasmic Reticulum Chaperone BiP, SUN Domain Proteins, and Dynein in Altering Nuclear Morphology during Human Cytomegalovirus Infection. J. Virol.; *84*: 7005-7017.

44. Butcher S. J., Aitken J., Mitchell J., Gowen B., Dargan D. J. (1998). Structure of the human cytomegalovirus B capsid by electron cryomicroscopy and image reconstruction. J. Struct. Biol.; *124*: 70-76.

45. Carrillo R.J., Privalov P.L. (2010). Unfolding of bZIP dimers formed by the ATF-2 and c-Jun transcription factors is not a simple two-state transition. Biophys. Chem.; *151*: 149-154.

46. Caumont A., Jamieson G., de Soultrait V. R., Parissi V., Fournier M., Zakharova O. D., Bayandin R., Litvak S., Tarrago-Litvak L., Nevinsky G. A. (1999). High affinity interaction of HIV-1 integrase with specific and non-specific single-stranded short oligonucleotides. FEBS. Lett.; *455*: 154-158.

47. Cepeda V., Esteban M., Fraile-Ramos A. (2010). Human cytomegalovirus final envelopment on membranes containing both trans-Golgi network and endosomal markers. Cellular. Microbiology.; *12*: 386–404.

48. Cha T.-A., Tom E., Kemble G. W., Duke G. M., Mocarski E. S., Spaete R. R. (1996). Human cytomegalovirus clinical isolates carry at least 19 genes not found in laboratory strains. J. Virol.; *70*, 78–83.

49. Chambers J., Angulo A., Amaratunga D., Guo H., Jiang Y., Wan J. S., Bittner A., Frueh K., Jackson M. R., Peterson P. A., Erlander M. G., Ghazal P. (1999). DNA microarrays of the complex human cytomegalovirus genome: profiling kinetic class with drug sensitivity of viral gene expression. J. Virol.; *73*: 5757-5766.

50. Chang Y. E., Poon A. P., Roizman B. **(**1996). Properties of the protein encoded by the UL32 open reading frame of herpes simplex virus type 1. J. Virol.; *70*: 3938-3946.

51. Chang Y. E., Van Sant C., Krug P. W., Sears A. E. Roizman B. (1997). The null mutant of the UL31 gene of herpes simplex virus 1: con struction and phenotype in infected cells. J. Virol.; *71*: 8307–8315.

52. Chee M. S., Bankier A. T., Beck S. (1990). Analysis of the protein-coding content of the sequence of human cytomegalovirus strain AD169. Curr. Top. Microbiol. Immunol.; *154*: 125–170.

53. Chee M., Rudolph S. A., Plachter B., Barrell B., Jahn G. (1989). Identification of the major capsid protein gene of human cytomegalovirus. J. Virol.; *63*: 1345-1353.

54. Chen D. H., Jiang H., Lee M., Liu F., Zhou Z. H. (1999). Three-dimensional visualization of tegument/capsid interactions in the intact human cytomegalovirus. Virology.; *260*: 10–16.

55. Cheung T. W., Teich S. A. **(**1999**).** Cytomegalovirus infection in patients with HIV infection. Mt Sinai J Med. *66*: 113-124.

56. Chi J. H., Wilson D. W. (2000). ATP-Dependent localization of the herpes simplex virus capsid protein VP26 to sites of procapsid maturation. J. Virol.; *74*: 1468-1476.

57. Chien C. T., Bartel P. L., Sternglanz R., Fields S. (1991). The two-hybrid system: a method to identify and clone genes for proteins that interact with a protein of interest. PNAS.; *88*: 9578-9582.

58. Child S. J., Hakki M., De Niro K. L., Geballe A. P. (2004). Evasion of cellular antiviral responses by human cytomegalovirus TRS1 and IRS1. J. Virol.; *78***:** 197-205.

59. Gleaves C. A., Smith T. F.,Shuster E. A., Pearson G. R. (1984) Rapid Detection of Cytomegalovirus in MRC-5 Cells Inoculated with Urine Specimens by Using Low-Speed Centrifugation and Monoclonal Antibody to an Early Antigen. J. Clin. Microbiol.; *19*: 917-919.

60. Cockrell S. K., Sanchez M. E., Erazo A., Homa F. L. **(**2009). Role of the UL25 Protein in Herpes Simplex Virus DNA encapsidation. J. Virol.; *83*: 47-57.

61. Cohen J. I., Corey G. R. **(**1985**).** Cytomegalovirus infection in the normal host. Medicine.; *64*: 100-114.

62. Compton T., Nepomuceno R. R., Nowlin D. M. **(**1992**).** Human cytomegalovirus penetrates host cells by pH-independent fusion at the cell surface. Virology*.; 191***:** 387-395.

63. Compton T., Nowlin D. M., Cooper N. R. (1993). Initiation of human cytomegalovirus infection requires initial interaction with cell surface heparan sulfate. Virology.; *193*: 834-841.

64. Conway J. F., Cockrell S. K., Copeland A. M., Newcomb W. W., Brown J. C., Homa F. L. (2010). Labeling and localization of the herpes simplex virus capsid protein UL25 and its interaction with the two triplexes closest to the penton. J. Mol. Biol.; *397*: 575-586.

65. Crough T., Khanna R. (2009) Immunobiology of human cytomegalovirus: from bench to bedside. Clin. Microbiol. Rev.; *22*: 76-98.

66. Crump C. M., Hung C. H., Thomas L., Wan L., Thomas G. (2003). Role of 575 PACS-1 in trafficking of human cytomegalovirus glycoprotein B and virus production. J. Virol.; *77*: 11105-11113.

67. Daikoku T., Ikenoya K., Yamada H., Goshima F., Nishiyama Y. (1998). Identification and characterization of the herpes simplex virus type 1 UL51 gene product. J. Gen. Virol.; *79*: 3027-3031.

68. Dargan D. J., Jamieson F. E., MacLean J., Dolan A., Addison C., McGeoch D. J. (1997). The published DNA sequence of human cytomegalovirus strain AD169 lacks 929 base pairs affecting genes UL42 and UL43. J. Virol.; *71*: 9833-9836.

69. Das S., Skomorovska-Prokvolit Y., Wang F. Z., Pellett P. E. (2006). Infection-dependent nuclear localization of US17, a member of the US12 family of human cytomegalovirus-encoded seven-transmembrane proteins. J. Virol.; *80*: 1191-1203.

70. Das S., Pellett P. E. (2007). Members of the HCMV US12 family of predicted heptaspanning membrane proteins have unique intracellular distributions, including association with the cytoplasmic virion assembly complex. Virology.; *361*: 263–273.

71. Das S., Vasanji A., Pellett P. E. (2007). Three-Dimensional Structure of the Human Cytomegalovirus Cytoplasmic Virion Assembly Complex Includes a Reoriented Secretory Apparatus. J. Virol.; *81*: 11861–11869.

72. Davison A. J., Akter P., Cunningham C., Dolan A., Addison C., Dargan, D. J., Hassan-Walker A. F., Emery V. C., Griffiths P. D., Wilkinson G. W. G. (2003). Homology between the humancytomegalovirus RL11 gene family and human adenovirus E3 genes. J. Gen. Virol.; *84*: 657–663.

73. de Bruyn Kops A, Knipe D. M. **(**1994**).** Preexisting nuclear architecture defines the intranuclear location of herpesvirus DNA replication structures. J. Virol.; *68*: 3512-3526.

74. de Bruyn Kops A., Uprichard S. L., Chen M., Knipe D. M. **(**1998**).** Comparison of the intranuclear distributions of herpes simplex virus proteins involved in various viral functions. Virology.; *252*: 162-178.

75. Demmler G. J. **(**1991**).** Infectious diseases society of america and centers disease control. Summary of a surveillance for congenital cytomegalovirus disease. Rev. Infect. Dis.; *13*: 315-329.

76. Diefenbach R. J., Miranda-Saksena M., Diefenbach E., Holland D. J., Boadle R. A., Armati P. J., Cunningham A. L. **(**2002**).** Herpes simplex virus tegument protein US11 interacts with conventional kinesin heavy chain. J. Virol.; *76*: 3282-3291.

77. Dittmer A., Bogner E. (2005). Analysis of the quaternary structure of the putative HCMV portal protein pUL104. Biochemistry.; *44*: 759-765.

78. Dittmer A., Drach J. C. , Townsend L. B. , Fischer A. , Bogner E. (2005). Interaction of the putative human cytomegalovirus portal protein pUL104 with the large terminase subunit pUL56 and its inhibition by benzimidazole-D-ribonucleosides. J. Virol.; *79*: 14660-14667.

79. Dittmer A., Bogner E. (2006). Specific short hairpin RNA-mediated inhibition of viral DNA packaging of human cytomegalovirus. FEBS Lett.; *580*: 6132-6138.

80. Dohner K., Wolfstein A., Prank U., Echeverri C., Dujardin D., Vallee R., Sodeik B. (2002)**.** Function of Dynein and dynactin in herpes simplex virus capsid transport. Mol. Biol. Cell.; *13*: 2795-2809.

81. Dolan A., Cunningham C., Hector R. D., Hassan-Walker A. F., Lee L.,Addison C., Dargan D. J., McGeoch D. J., Gatherer D., Emery V. C., Griffiths P. D., Sinzger C., McSharry B. P., Wilkinson G. W. and Davison A. J. (2004). Genetic content of wild-type human cytomegalovirus. J. Gen. Virol.; *85*: 1301-1312.

82. Dunn W., Chou C., Li H., Hai R., Patterson D., Stolc V., Zhu H., Liu F. (2003). Functional profiling of a human cytomegalovirus genome. PNAS.; *100*: 14223-14228.

83. Fiala, M., Honess, R.W., Heiner, D.C., Heine Jr., J.W., Murnane, J., Wallace, R., and Guze, L.B. (1976). Cytomegalovirus proteins. Polypeptides of virions and dense bodies. J. Virol.; *19*: 243-254.

84. Fields S., Song O.(1989). A novel genetic system to detect protein-protein interactions. Nature.; *340*: 245-246.

85. Fleckenstein B., Müller I., Collins J. (1982). Cloning of the complete human cytomegalovirus genome in cosmids. Gene.; *18*: 39-46.

86. Fowler K. B., Pass R. F. (1991). Sexually transmitted diseases in mothers of neonates with congenital cytomegalovirus infection. J. Infect. Dis.; *164*: 259–264.

87. Fraile-Ramos A., Pelchen-Matthews A., Kledal T. N., Browne H., Schwartz T. W., Marsh M. (2002). Localization of HCMV UL33 and US27 in Endocytic Compartments and Viral Membranes. Traffic.; *3*: 218-232.

88. Fuchs W., Klupp B. G., Granzow H., Osterrieder N., Mettenleiter T. C. (2002). The interacting UL31 and UL34 gene products of pseudorabies virus are involved in egress from the host-cell nucleus and represent components of primary enveloped but not of mature virions. J. Virol.; *76*: 364–378.

89. Gautier R., Douguet D., Antonny B., Drin G. (2008). HELIQUEST: a web server to screen sequences with specific α-helical properties. Bioinformatics.; *24*: 2101-2102.

90. Geballe A. P., Leach F. S., Mocarski E. S. **(**1986**).** Regulation of cytomegalovirus late gene expression: gamma genes are controlled by posttranscriptional events. J. Virol.; *57*: 864-874.

91. Gibson W. (2008) Structure and formation of the cytomegalovirus virion. Curr. Top. Microbiol. Immunol.; *325*: 187-204.

92. Gibson W., Baxter M. K., Clopper K. S. (1996). Cytomegalovirus "missing" capsid protein identified as heat-aggregable product of human cytomegalovirus UL46. J. Virol.; *70*: 7454-7461.

93. Giesen K., Radsak K., Bogner E. (2000). Targeting of the gene product encoded by ORF UL56 of human cytomegalovirus into viral replication centers. FEBS. Lett.; *471*: 215-218.

94. Glover J. N., Harrison S. C. (1995). Crystal structure of the heterodimeric bZIP transcription factor c-Fos–c-Jun bound to DNA. Nature.; *373*: 257–261.

95. Grünewald K., Desai P., Winkler D. C., Heymann J. B., Belnap D. M., Baumeister W., Steven A. C. (2003) Three-dimensional structure of herpes simplex virus from cryo-electron tomography. Science.; *302*: 1396-1398.

96. Hamel F., Boucher H., Simard C. (2002). Transcriptional and translational expression kinetics of the bovine herpesvirus 1 UL51 homologue gene. Virus. Res.; *84*: 125-134.

97. Hamprecht K., Jahn G. (2007). Human cytomegalovirus and congenital virus infection. Bundesgesundheitsblatt Gesundheitsforschung Gesundheitsschutz.; *50*: 1379-1392.

98. Heldwein E. E., Krummenacher C. (2008). Entry of herpesviruses into mammalian cells. Cell. Mol. Life. Sci.; *65*: 1653-1668.

99. Hensel G., Meyer, H. Gartner S., Brand G., Kern H. F. (1995). Nuclear localization of the human cytomegalovirus tegument protein pp150 (ppUL32). J. Gen. Virol.; *76*: 1591-1601.

100. Hofmann H., Sindre H., and Stamminger T. (2002). Functional interaction between the pp71 protein of human cytomegalovirus and the PML-interacting protein human Daxx. J. Virol.; *76*: 5769-5783.

101. Homman-Loudiyi M., Hultenby K.,Britt W., and Soderberg-Naucler C. (2003). Envelopment of human cytomegalovirus occurs by budding into Golgi-derived vacuole compartments positive for gB, Rab 3, trans-Golgi network 46, and mannosidase II. J. Virol.; *77*: 3191–3203.

102. Hu C. D., Chinenov Y., Kerppola T. K. (2002).Visualization of interactions among bZIP and Rel family proteins in living cells using bimolecular fluorescence complementation. Molecular. Cell.; *9*: 789–798.

103. Huang E. S., Chen S. T., Pagano J. S. **(**1975**).** Human Cytomegalovirus. Purification and Characterisation of viral DNA. J. Virol.; *12*: 1473-1481.

104. Huber M. T., Compton T. **(**1998**).** The human cytomegalovirus UL74 gene encodes the third component of the glycoprotein H-glycoprotein L-containing envelope complex. J. Virol.; *72*: 8191-8197.

105. Hwang J. S., Bogner E. **(**2002**).** ATPase activity of the terminase subunit pUL56 of human cytomegalovirus. J. Biol.Chem.; *277*: 6943-6948.

106. Hwang J. S., Kregler O., Schilf R., Bannert N., Drach J. C., Townsend L. B., Bogner E. (2007). Identification of acetylated, tetrahalogenated benzimidazole D-ribonucleosides with enhanced activity against human cytomegalovirus. J. Virol.; *81*: 11604-11611.

107. Hwang J. S., Schilf R., Drach J. C., Townsend L. B., Bogner E. (2009). Susceptibilities of human cytomegalovirus clinical isolates and other herpesviruses to new acetylated, tetrahalogenated benzimidazole D-ribonucleosides. Antimicrob. Agents. Chemother.; *53*: 5095-5101.

108. Irmiere A., Gibson W. (1983). Isolation and characterization of a noninfectious virion-like particle released from cells infected with human strains of cytomegalovirus. Virology.; *130*: 118-133.

109. Jahn G., Scholl B. C., Traupe B., Fleckenstein B. (1987). The two major structural phosphoproteins (pp65 and pp150) of human cytomegalovirus and their antigenic properties. J. Gen. Virol.; *68*: 1327-1237.

110. Jahn G., Harthus H. P., Broker M., Borisch B., Platzer B., Plachter B. (1990). Generation and application of a monoclonal antibody raised against a recombinant cytomegalovirus-specific polypeptide. Klin. Wochenschr.; *68*: 1003-1007.

111. Jones D. T. (1999) Protein secondary structure prediction based on position-specific scoring matrices. J. Mol. Biol.; *292*: 195-202.

112. Kalejta R. F. (2008). Tegument proteins of human cytomegalovirus. Microbiol. Mol. Biol. Rev.; *72*: 249-265.

113. Kari B., Gehrtz . (1992). A human cytomegalovirus glycoprotein complex designated gC-II is a major heparin-binding component of the envelope. J. Virol.; *66*: 1761-1764.

114. Keay S., Baldwin B. **(**1992**).** The human fibroblast receptor for gp86 of human cytomegalovirus is a phosphorylated glycoprotein. J. Virol*.; 66*: 4834-4838.

115. Kemble G. W., Mocarski E. S. (1989). A host cell protein binds to a highly conserved sequence element (pac-2) within the cytomegalovirus a sequence. J. Virol.; *63*: 4715-4728.

116. Kerppola T. K. (2008). Bimolecular fluorescence complementation (BiFC) analysis as a probe of protein interactions in living cells. Annu. Rev. Biophys.; *37*: 465-487.

117. Klemola E. **(**1973**).** Cytomegalovirus infection in previously healthy adults. AnnIntern. Med. *79*: 267-268.

118. Klupp, B. G., Granzow H., Keil G. M., Mettenleiter T. C. **(**2006). The capsid-associated UL25 protein of the alphaherpesvirus pseudorabies virus is nonessential for cleavage and encapsidation of genomic DNA but is required for nuclear egress of capsids. J. Virol.; *80***:** 6235–6246.

119. Klupp B. G., Granzow H., Klopfleisch R., Fuchs W., Kopp M., Lenk M., Mettenleiter T. C. (2005). Functional analysis of the pseudorabies virus UL51 protein. J. Virol.; *79*: 3831-3840.

120. Kim E. T., Oh S. E., Lee Y. O., Gibson W., Ahn J. H. (2009). Cleavage specificity of the UL48 deubiquitinating protease activity of human cytomegalovirus and the growth of an active-site mutant virus in cultured cells. J. Virol.; *83*: 12046-12056.

121. Kouzarides T., Ziff E. **(**1988). The role of the leucine zipper in the fos-jun interaction. Nature.; *336***:** 646–651.

122. Krosky P. M., Baek M. C., Coen D. M. **(**2003**).** The human cytomegalovirus UL97 protein kinase, an antiviral drug target, is required at the stage of nuclear egress. J. Virol.; *77*: 905-914.

123. Krzyzaniak M. A., Mach M., Britt W. J. **(**2009). HCMV-encoded glycoprotein M (UL100) interacts with Rab11 effector protein FIP4. Traffic.; *10*: 1439 –1457.

124. Kuhn J., Leege T., Klupp B. G., Granzow H., Fuchs W., Mettenleiter T.C. **(**2008). Partial functional complementation of a pseudorabies virus UL25 deletion mutant by herpes simplex virus type 1 pUL25 indicates overlapping functions of alphaherpesvirus pUL25 proteins. J. Virol.; *82*: 5725-5734.

125. Ladin B. F., Blankenship M. L., Ben-Porat T. **(**1980**).** Replication of herpesvirus DNA. V. The maturation of concatemeric DNA of pseudorabies virus to genome length is related to capsid formation. J. Virol*.; 33***:** 1151-1164.

126. Laemmli, U. K. (1970). Cleavage of structural proteins during the assembly of the head of bacteriophages T4. Nature.; *227*: 680-685.

127. Lai L., Britt W. J. (2003). The interaction between the major capsid protein and the smallest capsid protein of human cytomegalovirus is dependent on two linear sequences in the smallest capsid protein. J. Virol.; *77*: 2730-2735.

128. Lamberti C, Weller S. K. (1996). The herpes simplex virus type 1 UL6 protein is essentiell for cleavage and packaging but not for genomic inversion. Virology.; *226*: 403-407.

129. Landini M. P., Severi B., Badiali L., Gonczol E., Mirolo G. (1987). Structural components of human cytomegalovirus: in situ localization of the major glycoprotein. Intervirology.; *27*: 154-160.

130. Landschulz W. H., Johnson P. F., McKnight S. L. (1988).The Leucine Zipper: A Hypothetical Structure Common to a New Class of DNA Binding Proteins. Science.; *240*: 1759- 1764.

131. Lenk M., Visser N., Mettenleiter T. C. (1997). The pseudorabies virus UL51 gene product is a 30-kilodalton virion component. J. Virol.; *71*: 5635-5638.

132. Li L., Nelson J. A., Britt W. J. **(**1997**).** Glycoprotein H-related complexes of human cytomegalovirus: identification of a third protein in the gCIII complex. J. Virol.; *71*: 3090-3097.

133. Liu B., Stinski M. F. **(**1992**).** Human cytomegalovirus contains a tegument protein that enhances transcription from promoters with upstream ATF and AP-1 cisacting elements. J. Virol.; *66*: 4434-4444.

134. Louvet O., Doignon F., Crouzet M. (1997). Stable DNA-binding yeast vector allowing high-bait expression for use in the two-hybrid system. Biotechniques.; *23*: 816-818, 820.

135. Luckow V. A., Lee S. C., Barry G. F., Olins P. O. (1993). Efficient generation of infectious recombinant baculoviruses by site-specific transposon-mediated insertion of foreign genes into a baculovirus genome propagated in Escherichia coli. J. Virol.; *67*: 4566-4579.

136. Luxton G. W. G., Haverlock S., Coller K. E., Antinone S. E., Pincetic A., Smith G. A. (2005). Targeting of herpesvirus capsid transport in axons is coupled to association with specific sets of tegument proteins. PNAS.; *102***:** 5832-5837.

137. Mach M., Kropff B., Dal Monte P., Britt W. **(**2000**).** Complex formation by human cytomegalovirus glycoproteins M (gpUL100) and N (gpUL73). J. Virol.; *74*: 11881-11892.

138. Mach M., Kropff B., Kryzaniak M,. Britt W. (2005). Complex formation by glycoproteins M and N of human cytomegalovirus: structural and functional aspects. J. Virol.; *79*: 2160-2170.

139. Malik A. K., Weller S. K. **(**1996). Use of transdominant mutants of the origin-binding protein (UL9) of herpes simplex virus type 1 to define functional domains. J. Virol.; *70***:** 7859–7866.

140. Marchler-Bauer A., Anderson J. B., Chitsaz F., Derbyshire M. K., DeWeese-Scott C., Fong J. H., Geer L. Y., Geer R. C., Gonzales N. R., Gwadz M., He S., Hurwitz D. I., Jackson J. D., Ke Z., Lanczycki C. J., Liebert C. A., Liu C., Lu F., Lu S., Marchler G. H., Mullokandov M., Song J. S., Tasneem A., Thanki N., Yamashita R. A., Zhang D., Zhang N., Bryant S. H. **(**2009). CDD: specific functional annotation with the Conserved Domain Database. Nucleic. Acids. Res.; *37*: D205–D210.

141. Martínez-Turiño S., Hernández C. (2011) A membrane-associated movement protein of Pelargonium flower break virus shows RNA-binding activity and contains a biologically relevant leucine zipper-like motif. Virology.; *413*: 310-309.

142. Maurer U. E., Sodeik B., Grünewald K. (2008). Native 3D intermediates of membrane fusion in herpes simplex virus 1 entry. PNAS.; *105*: 10559-10564.

143. McCormac L. P., Grundy J. E. **(**1999**).** Two clinical isolates and the Toledo strain of cytomegalovirus contain endothelial cell tropic variants that are not present in the AD169, Towne, or Davis strains. J. Med. Virol.; *57*: 298-307.

144. McNab A. R., Desai P., Person S., Roof L. L., Thomsen D. R., Newcomb W. W., Brown J. C., Homa F. L. **(**1998). The product of the herpes simplex virus type 1 UL25 gene is required for encapsidation but not for cleavage of replicated viral DNA. J. Virol.; *72***:** 1060–1070.

145. McVoy M. A., Adler S. P. (1994). Human cytomegalovirus DNA replicates after early circularization by concatemer formation, and inversion occurs within the concatemer. J. Virol.; *68*: 1040-1051.

146. McVoy M. A., Nixon D. E., Adler S. P., Mocarski E. S. **(**1998**).** Sequences within the herpesvirus-conserved pac1 and pac2 motifs are required for cleavage and packaging of the murine cytomegalovirus genome. J. Virol.; *72*: 48-56.

147. Meier J., Lienicke U., Tschirch E., Krüger D. H., Wauer R. R., Prösch S. (2005) Human cytomegalovirus reactivation during lactation and mother-to-child transmission in preterm infants. J. Clin. Microbiol.; *43*: 1318-1324.

148. Meier J. L., Stinski M. F. (1996). Regulation of human cytomegalovirus immediate-early gene expression. Intervirology.; *39*: 331-342.

149. Meissner, C.S., Köppen-Rung P., Dittmer A., Lapp S., Bogner E. (2011) A "Coiled-coil" motif is important for oligomerization and DNA binding properties of human cytomegalovirus protein UL77. J. Virol.*; Under Review.*

150. Meissner, C.S., Suffner S., Schaufflinger M., von Einem J., Bogner E. (2011) A leucine zipper motif of human cytomegalovirus tegument protein pUL71 is important for oligomerization. In Prep.

151. Mettenleiter, T. C. **(**2002). Herpesvirus assembly and egress. J. Virol.; *76*:1537-1547.

152. Mettenleiter, T. C. **(**2004). Budding events in herpesvirus morphogenesis. Virus Research.; *106*:167-180.

153. Mettenleiter, T. C. **(**2006). Intriguing interplay between viral proteins during herpesvirus assembly or: the herpesvirus assembly puzzle. Vet. Microbiol.; *113*:163-169.

154. Mettenleiter, T. C., B. G. Klupp, and H. Granzow. (2009). Herpesvirus assembly: an update. Virus. Res.; *143*:222-234.

155. Meyer G. A., Radsak K. **(**2000**).** Identifikation of a novel signal sequence that targets transmembrane proteins to the nuclear envelope inner membrane. J. Biol. Chem.; *275*: 3857-3866.

156. Meyer H. H., Ripalti A., Landini M. P., Radsak K., Kern H. F., Hensel G. M. **(**1997**).** Human cytomegalovirus late-phase maturation is blocked by stably expressedUL32 antisense mRNA in astrocytoma cells. J. Gen. Virol.; *78*: 2621-2631.

157. Milbradt J., Auerochs S., Marschall M. (2007). The cytomegaloviral proteins pUL50 and pUL53 are associated with the nuclear lamina and interact with cellular protein kinase C. J. Gen. Virol., *88*: 2642-2650.

158. Milbradt J., Auerochs S., Sticht H., Marschall M. (2009). Cytomegalo-viral proteins that associate with the nuclear lamina: components of a postulated nuclear egress complex. J. Gen. Virol.; *90*: 579–590.

159. Mocarski E. S., Liu A. C., Spaete, R. R. **(**1987**).** Structure and variability of the a sequence in the genome of human cytomegalovirus (Towne strain). J. Gen. Virol.; *68*: 2223-2230.

160. Mockenhaupt T., Reschke M., Bogner E., Reis B., Radsak K. (1994). Structural analysis of the US-segment of a viable temperature sensitive human cytomegalovirus mutant. Arch Virol.; *137*: 161-169.

161. Murphy E., Shenk T. (2008). Human cytomegalovirus genome. Curr Top Microbiol Immunol.; *325*: 1-19.

162. Napoli A., Kvaratskelia M., White M. F., Rossi M., Ciaramella M. (2001). A novel member of the bacterial-archaeal regulator family is a nonspecific dna-binding protein and induces positive supercoiling. J Biol Chem*.; 276*: 10745-10752.

163. Nasseri M., Mocarski E. S. (1988). The cleavage recognition signal is contained within sequences surrounding an a-a junction in herpes simplex virus DNA. Virology.; *167*: 25-30.

164. Newcomb W. W., Homa F. L., Booy F. P., Thomsen D. R., Trus B. L. Steven A. C., Spencer J. V. & Brown J. C. **(**1996**).** Assembly of the herpes simplex virus capsid: characterization of intermediates observed during cell-free capsid formation. J. Mol. Biol*.; 263***:** 432-446.

165. Newcomb W. W., Homa D. L., Brown J. C. **(**2006). Herpes simplex virus capsid structure: DNA packaging protein UL25 is located on the external surface of the capsid near the vertices. J. Virol.; *80*: 6286-6294.

166. Newcomb W. W., Juhas R. M., Thomsen D. R., Homa F. L., Burch A. D., Weller S. K., Brown J. C. (2001). The UL6 gene product forms the portal for entry of DNA into herpes simplex virus capsid. J. Virol.; *75*: 10923-10932.

167. Newcomb W. W., Thomsen D. R., Homa F. L., Brown J. C. (2003). Assembly of the herpes simplex virus capsid: identification of soluble scaffold-portal complexes and their role in formation of portal-containing capsids. J. Virol.; *77*: 9862–9871.

168. Nicola A. V., Hou J., Major E. O., Straus S. E. *(*2005*).* Herpes simplex virus type 1 enters human epidermal keratinocytes, but not neurons, via a pH-dependent endocytic pathway. J. Virol.; *79*: 7609-7616.

169. Nozawa N, Daikoku T, Koshizuka T, Yamauchi Y, Yoshikawa T, Nishiyama Y. (2003). Subcellular localization of herpes simplex virus type 1 UL51 protein and role of palmitoylation in Golgi apparatus targeting. J. Virol.; *77*: 3204-3216.

170. Nozawa N, Kawaguchi Y, Tanaka M, Kato A, Kato A, Kimura H, Nishiyama Y. (2005). Herpes simplex virus type 1 UL51 protein is involved in maturation and egress of virus particles. J. Virol.; *79*: 6947-6956.

171. Ogasawara M., Suzutani T., Yoshida I., Azuma M. **(**2001). Role of the UL25 gene product in packaging DNA into the herpes simplex virus capsid: location of UL25 product in the capsid and demonstration that it binds DNA. J. Virol.; *75***:** 1427–1436.

172. Ojala P. M., Sodeik B., Ebersold M. W., Kutay U., Helenius A. **(**2000**).** Herpes simplex virus type 1 entry into host cells: reconstitution of capsid binding and uncoating at the nuclear pore complex in vitro. Mol. Cell. Biol.; *20*: 4922-4931.

173. O'Shea E. K., Rutkowski R., Kim P. S. (1989). Evidence that the leucine zipper is a coiled coil. Science.; *243*: 538-542.

174. O'Shea E. K., Klemm J. D., Kim P. S., Alber T. (1991). X-ray Structure of the GCN4 Leucine Zipper, a Two-Stranded, Parallel Coiled Coil. Science*.; 254*: 539-544.

175. Pasdeloup D., Blondel D., Isidro A. L., Rixon F. J. **(**2009). Herpesvirus capsid association with the nuclear pore complex and viral DNA release involve the nucleoporin CAN/Nup214 and the capsid protein pUL25. J. Virol.; *83***:** 6610–6623.

176. Patel A. H., MacLean J. B. **(**1995). The product of the UL6 gene of herpes simplex virus type 1 is associated with virus capsids. Virology.; *206*: 465-478.

177. Pear W. S., Nolan G. P., Scott M. L., Baltimore D. (1993). Production of high-titer helper-free retroviruses by transient transfection. PNAS.; *90*: 8392-8396.

178. Pepperl S., Münster J., Mach M., Harris J. R., Plachter B. (2000). Dense bodies of human cytomegalovirus induce both humoral and cellular immune responses in the absence of viral gene expression. J. Virol.; *74*: 6132-6146.

179. Perdue M. L., Cohen J. C., Randall C. C., O'Callaghan D. J. **(**1976**).** Biochemical studies of the maturation of herpes virus nucleocapsid species. Virology*.; 74*: 197-208.

180. Peters J., Nitsch M., Kühlmorgen B., Golbik R., Lupas A., Kellermann J., Engelhardt H., Pfander J. P., MüllerS. , Goldie K., Engel A., Stette K.-O., Baumeister W. (1995). Tetrabrachion: a filamentous archaebacterial surface protein assembly of unusual structure and extreme stability. J. Mol. Biol.; *257*: 385-340.

181. Phillips S. L., Bresnahan W. A. (2011). Identification of binary interactions between human cytomegalovirus virion proteins. J. Virol.; *85*: 440-447.

182. Pietropaolo R., Compton T. (1999). Interference with annexin II has no effect on entry of human cytomegalovirus into fibroblast cells. J. Gen. Virol.; *80*: 1807–1816.

183. Plachter B., Britt W., Vornhagen R.,Stamminger T., Jahn G. (1993). Analysis of Proteins Encoded by IE Regions 1 and 2 of Human Cytomegalovirus Using Monoclonal Antibodies Generated against Recombinant Antigens. Virology.; *193*: 642-652.

184. Radsak K., Brucher K. H., Georgatos S. D. **(**1991**).** Focal nuclear envelope lesions and specific nuclear lamin A/C dephosphorylation during infection with human cytomegalovirus. Eur. J. Cell. Biol.; *54*: 299-304.

185. Radsak K., Eickmann M., Mockenhaupt T., Bogner E., Kern H., Eis-Hubinger A., Reschke M. **(**1996**).** Retrieval of human cytomegalovirus glycoprotein B from the infected cell surface for virus envelopment. Arch. Virol.; *141*: 557-572.

186. Radsak K., Schneider D., Jost E., Brücher K. H. **(**1989**).** Alteration of nuclear lamina protein in human fibroblasts infected with cytomegalovirus (HCMV). Arch. Virol.; *105*: 103-112.

187. Radtke K., Döhner K., Sodeik B. (2006). Viral interactions with the cytoskeleton: a hitchhiker's guide to the cell. Cell Microbiol.; *8*: 387-400.

188. Raynor C. M., Wright J. F., Waisman D. M., Pryzdial E. L. (1999). Annexin II enhances cytomegalovirus binding and fusion to phospholipid membranes. Biochemistry.; *38* : 5089–5095.

189. Reinke A. W., Grigoryan G. ,Keating A.E. (2011). Identification of bZIP Interaction Partners of Viral Proteins HBZ, MEQ, BZLF1, and K-bZIP Using Coiled-Coil Arrays. Biochemistry.; *49*: 1985-1997.

190. Reschke M., Reis B., Noding K., Rohsiepe D., Richter A., Mockenhaupt T., Garten W., Radsak K. **(**1995**).** Constitutive expression of human cytomegalovirus glycoprotein B (gpUL55) with mutagenized carboxy-terminal hydrophobic domains. J. Gen. Virol.; *76*: 113-122.

191. Revello M. G., Zavattoni M., Furione M., Lilleri D., Gorini G., Gerna G. **(**2002**).** Diagnosis and outcome of preconceptional and periconceptional primary human cytomegalovirus infections. J. Infect. Dis. *186*: 553-557.

192. Rixon F. J. **(**1993**).** Structure and assembly of herpesviruses. Semin. Virol.*; 4*: 135-144.

193. Rode K., Döhner K., Binz A., Glass M., Strive T., Bauerfeind R., Sodeik B. (2011). Uncoupling uncoating of herpes simplex virus genomes from their nuclear import and gene expression. J. Virol.; *85*: 4271-4283.

194. Roizmann B., Desrosiers R. C., Fleckenstein B., Lopez C., Minson A. C., Studdert M. J. (1992) The family Herpesviridae: an update. The Herpesvirus Study Group of the International Committee on Taxonomy of Viruses. Arch. Virol.; *123*: 425-449.

195. Roller R., Zhou Y., Schnetzer R., Ferguson J., DeSalvo D. (2000). Herpes simplex virus type 1 UL34 gene product is required for viral envelopment. J. Virol.; *74*: 117–129.

196. Rowe W. P., Hartley J.W., Waterman S., Turner H. C., Huebner R. J. (1956). Cytopathogenic agent resembling human salivary gland virus recovered from tissue cultures of human adenoids. Proc Soc Exp Biol Med.; *92*: 418-424.

197. Rowshani A. T., Bemelman F. J., van Leeuwen E. M., van Lier R. A., ten Berge I. J. **(**2005**).** Clinical and immunologic aspects of cytomegalovirus infection in solidorgan transplant recipients. Transplantation. *79*: 381-386.

198. Ryckman B. J., Chase M. C., Johnson D. C. (2008). HCMV gH/gL/UL128-131 interferes with virus entry into epithelial cells: evidence for cell type-specific receptors. PNAS.**;** *105*: 14118-14123.

199. Salmon B., Cunningham, Davison A. J., Harris W. J., Baines J. D. (1998). The herpes simplex virus type 1 U(L)17 gene encodes virion tegument proteins that are required for cleavage and packaging of viral DNA. J. Virol.; *72*: 3779-3788.

200. Sam M. D., Evans B. T., Coen D. M., Hogle J. M. (2009). Biochemical, biophysical, and mutational analyses of subunit interactions of the human cytomegalovirus nuclear egress complex. J Virol.; *83*: 2996-3006.

201. Sanchez V., Angeletti P. C., Engler J. A., Britt W. J. **(**1998**).** Localization of human cytomegalovirus structural proteins to the nuclear matrix of infected human fibroblasts. J. Virol.*; 72***:** 3321-3329.

202. Sanchez V., Greis K. D., Sztul E., Britt W.J. (2000). Accumulation of Virion Tegument and Envelope Proteins in a Stable Cytoplasmic Compartment during Human Cytomegalovirus Replication: Characterization of a Potential Site of Virus Assembly. J. Virol.; *74*: 975-986.

203. Sanchez V., Sztul E., Britt W. J. (2000). Human cytomegalovirus pp28 (UL99) localizes to a cytoplasmic compartment which overlaps the endoplasmic reticulum-golgi-intermediate compartment. J. Virol.; *74*: 3842-3851.

204. Sarov, I., Abady, I. (1975). The morphogenesis of human cytomegalovirus. Isolation and polypeptide characterization of cytomegalovirions and dense bodies. Virology; *66*: 464-473.

205. Schauflinger M., Fischer D., Schreiber A., Chevillotte M., Walther P., Mertens T., von Einem J. (2011). The tegument protein UL71 of human cytomegalovirus is involved in late envelopment and affects multivesicular bodies. J. Virol.; *85*: 3821-3832.

206. Scheffczik H., Savva C. G., Holzenburg A., Kolesnikova L., Bogner E. **(**2002**).** The terminase subunits pUL56 and pUL89 of human cytomegalovirus are DNAmetabolizing proteins with toroidal structure. Nucleic. Acids. Res.; *30*: 1695- 1703.

207. Scholz B., Rechter S., Drach J. C., Townsend L. B., Bogner E. **(**2003**).** Identification of the ATP-binding site in the terminase subunit pUL56 of human cytomegalovirus. Nucleic. Acids. Res.; *31*: 1426-1433.

208. Scott J. E., Willett I. H. (1966). Binding of cationic dyes to nucleic acids and their biological polyanions. Nature.; *209*: 985-987.

209. Seo J-Y., Britt W. J. (2008). Multimerization of Tegument Protein pp28 within the Assembly Compartment Is Required for Cytoplasmic Envelopment of Human Cytomegalovirus. J. Virol.; *82*: 6272–6287.

210. Shaner N. C., Campbell R. E., Steinbach P. A., Giepmans B. N., Palmer A. E., Tsien R. Y. (2004). Improved monomeric red, orange and yellow fluorescent proteins derived from Discosoma sp. red fluorescent protein. Nat Biotechnol.; *22*: 1567-1572.

211. Shu X., Shaner N. C., Yarbrough C. A., Tsien R. Y., Remington S. J. (2006). Novel chromophores and buried charges control color in mFruits. Biochemistry.; *45*: 9639-9647.

212. Silva, M. C., Schroer J., Shenk T. (2005). Human cytomegalovirus cell-to-cell spread in the absence of an essential assembly protein. PNAS.; *102*: 2081-2086.

213. Singer G. P., Newcomb W. W., Thomsen D. R., Homa F. L., Brown J. C. (2005). Identification of a region in the herpes simplex virus scaffolding protein required for interaction with the portal. J. Virol.; *79*: 132–139.

214. Sinzger C., Digel M., Jahn G.. (2008) Cytomegalovirus cell tropism. Curr. Top. Microbiol. Immunol.; *325*: 63-83.

215. Sinzger C., Hahn G., Digel M., Katona R., Sampaio K. L., Messerle M., Hengel H., Koszinowski U., Brune W., Adler B. (2008). Cloning and sequencing of a highly productive, endotheliotropic virus strain derived from human cytomegalovirus TB40/E. J. Gen. Virol.; *89*: 359-368.

216. Sinzger C., Kahl M., Laib K., Klingel K., Rieger P., Plachter B., Jahn G. **(**2000**).** Tropism of human cytomegalovirus for endothelial cells is determined by apost-entry step dependent on efficient translocation to the nucleus. J. Gen.Virol.; *81*: 3021-3035.

217. Sodeik B., Ebershold M. W., Helenius A. **(**1997**).** Microtubule-mediated transport of incoming herpes simplex virus 1 capsids to the nucleus. J. Cell. Biol.; *136*: 1007-1021.

218. Söderberg C., Giugni T. D., Zaia J. A., Larson S., Wahlberg J. M., Möller E. **(**1993**).** CD13 (human aminopeptidase-N) mediates Human Cytomegalovirus infection. J. Virol*.; 67***:** 6576-6585.

219. Spaete R. R., Mocarski E. S. **(**1985**).** Regulation of cytomegalovirus gene expression: alpha and beta promoters are trans activated by viral functions in permissive human fibroblasts. J. Virol.; *56*: 135-143.

220. Stinski M. F. (1977). Synthesis of proteins and glycoproteins in cells infected with human cytomegalovirus. J. Virol.; *23*: 751-767.

221. Stinski M. F., Thomsen D. R., Stenberg R. M., Goldstein L. C. **(**1983**).** Organization and expression of the immediate early genes of human cytomegalovirus. J. Virol.; *46*: 1-14.

222. Stow N. D. (2001). Packaging of genomic and amplicon DNA by the herpes simplex virus type 1 UL25-null mutant KUL25NS. J. Virol.; *75*: 10755-10765.

223. Studier F. W., Moffat B. A. (1986). Use of bacteriophage T7 RNA polymerase to direct selective high-level expression of cloned genes. J. Mol. Biol.; *189*: 113-130.

224. Talbot, P., and J.D. Almeida. (1977). Human cytomegalovirus: purification of enveloped virions and dense bodies. J.Gen.Virol.; *36*: 345-349.

225. Tandon R., AuCoin D. P., Mocarski E. S. (2009). Human cytomegalovirus exploits ESCRT machinery in the process of virion maturation. J. Virol.; *83*: 10797-10807.

226. Tengelsen L. A., Pederson N. E., Shaver P. R., Wathen M. W., Homa F. L. **(**1993). Herpes simplex virus type 1 DNA cleavage and encapsidation require the product of the UL28 gene: isolation and characterization of two UL28 deletion mutants. J. Virol.; *67*: 3470-3480.

227. Theiler R. N., Compton T. (2002). Distinct Glycoprotein O Complexes Arise in a Post-Golgi Compartment of Cytomegalovirus-Infected Cells. J. Virol.; *76*: 2890-2898.

228. Thoma, C.,Borst, E., Messerle, M., Rieger,M., Hwang, J.,Bogner, E. (2006). Identification of the interaction domain of the small terminase subunit pUL89 with the large subunit pUL56 of human cytomegalovirus. Biochemistry.; *45*: 8855-8863.

229. Thurlow J. K., Murphy M., Stow N. D., Preston V. G. (2006). Herpes simplex virus type 1 DNA-packaging protein UL17 is required for efficient binding of UL25 to capsids. J. Virol.; *80*: 2118-2126.

230. Thurlow J. K., Rixon F. J., Murphy M., Targett-Adams P., Hughes M., Preston V. G. (2005). The herpes simplex virus type 1 DNA packaging protein UL17 is a virion protein that is present in both the capsid and the tegument compartments. J. Virol.; *79*: 150-158.

231. Tischer, B. K., von Einem, J., Kaufer, B., Osterrieder, N. (2006). Two-step red-mediated recombination for versatile high-efficiency markerless DNA manipulation in Escherichia coli. Biotechniques.; *40*: 191-197.

232: To A., Bai Y., Shen A., Gong H., Umamoto S., Lu S., Liu F. (2011). Yeast Two Hybrid Analyses Reveal Novel Binary Interactions between Human Cytomegalovirus-Encoded Virion Proteins. PLoS One.; *6*: e17796.

233. Tooze J., Hollinshead M., Reis B., Radsak K., Kern H. (1993). Progeny vaccinia and human cytomegalovirus particles utilize early endosomal cisternae for their envelopes. Eur. J. Cell. Biol.; *60*: 163-178.

234. Trus B. L., Gibson W., Cheng N., Steven A. C. **(**1999**).** Capsid structure of simian cytomegalovirus from cryoelectron microscopy: evidence for tegument attachment sites. J. Virol*.; 73***:** 2181-2192.

235. Trus B. L., Newcomb W. W., Cheng N., Cardone G., Marekov L., Homa F. L., Brown J. C., Steven A. C. (2007). Allosteric signaling and a nuclear exit strategy: binding of UL25/UL17 heterodimers to DNA-filled HSV-1 capsids. Mol. Cell.; *26***:** 479–489.

236. Uetz, P., Dong, Y. A., Zeretzke, C., Atzler, C., Baiker, A. (2006). Herpesviral protein networks and their interaction with the human proteome. Science; *311*: 239-242.

237. Ufaz, S., Shukla, V., Soloveichik, Y., Golan, Y., Breuer, F., Koncz, Z., Galili, G., Koncz, C., Zilberstein, A. (2011). Transcriptional control of aspartate kinase expression during darkness and sugar depletion in Arabidopsis: involvement of bZIP transcription factors. Planta.; *233*: 1025-1040.

238. Valentine R., Shapiro C., Stadtman E. R. **(**1968**).** Regulation of glutamine synthetase. XII. Electron microscopy of the enzyme from Escherichia coli. Biochemistry.; *7*: 2143–2152.

239. Varnum, S. M., Streblow, D. N., Monroe, M. E., Smith, P., Auberry, K. J., Pasa-Tolic, L., Wang, D., Camp, D. G. 2nd, Rodland, K., Wiley, S., Britt, W., Shenk, T., Smith, R. D., Nelson, J. A. (2004). Identification of proteins in human cytomegalovirus (HCMV) particles: the HCMV proteome. J Virol.; *78*: 10960-10966. Erratum in J Virol.; *78*: 13395.

240. Waldeck-Weiermair M., Jean-Quartier C., Rost R., Khan M. J., Vishnu N., Bondarenko A. I., Imamura H., Malli R., Graier W. F. (2011). The leucine zipper EF hand-containing transmembrane protein 1 (LETM1) and uncoupling proteins- 2 and 3 (UCP2/3) contribute to two distinct mitochondrial Ca2+ uptake pathways. J. Biol. Chem.; [Epub ahead of print]

241. Wang, L., Jackson, W. C., Steinbach, P. A., Tsien, R. Y. (2004). Evolution of new nonantibody proteins via iterative somatic hypermutation. PNAS.*; 101*: 16745–16749.

242. Wang X., Huang D. Y., Huong S. M., Huang E. S. **(**2005**).** Integrin alphavbeta3 is a coreceptor for human cytomegalovirus. Nat. Med.; *11*: 515-521.

243. Wang X., Huong S. M., Chiu M. L., Raab-Traub N., Huang E. S. (2003). Epidermal growth factor receptor is a cellular receptor for human cytomegalovirus. Nature.; *424*: 456–461.

244. Wathen M. W., Stinski M. F. **(**1982**).** Temporal patterns of human cytomegalovirus transcription: mapping the viral RNAs synthesized at immediate early, early, and late times after infection. J. Virol.; *41*: 462-477.

245. Welch A. R., Woods A. S., McNally L. M., Cotter R. J., Gibson W. **(**1991**).** A herpesvirus maturational protease, assemblin: identification of its gene, putative active site domain, and cleavage site. PNAS.; *88*: 10792-10796.

246. Williamson M. P., Sutcliffe M. J. (2010). Protein-protein interactions. Biochem. Soc. Trans.; *38*: 875-878.

247. Winkler M., Schmolke S., Plachter B., Stamminger T. **(**1995**).** The pUL69 protein of human cytomegalovirus (HCMV), a homologue of the herpes simplex virus ICP27, is contained within the tegument of virions and activates the major immediate-early enhancer of HCMV in synergy with the tegument protein pp71 (ppUL82). Scand. J. Infect. Dis. Suppl.; *99*: 8-9.

248. Womack, A., Shenk, T. (2010). Human Cytomegalovirus Tegument Protein pUL71 Is Required for Efficient Virion Egress. MBio.; *1*: e00282-10.

249. Wright H. T. Jr., Goodheart C. R., Lielausis A. **(**1964**).** Human cytomegalovirus. Morphology by negative staining. Virology.*; 23*: 419-424.

250. Yang K., Wills E., Baines J. D. (2009). The putative leucine zipper of the UL6-encoded portal protein of herpes simplex virus 1 is necessary for interaction with pUL15 and pUL28 and their association with capsids. J. Virol.; *83*: 4557-4564.

251. Yu D., Silva M. C., Shenk T. (2003). Functional map of human cytomegalovirus AD169 defined by global mutational analysis. PNAS.; *100*: 12396- 12401.

252. Yu D., Smith G. A., Enquist L. W., Shenk T. (2002). Constructionof a self-excisable bacterial artificial chromosome containing thehuman cytomegalovirus genome and mutagenesis of the diploid TRL/IRL13 gene. J. Virol.; *76*: 2316–2328.

253. Yu D., Weller S. K. (1998). Herpes simplex virus type 1 cleavage and packaging proteins UL15 and UL28 are associated with B but not C capsids during packaging. J. Virol.; *72*: 7428-7439.

254. Yu, X., Shah, S., Lee, M., Dai, W., Lo, P., Britt, W., Zhu, H., Liu, F., Hong Zhou, Z. (2011). Biochemical and structural characterization of the capsid-bound tegument proteins of human cytomegalovirus. J. Struct. Biol.; [Epub ahead of print]

255. Zhou Z. H., Chen D. H., Jakana J., Rixon F. J., Chiu W. (1999). Visualization of tegument–capsid interactions and DNA in intact herpes simplex virus type 1 virions. J. Virol.; *73*: 3210–3218.

256. Zhou Z. H., Dougherty M., Jakana J., He J., Rixon F. J., Chiu W. (2000). Seeing the herpesvirus capsid at 8.5 A. Science.; *288*: 877–880.

Anhang

Abbreviations

Abbreviations for chemical compounds are found in the chemical list (2.1.1.1).

^{35}S	Sulphur radioactive isotope
aa	amino acids
AC	Assembly compartment or assembly complex
AIDS	Acquired immune deficiency syndrome
ATP	Adenosine triphosphate
BAC	Bacterial artificial chromosome
bp	Base pair
BE	Binding efficiency
BiFC	Bi-molecular fluorescence complementation
BSA	Bovine serum albumin
cAMP	Cyclic adenosine monophosphate
CCD	Charged coupled device
cf.	*lat. conferre*, compare
cGMP	cyclic guanosine monophosphate
cm^2	Square centimetre
DB	Dense body
DNA	Deoxyribonucleic acid
dNTP	Deoxyribonucleotide
ds	double strand
EBV	Epstein-Barr-Virus (Herpesvirus)
ECL	Enhanced chemiluminescence
E. coli	*Escherichia coli*
e.g.	*lat. exampli gratia,* for example
EGFR	Epidermal growth factor receptor
EM	Electron microscope
ER	Endoplasmatic reticulum (cellular)
ESCRT	Endosomal sorting complex required for transport (cellular)
FCS	Fetal calf serum
g	g-force (centrifugation)

g	Gramm (10^{-3} kg)
GST	Glutathione S-transferase
h	hour
HCMV	Human cytomegalovirus
HEK	Human Embryonic Kidney cells
HELF	human embryonic lung fibroblast cells
HFF	Human foreskin fibroblast cells
HHV-6	human herpes virus type 6 (Herpesvirus)
HHV-7	human herpes virus type 7 (Herpesvirus)
HHV-8	human herpes virus type 8 (Herpesvirus)
HSV-1	herpes simplex virus type 1 (Herpesvirus)
HSV-2	herpes simplex virus type 2 (Herpesvirus)
I_{BiFC}	BiFC intensity
ICTV	international committee on virus taxonomy
IgG	Immunoglobulin G
IF	Immunofluorescence
$I_{mCherry}$	mCherry (red) intensity
IP	Immunoprecipitation
IRL	Internal repeat long; region in Herpesvirus genome
IRS	Internal repeat short; region in Herpesvirus genome
I_{YFP}	YFP intensity
kb	Kilo bases (1000 bases)
kDa	Kilo Dalton (1Da~ 1/ N_A gram)
kg	Kilo gram
L	litre
M	Mole
mA	Miliampere, unit of electric current
mCi	Milicurie, unit of radioactivity
mg	Miligram (10^{-3} g)
µg	Micro gram (10^{-6} g)
ml	Mililitre (10^{-3} L)
µl	Micro litre (10^{-6} L)
MOI	Multiplicity of infection

mol	Mole, mass entity of N_A (Avogadro's number ((6.02214179 ±3x 10^{-7}) x 10^{23} mol^{-1}) pieces
MW	Molecular weight
NC	Nitrocellulose membrane
NIEP	Non-infectious enveloped viral particle
ng	Nanogram (10^{-9} g)
nm	Nanometre (10^{-9} m)
OD_{600}	Optical density 600 at nm
ORF	Open reading frame
OVA	Ovalbumine
o/n	Over night (16h)
PAGE	Poliacrylamide gel electrophoresis
pAP	Assembly protein precursor (encoded by *HCMV* UL80)
PCR	Polymerase chain reaction
pH	negative decimal logarithm of hydrogen ion activity in solution
pI	Isoelectric point
p.i.	Post infection
PrV	Pseudorabies virus (*α-Herpesvirinae* in swine)
RT	Room temperature (~20°C)
T	Triangulation Number (T-Number) $T = h^2 + k^2 + hk$ (*h, k* non-neg. integers)
TEM	transmission electron microscopy
TGN	Trans Golgi network (cellular)
TRL	Terminal repeat long; region in Herpesvirus genome
TRS	Terminal repeat short; region in Herpesvirus genome
UL	Unique long segment; region in Herpesvirus genome
US	Unique short segment; region in Herpesvirus genome
V	Volt, unit of electronic force
VZV	varizella zoster virus (Herpesvirus)
WB	Western blot (= immunostaining)
WM	Whatmann blotting paper
Y2H	Yeast two hybrid
YC	C-terminal part of YFP (used for BiFC)
YFP	Yellow fluorescent protein; Fluorophore in BiFC (=citrin)

YN	N-terminal part of YFP (used for BiFC)
‘	minute
°C	degree Celsius

Herpes gene products and proteins (239)

gB	Glycoprotein B, encoded by *HCMV* UL55
gCI	Glycoprotein complex I
gCII	Glycoprotein complex II
gCIII	Glycoprotein complex III
gH	Glycoprotein H, encodes by *HCMV* UL75
gL	Glycoprotein L, encodes by *HCMV* UL115
gM	Glycoprotein M, encodes by *HCMV* UL100
gN	Glycoprotein N, encodes by *HCMV* UL73
gO	Glycoprotein O, encodes by *HCMV* UL74
IE1/2	Immediate early gene 1/2, IE1 encodes by *HCMV* UL123 IE2 encodes by *HCMV* UL122
mC-BP	minor capsid binding protein, encodes by *HCMV* UL46
mCP	minor capsid protein, encodes by *HCMV* UL85
MCP	major capsid protein, encodes by *HCMV* UL86
pAP	Assembly protein precursor (encoded by *HCMV* UL80)
pp28	“Phosphor protein 28”; *HCMV* tegument protein, encoded by UL99
pp65	“Phosphor protein 65”; *HCMV* tegument protein, encoded by UL83
pp71	“Phosphor protein 71”; *HCMV* tegument protein, encoded by UL82
pp150	“Phosphor protein 150”; *HCMV* tegument protein, encoded by UL32
pPR	Proteinase precursor (encoded by *HCMV* UL80)
pTRS1	*HCMV* short terminal repeat gene product 1; Transcription-replication
U44	Class of Herpesvirus proteins
pUL14	*HCMV* type 1 membrane protein, encoded by UL14
pUL31	*α-Herpesvirinae* protein that facilitates nuclear egress
pUL34	*α-Herpesvirinae* protein that facilitates nuclear egress
pUL44	*HCMV* polymerase co-factor, encoded by UL44
pUL47	*HCMV* tegument protein, encoded by UL47

pUL48	*HCMV* large tegument protein, encoded by UL48
pUL50	*HCMV* type 2 membrane protein, encoded by UL50
pUL51	*HCMV* DNA packaging protein, encoded by UL51
pUL52	*HCMV* DNA packaging protein, encoded by UL52
pUL56	*HCMV* large terminase subunit, encoded by UL56
pUL57	*HCMV* single strand binding protein, encoded by UL57
pUL69	*HCMV* RNA-binding protein, encoded by UL69
pUL71	*HCMV* tegument protein, encoded by UL71 (this study)
pUL76	*HCMV* nuclear protein, encoded by UL76
pUL77	*HCMV* capsid associated protein, encoded by UL77 (this study)
pUL88	*HCMV* Tegument protein, encoded by UL88
pUL89	*HCMV* short terminase subunit, encoded by UL89
pUL93	*HCMV* capsid associated protein, encoded by UL93
pUL97	*HCMV* viral kinase, encoded by UL97
pUL104	*HCMV* portal protein, encoded by UL104
pUS14	*HCMV* type 3 membrane protein, encoded by US14
pUS17	*HCMV* type 3 membrane protein, encoded by US17
pUS20	*HCMV* type 3 membrane protein, encoded by US20
pUS29	*HCMV* putative membrane protein, encoded by US29
RL5A	*HCMV* envelope glycoprotein, encoded by RL5A
RL13	*HCMV* membrane protein, encoded by RL13
SCP	small capsid protein, encodes by *HCMV* UL48A
UL6	encodes *HSV-1* portal protein (=*HCMV* UL104)
UL15	encodes *HSV-1* terminase subunit (=*HCMV* UL89)
UL17	encodes *HSV-1* tegument protein (=*HCMV* UL93)
UL25	encodes *HSV*-1 capsid associated protein (=*HCMV* UL77)
UL28	encodes *HSV-1* terminase subunit (=*HCMV* UL56)
UL32	encodes *HSV-1* packaging protein (=*HCMV* UL52)
UL33	encodes *HSV-1* packaging protein (=*HCMV* UL52)
UL36	encodes *HCMV* tegument protein pUL36
UL70	encodes *HCMV* helicase-primase primase subunit pUL70
UL71	encodes *HCMV* tegument protein pUL71
UL72	encodes *HCMV* deoxyuridine triphosphatase pUL72

UL76	encodes *HCMV* nuclear protein pUL76
UL77	encodes *HCMV* capsid-associated protein pUL77
UL78	encodes *HCMV* envelope protein pUL78
UL80	encodes *HCMV* scaffold proteins pAP, pPR
UL131A	encodes *HCMV* envelope protein pUL131A

Amino acids

A (Ala)	Alanine
D (Asp)	Aspartic acid
E (Glu)	Glutamic acid
F (Phe)	Phenylalanine
H (His)	Histidine
I (Ile)	Isoleucine
K (Lys)	Lysine
L (Leu)	Leucine
N (Asn)	Asparagine
P (Pro)	Proline
Q (Gln)	Glutamine
R (Arg)	Arginine
T (Thr)	Threonine
W (Trp)	Trypophane

In silico analysis HSV-1 UL51 in comparison to HCMV UL71

```
Psi-pred HHHHHHHHHH HHHCCCCCCC CCCCCCCCCC HHHHHHHHHH HHHCCCCCCC CHHHHHHCCC
HCMV   1 mqlaqrlcel lmcrrkaapv adyvllqpse dvelrelqaf ldenfkqlei tpadlrtfsr
HSV-1  1 masllgaicg wgarpeeqye miraavppse aeprlqeala vvnallpapi tlddalgsld
Psi-pred CHHHHHHHHC CCCCCHHHHH HHHHCCCCCC CHHHHHHHHH HHHHHCCCC CCHHHHHHCHH

Psi-pred CCHHHHHHHH HHHHHHHHHH HHHHHHHHHH HCCCCCCCCC HHHHHHHHHH HHHHHHHHHH
HCMV  61 dtdvvnhllk llplyrqcqs kcaflkgyls egclphtrpa aeveckksqr ilealdilil
HSV-1 61 dtrrlvkara lartyhacmv nlerlarhhp gfeaptidga vaahqdkmrr ladtcmatil
Psi-pred HHHHHHHHHH HHHHHHHHHH HHHHHHHCCC CCCCCCCHHH HHHHHHHHHH HHHHHHHHHH

Psi-pred  HHHHHCCCCC CHHHHHHHHH HHHCCCHHHH HHHHHHHHHC CCCHHHHHHH HHCCCCCCCC
HCMV  121 klvvgefams eadslemlld kfstdqaslv evqrvmglvd mdceksayml eagaaatvap
HSV-1 121 qmymsvgaad ksadvlvsqa irsmaesdvv medvaiaera lglsafgvag gtrsggigvt
Psi-pred  HHHHHCCCCC CCHHHHHHHH HHHHHHHHHH HHHHHHHHHH HCCCCCCCCC CCCCCCCCCC

Psi-pred  CCCCCEEECC CCCCCCCCEE EEEECCCCCC CCCCCCCCCC CCCCCCCCCC CCCCCCCCCH
HCMV  181 ptppavvqge sgvredgetv aavsafacps vsdslipeet gvtrpmmslah intvscptv
HSV-1 181 eapslghpht pppevtlapa arngdalpdp kpescprvsv prptasptap rpgpsraapc
Psi-pred  CCCCCCCCCC CCCCCCCCCC CCCCCCCCCC CCCCCCCCCC CCCCCCCCCC CCCCCCCCCC

Psi-pred  HHHHHHHHHC CCCCCCEEEE CCCCCCCCCC CCCCCCCCCC CCCCCCCCCC CCCCCCCCC
HCMV  241 mrfdqrllee gdeedevtvm spspepvqqq ppvepvqqqp qgrgshrrry kesapqetlp
HSV-1 241 vlgq
Psi-pred  CCCC

Psi-pred  CCHHHHHHHH HHCCCCCCCC CCCCCCEEEC CCCCCCCCCC HHHHCCCCCC CCHHHHHCCC
HCMV  301 tnhereildl mrhspdvpre avmsptmvti pppqipfvgs arelrgvkkk kptaaallss

Psi-pred C
HCMV  361 a
```

p-coils: predicted coiled-coil motifs in orange

Psi-pred: H...Helix, E.. strand, C..coil

HSV-1 UL51 aa.31-52 Hydrophobic core: $l_{45}a_{31}a_{38}r_{49}v_{42}l_{35}l_{46}l_{39}$ (Heliquest prediction)

HCMV UL71 aa. 34-55 Leucien zipper-like motif lrelqaf ldenfkqlei tpadl(Motif scan prediction)

Hydrophobic aa. i..isoleucine, l..leucine in yellow

Danksagung

Ich möchte mich an dieser Stelle ganz herzlich bei all denjenigen bedanken, die mich während meiner Promotion unterstützt haben.

Herrn Prof. Dr. Detlev H. Krüger möchte ich für die Möglichkeit, am Institut für Medizinische Virologie der Charité- Universitätsklinikum Berlin zu promovieren und für die Vertretung der Arbeit vor dem Fachbereich Biologie der Humboldt Universität zu Berlin danken.

Meiner Arbeitsgruppenleiterin Frau Prof. Dr. Elke Bogner danke ich für die Bereitstellung des vielseitigen und interessanten Themas sowie für die Unterstützung bei der Planung und Ausführung der experimentellen Arbeiten.

Prof. Dr. Thomas Mertens möchte ich für die Möglichkeit danken Teile meiner praktischen Arbeiten am Universitätsklinikum Ulm durchzuführen. Im besonderem danke ich Dr. Jens von Einem für die Bereitstellung der rekombinanten Viren und für die anregenden Diskussionen im Rahmen dieser in Ulm durchgeführten Arbeiten.

Ich danke der ZIBI Graduate School Berlin und insbesondere Frau Dr. Martina Sick und Frau Dr. Susann Beetz für die sehr persönliche und motivierende Begleitung der Promotion.

Den ehemaligen und aktuellen Mitarbeitern der Arbeitsgruppe Bogner: Angelika Lander, Christina Priemer, Ina Woskobojnik, Jae-Seon Hwang, Kathrin Dezer, Marion Kaspari, Oliver Kregler, Panja Köppen-Rung, Rita Schilf, Sara Lapp; möchte ich für die gute Zusammenarbeit, die nette und kollegiale Arbeitsatmosphäre, die große Hilfsbereitschaft sowie die anregenden Diskussionen danken. Viele von euch sind nicht nur Kollegen sondern auch zu gute Freunde geworden.

Meinen Praktikanten Sigrun Schmähling und im besonderen Silke Pollack, sind für ihre tatkräftige Unterstützung bei den experimentellen Arbeiten zu erwähnen.

Publikationen:

“Peer review” Journals

Meissner, C.S., Köppen-Rung P., Dittmer A., Lapp S., Bogner E. (2011) A “Coiled-coil” motif is important for oligomerization and DNA binding properties of human cytomegalovirus protein UL77. PLoS ONE 6(10): e25115.

Meissner, C.S., Suffner S., Schaufflinger M., von Einem J., Bogner E. (2011) A leucine zipper motif of human cytomegalovirus tegument protein pUL71 is important for oligomerization. In Prep.

Vorträge and Posterpräsentationen:

Christina S. Meissner, Elke Bogner. (2008). Identification of viral and cellular interaction partners during intracellular maturation of HCMV. Posterpräsentation beim “Annual Retreat of ZIBI Graduate School”, Meissen, 3-5. December 2008.

Christina S. Meissner , Alexandra Dittmer and Elke Bogner (2009). Human cytomegalovirus capsid associated protein pUL77 interacts with other DNA packaging proteins. Posterpräsentation beim “34th Annual International Herpesvirus Workshop”, Ithaca, New York USA, 25 –31. Juli 2009.

Christina S. Meissner and Elke Bogner (2009). Characterisation of HCMV pUL71 in context of nuclear egress. Posterpräsentation beim “34th Annual International Herpesvirus Workshop”, Ithaca, New York USA, 25 –31. Juli 2009.

Christina S. Meissner , Alexandra Dittmer and Elke Bogner (2009). Human cytomegalovirus capsid associated protein pUL77 interacts with other DNA packaging proteins .Vortrag beim “4th Mini-Herpesvirus Workshop”, Berlin, 11. September 2009.

Berlin, den

Christina Sylvia Meissner

Christina S. Meissner and Elke Bogner (2010). Functional analysis of pUL71 and pUL77 in context of HCMV egress. Posterpräsentation beim "Annual Retreat of ZIBI Graduate School", Woltersdorf, 6-8. Januar 2010.

Christina S. Meissner and Elke Bogner (2010) Function of HCMV pUL71 – a stabilizing factor in the virion? Posterpräsentation beim "35th International Herpesvirus Workshop", Salt Lake City, Utah USA, 24 –29. Juli, 2010.

Christina S. Meissner and Elke Bogner (2011) HCMV pUL71 – a stabilizing factor in the virion? Vortrag beim "Annual Retreat of ZIBI Graduate School", Potsdam, 21 –22. Februar 2011.

Christina S. Meissner, Jens von Einem and Elke Bogner (2011). A leucine zipper motif of human cytomegalovirus tegument protein pUL71 is important for oligomerisation. Posterpräsentation beim "21st Annual Meeting of the GfV (Gesellschaft für Virologie)", Freiburg, 23-26. März 2011.

Pánja Köppen-Rung, Christina S. Meissner, Sara M. Lapp, Alexandra Dittmer and Elke Bogner (2011). Coiled-coil motif important for oligomerisation and DNA binding properties of human cytomegalovirus protein UL77. Posterpräsentation beim "21st Annual Meeting of the GfV (Gesellschaft für Virologie)", Freiburg, 23-26. März 2011.

Christina S. Meissner, Sascha Suffner, Jens von Einem and Elke Bogner (2011) A leucine zipper motif mediates oligomerization of human cytomegalovirus tegument protein pUL71 and is crucial for its function. Vortrag beim "36th International Herpesvirus Workshop", Gdansk, Polen, 24 –28. Juli, 2011.

Berlin, den

Christina Sylvia Meissner

Eidesstattliche Erklärung

Hiermit erkläre ich, die vorliegende Doktorarbeit selbständig und nur unter Verwendung der angegebenen Literatur und Hilfsmittel angefertigt zu haben.

Berlin, den

Christina Sylvia Meissner